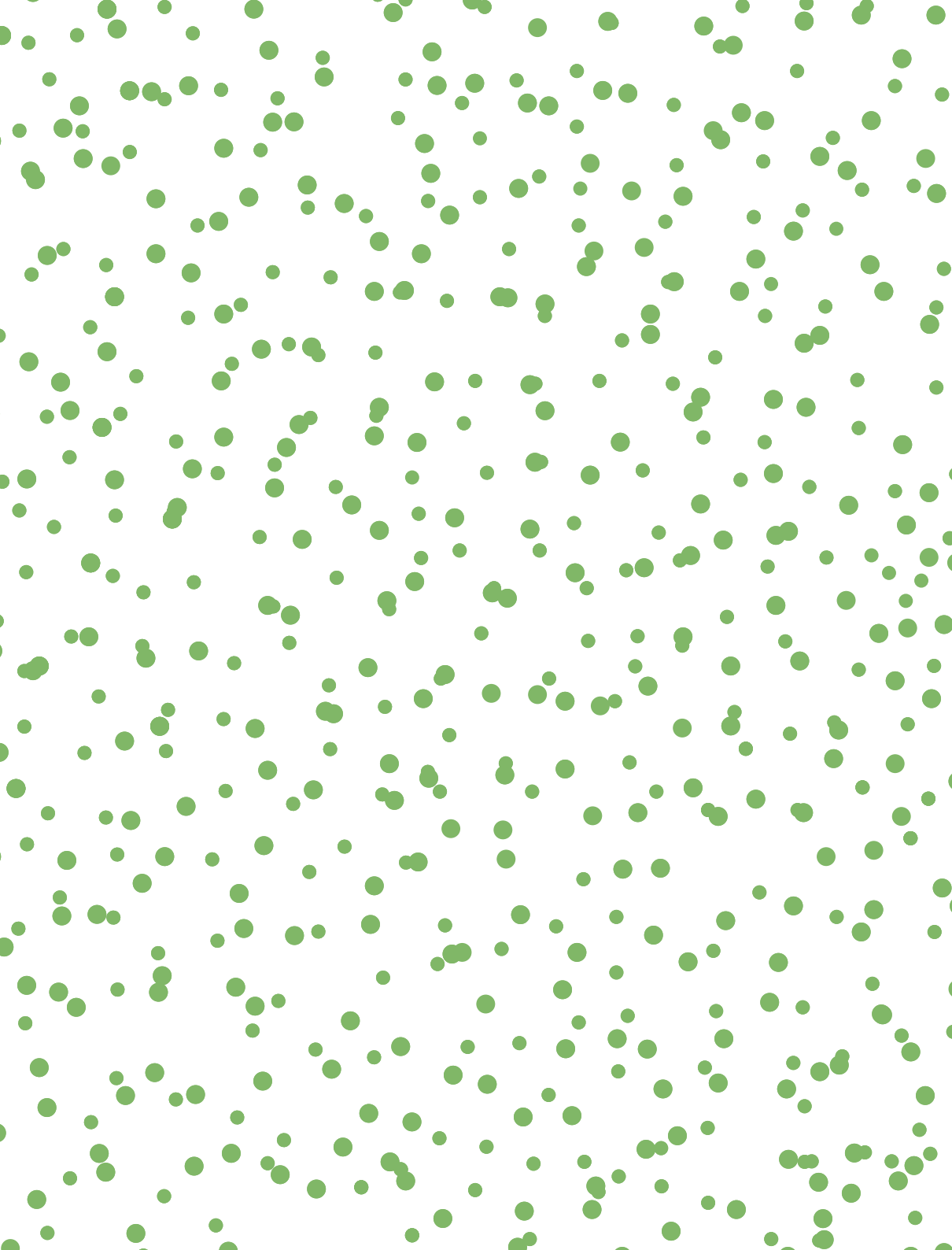


FLUORESCENCE-GUIDED
CANCER SURGERY

*Clinical translation of
tumor-targeted agents*

CHARLOTTE HOOGSTINS



Fluorescence-guided cancer surgery

Clinical translation of tumor-targeted agents

© Charlotte E.S. Hoogstins

Design: Caroline de Lint, Voorburg (caro@delint.nl)

All rights reserved. No part from this thesis may be reproduced, distributed or transmitted in any form or by any means, without prior written permission of the author.

Publication of this thesis was financially supported by the foundation Centre for Human Drug Research, Leiden, the Netherlands

PROEFSCHRIFT

ter verkrijging van de graad van Doctor
aan de Universiteit Leiden, op gezag van
Rector Magnificus prof. mr. C.J.J.M. Stolker,
volgens besluit van het College voor Promoties
te verdedigen op dinsdag 25 september 2018
klokke 11:15 uur

DOOR

Charlotte Egberdina Sophie Hoogstins
geboren te Amsterdam
in 1987

PROMOTORES

Prof. dr. J. Burggraaf

Prof. dr. A.F. Cohen

CO-PROMOTOR

Dr. A.L. Vahrmeijer

LEDEN PROMOTIECOMMISSIE

Prof. dr. C.J.H. van de Velde

Prof. dr. S. Osanto

Prof. dr. C. Löwik (Erasmus Medisch Centrum, Rotterdam)

Prof. dr. H.J.T. Rutten (Catharinaziekenhuis, Eindhoven)

PART I ROAD TOWARDS TUMOR-TARGETED AGENTS

- 1 Introduction and outline of the thesis – **8**
- 2 The value of intraoperative near-infrared fluorescence imaging based on enhanced permeability and retention of indocyanine green: feasibility and false-positives in ovarian cancer – **14**
- 3 In search for optimal targets for intraoperative fluorescence imaging of peritoneal carcinomatosis from colorectal cancer – **30**

PART II CLINICAL TRANSLATION OF TUMOR-TARGETED AGENTS

- 4 Intraoperative imaging of folate receptor alpha positive ovarian and breast cancer using the tumor specific agent EC17 – **46**
- 5 A novel tumor-specific agent for intraoperative near-infrared fluorescence imaging: a translational study in healthy volunteers and patients with ovarian cancer – **67**
- 6 Feasibility of folate receptor-targeted intraoperative fluorescence imaging during staging procedures for early ovarian cancer – **88**
- 7 Image-guided surgery in patients with pancreatic cancer: first results of a clinical trial using SGM-101, a novel carcinoembryonic antigen-targeting, near-infrared fluorescent agent – **103**

PART III FUTURE PERSPECTIVES

- 8 Image guided surgery using near-infrared fluorescence: road to clinical translation of novel probes for real time tumor visualization – **120**
- 9 Setting standards for reporting and quantification in fluorescence-guided surgery – **130**

PART IV SUMMARY AND APPENDICES

- 10 Summary – **148**
- 11 Nederlandse samenvatting – **152**
List of publications – **156**
Curriculum vitae – **158**

PART I

ROAD TOWARDS

TUMOR-TARGETED AGENTS

Chapter 1

Introduction and outline of the thesis

IMAGE-GUIDED SURGERY ● Novel insights into the complex biology of cancer have instigated major changes in daily clinical practice over the last decade. These changes mainly apply to chemotherapy, hormonal therapy, immunotherapy and new targeted therapies. In spite of these advancements in non-surgical therapies, surgery remains the primary treatment modality for solid tumors. Strikingly oncologic surgeons still rely on non-specific visual changes and palpation of subtle irregularities to guide their resections. Consequently, clinical outcome of cancer surgery for most cancer types has only gradually improved over the last decades. The importance of clear intraoperative tumor visualization is evident from the impact that irradical or incomplete tumor resections have on survival as illustrated by two examples. The status of the resection margins is an important independent prognostic factor in pancreatic cancer for which it has been shown that survival time of patients doubles when comparing microscopically radical resection (R0; mean survival 20.3 months) and with irradical resections (R1; median survival 10.3 months) [1]. In ovarian cancer, several studies have shown that the amount of residual tumor following cytoreductive surgery is the most important prognostic indicator of survival [2]. In order to improve surgical outcomes, real-time intraoperative distinction between malignant and normal tissue is urgently needed.

NEAR-INFRARED (NIR) FLUORESCENCE ● Fluorescence imaging appears to be ideal for intraoperative application. It has fast acquisition times (in millisecond range), flexibility in application and portability [3]. Particularly, the use of near infrared (NIR) fluorescence (wavelengths 700-900 nm) is interesting as NIR light increases tissue penetration depth (up to 1 cm) and decreases autofluorescence (signals arising from background tissue). Noticeably, this imaging modality requires endogenous contrast or, more commonly, the administration of an exogenous contrast agent. As fluorescent light is invisible to the human eye, a dedicated imaging system is needed to detect the fluorescence signal and to procedure a two-dimensional (2D) image demarking its distribution. Figure 1.

IMAGING SYSTEMS ● The increasing interest in fluorescence imaging has led to the development of a variety of commercial and experimental fluorescence imaging systems. Imaging systems are available at different wavelengths and can be adapted for different types of surgery (open or laparoscopic). As a complementary combination of fluorescent agent and imaging system is essential for a successful application, manufacturing of imaging systems is governed mainly by the optical properties of the fluorescent agents. Although sensitivity of the

imaging system has been suggested the most important factor for the intraoperative detection of an imaging agent, other key features also play an important role in the selection of an imaging system and its adoption in the clinic. These features can be summarized as (i) maximized ergonomics, (ii) real-time overlay of white-light and fluorescence images with (iii) minimal hindrance from ambient room light, and (iv) the ability to quantify fluorophores in situ [4,5]. Given the recent advancements in the field, the ability to image multiple fluorescent agents simultaneously while maintaining high sensitivity for each individual agent will also be of importance.

FLUORESCENT AGENTS • Exogenous contrast agents can either be nonspecific (i.e. indocyanine green (ICG)) or molecularly targeting fluorescent imaging agents. At first, the fluorescence-imaging field focused predominantly on ICG imaging because ICG is available for clinical use. Other clinically available agents include methylene blue (MB) and 5-aminolevulinic acid (5-ALA). Although these agents have demonstrated to be of value in certain indications, they are not universally applicable and for a large number of indications, therefore the need for specific imaging agents remains. The improved knowledge regarding the hallmarks of cancer combined with the ability to conjugate fluorescent dyes to targeting molecules has shifted the focus of the fluorescence imaging field towards specific tumor-targeted agents [6]. These agents actively bind and cumulate in tumor cells, allowing more specific intraoperative fluorescence imaging.

For tumor specific imaging a variety of fluorophores at different wavelengths (CY5, IRDYE800CW, ZW800-1) can be used. The fluorophore is coupled to a targeting moiety that specifically binds a biomarker expressed by a tumor cell. Targeting moieties range from monoclonal antibodies, antibody fragments, small peptides to small molecules. A certain combination of fluorophore and targeting moiety will have specific characteristics in terms of tumor binding affinity, affinity for normal tissue and pharmacokinetics. These characteristics will greatly determine the added value associated with the use of the agent. For instance, antibodies have a strong tumor binding affinity, but slow clearance and a long half-life preclude imaging directly after dosing.

REGULATORY • Rules and regulations for new fluorescent agents and imaging systems are set by the United States of America's Food and Drug Administration (FDA) and its European counterpart the European Medicines Agency (EMA). Despite a lack of therapeutic effect, for regulatory approval of a fluorescent agent, an investigational new drug (IND) application is required. The IND must include

detailed information about Good Manufacturing Practices (GMP) production, manufacturing, pharmacology, toxicology and, if available, previous human experience with related compounds. This complex process as well as the associated time and cost, poses a challenge for developers of novel tumor specific agents to bring these compounds into the clinic. Notwithstanding, various tumor-targeted agents have been successfully studied in clinical trials [7-9]. Moreover a great potential for a broad range of clinical applications remains [10].

OUTLINE OF THE THESIS • This thesis is divided into three parts. In the first part the road towards tumor-targeted agents is discussed. Chapter 2 focusses on the value of the non-targeted agent ICG for the intra-operative detection of ovarian cancer in patients. In Chapter 3 potential biomarkers for the detection of peritoneal carcinomatosis from colorectal cancer are evaluated.

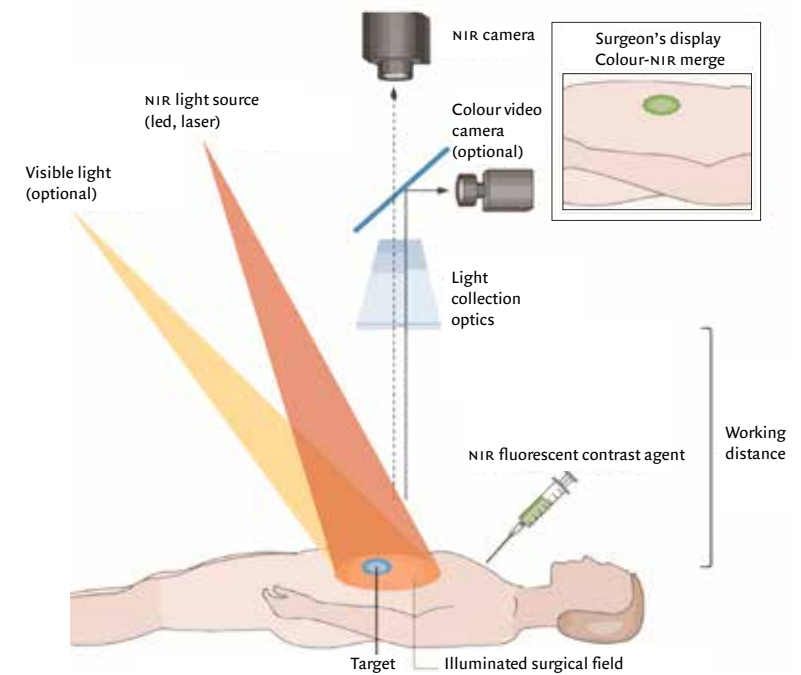
Part 1 is the foundation for part 2, in which the clinical application of various tumor-targeted agents are described. Chapter 4 describes the use of a small molecule (EC17) as an agent for intraoperative ovarian cancer imaging. The use of an improved version of EC17, OTL38, is described in Chapters 5 and 6. This part is concluded with Chapter 7 in which the use of SGM-101, an fluorescent labelled antibody for intraoperative imaging of pancreatic cancer, is described.

In the last part the future perspectives of fluorescence-guided cancer surgery are described. Chapter 8 highlights some of the challenges for clinical application of fluorescence-guided cancer surgery and in Chapter 9 suggestions are given to overcome some of these challenges by providing recommendations regarding standardization of imaging system assessment and image analysis.

REFERENCES

- 1 Garcea G, Dennison AR, Pattenden CJ, Neal CP, Sutton CD, Berry DP. Survival following curative resection for pancreatic ductal adenocarcinoma. A systematic review of the literature. *JOP*. 2008;9(2):99-132.
- 2 Chang SJ, Bristow RE, Ryu HS. Impact of complete cytoreduction leaving no gross residual disease associated with radical cytoreductive surgical procedures on survival in advanced ovarian cancer. *Ann Surg Oncol*. 2012;19(13):4059-67.
- 3 Themelis G, Yoo JS, Soh KS, Schulz R, Ntziachristos V. Real-time intraoperative fluorescence imaging system using light-absorption correction. *J Biomed Opt*. 2009;14(6):064012.
- 4 Zhang RR, Schroeder AB, Grudzinski JJ, Rosenthal EL, Warram JM, Pinchuk AN, et al. Beyond the margins: real-time detection of cancer using targeted fluorophores. *Nat Rev Clin Oncol*. 2017;14(6):347-64.
- 5 AV DS, Lin H, Henderson ER, Samkoe KS, Pogue BW. Review of fluorescence guided surgery systems: identification of key performance capabilities beyond indocyanine green imaging. *J Biomed Opt*. 2016;21(8):80901.
- 6 Hanahan D, Weinberg RA. The hallmarks of cancer. *Cell*. 2000;100(1):57-70.
- 7 Hoogstins CE, Tummers QR, Gaarenstroom KN, de Kroon CD, Trimbos JB, Bosse T, et al. A Novel Tumor-Specific Agent for Intraoperative Near-Infrared Fluorescence Imaging: A Translational Study in Healthy Volunteers and Patients with Ovarian Cancer. *Clin Cancer Res*. 2016;22(12):2929-38.
- 8 Rosenthal EL, Warram JM, de Boer E, Chung TK, Korb ML, Brandwein-Gensler M, et al. Safety and Tumor Specificity of Cetuximab-IRDye800 for Surgical Navigation in Head and Neck Cancer. *Clin Cancer Res*. 2015;21(16):3658-66.
- 9 Harlaar NJ, Koller M, de Jongh SJ, van Leeuwen BL, Hemmer PH, Kruijff S, et al. Molecular fluorescence-guided surgery of peritoneal carcinomatosis of colorectal origin: a single-centre feasibility study. *Lancet Gastroenterol Hepatol*. 2016;1(4):283-90.
- 10 Tipirneni KE, Rosenthal EL, Moore LS, Haskins AD, Udayakumar N, Jani AH, et al. Fluorescence Imaging for Cancer Screening and Surveillance. *Mol Imaging Biol*. 2017

FIGURE 1 FLUORESCENCE IMAGING



Fluorescent contrast agents are administered intravenously. During surgery, the agent is visualized using a fluorescent imaging system. An optimal system includes simultaneous visible (white light) illumination of the surgical field, which can be merged with the fluorescence images. Illustration and caption adapted from Vahrmeijer et al., *Nat Rev* 2013

Chapter 2

The value of intraoperative near-infrared fluorescence imaging based on enhanced permeability and retention of indocyanine green: feasibility and false-positives in ovarian cancer

PLoS One. 2015 Jun 25

QUIRIJN TUMMERS*, CHARLOTTE HOOGSTINS*, ALEXANDER PETERS, COR DE KROON, BAPTIST TRIMBOS, CORNELIS VAN DE VELDE, JOHN FRANGIONI, ALEXANDER VAHRMEIJER, KATJA GAARENSTROOM

* Shared first authorship

ABSTRACT

OBJECTIVE In ovarian cancer, two of the most important prognostic factors for survival are completeness of staging and completeness of cytoreductive surgery. Therefore, intra-operative visualization of tumor lesions is of great importance. Preclinical data already demonstrated tumor visualization in a mouse-model using near-infrared (NIR) fluorescence imaging and indocyanine green (ICG) as a result of enhanced permeability and retention (EPR). The aim of this study was to determine feasibility of intraoperative ovarian cancer metastases imaging using NIR fluorescence imaging and ICG in a clinical setting.

METHODS Ten patients suspected of ovarian cancer scheduled for staging or cytoreductive surgery were included. Patients received 20 mg ICG intravenously after opening the abdominal cavity. The mini-FLARE™ NIR fluorescence imaging system was used to detect NIR fluorescent lesions.

RESULTS 6 out of 10 patients had malignant disease of the ovary or fallopian tube, of which 2 had metastatic disease outside the pelvis. Eight metastatic lesions were detected in these 2 patients, which were all NIR fluorescent. However, 13 non-malignant lesions were also NIR fluorescent, resulting in a false-positive rate of 62%. There was no significant difference in tumor-to-background ratio between malignant and benign lesions (2.0 vs 2.0; $P=0.99$).

CONCLUSIONS This is the first clinical trial demonstrating intraoperative detection of ovarian cancer metastases using NIR fluorescence imaging and ICG. Despite detection of all malignant lesions, a high false-positive rate was observed. Therefore, NIR fluorescence imaging using ICG based on the EPR effect is not satisfactory for the detection of ovarian cancer metastases. The need for tumor-specific intraoperative agents remains.

INTRODUCTION

Ovarian cancer has a worldwide incidence of 225,500 making it the 6th most common cancer in women. With 140,200 deaths worldwide per year, it has the highest mortality rates amongst all gynaecological cancers [1–3]. In general, ovarian cancer can be classified as early stage (FIGO I to IIa) or advanced stage (FIGO IIb-IV). Prognosis and treatment are mainly dependent on this classification.

Early stage ovarian cancer has a 5 year survival of 75-100%, with the most important factors influencing survival being differentiation grade of the tumor and the completeness of staging [1]. During surgical staging, blind biopsy samples of predefined areas and biopsy samples of suspected lesions are obtained. The primary aim of the staging procedure is to determine whether there is occult metastatic disease not primarily visible by the naked eye. When no metastases are present, resection of the primary tumor is the treatment of choice and chemotherapy can be avoided [4]. When metastases are present, surgical resection is supplemented with chemotherapy. Optimal staging has been shown to improve survival in low stage ovarian cancer because it discriminates true early stage ovarian cancer from occult tumor spread, which results in more advanced disease [4].

However, most patients (around 75%) present with advanced disease [5]. The most important prognostic factor for overall survival in advanced stage disease is the amount of residual tumor after cytoreductive surgery [6–8]. Therefore complete cytoreduction, defined as no visible residual tumor left after surgery, or optimal cytoreduction, not consistently defined as a maximal diameter of residual tumor of 0-2 cm [5,9-11], is the goal for advanced stage ovarian cancer surgery.

In order to achieve either optimal staging or complete or optimal cytoreduction, visualization of tumor lesions is of great importance. With imaging modalities such as CT and MRI, pre-operative identification and localization of tumor lesions is reasonably achievable, however intraoperative visualization of tumor tissue can be challenging.

Near-infrared (NIR) fluorescence imaging is a promising technique to assist in the real time intraoperative identification of malignant lesions [12]. This technique makes use of NIR fluorescent light (700-900 nm) emitted by contrast agents after excitation by an imaging system able to detect this NIR fluorescent signal. NIR fluorescence is relatively easy and provides sufficient contrast due to high tissue penetration and low auto-fluorescence [13].

For tumor identification, it is essential that contrast agents accumulate in tumor tissue either actively or passively. Active accumulation can be achieved by targeting ligands that are over-expressed on tumor tissue. Van Dam *et al.* were the first to show tumor identification using a folate receptor alpha (FR α) targeting agent [14]. In their series they were able to identify tumor tissue in 3 patients with FR α positive ovarian cancer intraoperatively. However, these results have not yet been reproduced in other studies using a FR α or different targeting agents. A possible cause for this may be the expensive and time-consuming nature of the development of these tumor-specific agents. Therefore, it is of great importance to exploit clinically available contrast agents, such as indocyanine green (ICG) [15].

In vivo ICG binds to serum proteins and therefore behaves as a macromolecule in the circulation. It is known that macromolecules accumulate in tumor tissue due to increased vascular permeability and reduced drainage. This phenomenon is called the ‘enhanced permeability and retention’ (EPR) effect and has been observed in most solid tumors [16,17].

Clinical feasibility trials using this effect with ICG in breast cancer patients in a pre-operative diagnostic setting and in gastric cancer patients during endoscopic surgery showed that it was possible to distinguish tumor from surrounding tissue [18–23]. In addition, Kosaka *et al.* [24] detected small ovarian (1-2 mm in size) cancer implants using NIR fluorescent imaging after intravenous (IV) administration of ICG in a mouse model. Pathophysiological heterogeneity of solid tumors, for examples in size, presence of necrosis, or presence of vascular mediators may influence accumulation of macromolecules in tumor tissue [25,26]. It is therefore not clear if all preclinical results can be translated to the clinic.

The primary aim of the current study was to determine the feasibility of ovarian cancer metastases detection using ICG and NIR fluorescence imaging in a clinical setting. Secondary aim was to assess concordance between fluorescence signal and tumor status on histopathology. In addition, we sought to determine if a sufficient tumor-to-background ratio (TBR), based on the EPR effect, could be obtained to discriminate between malignant and non-malignant tissue.

MATERIAL AND METHODS

TRACER PREPARATION ● ICG was prepared in the operating room following preparation instructions of the institutional pharmacist. ICG (25 mg vials, purchased from Pulsion Medical Systems Munich, Germany) was diluted in 10 cc of sterile water for injection to yield a 2.5mg/ml (3.2 mM) stock solution.

CLINICAL TRIAL ● The study was approved by the Local Medical Ethics Committee of the Leiden University Medical Center (LUMC) on 27-06-2012 and was performed in accordance with the ethical standards of the Helsinki Declaration of 1975. Due to administrative error, trial registration was performed after the start of the study (date trial registration 11-09-2014; IS-RCTN16945066). The authors confirm that all ongoing and related trials for this intervention are registered. Because this study was set up as feasibility study, no formal sample size could be calculated. Determination of feasibility was expected after inclusion of 15 patients. In case apparent non-feasibility was observed, earlier termination of the study could be performed.

Eventually, ten patients presenting at the department of Gynaecological Oncology of LUMC between 14 October 2012 and 11 December 2013 suspected of either early stage ovarian cancer scheduled to undergo staging surgery or of advanced ovarian cancer scheduled to undergo cytoreductive surgery, were included. All surgical procedures were performed by laparotomy through a mid-line abdominal incision. All patients gave written informed consent. Exclusion criteria were pregnancy, severe renal insufficiency ($\text{GFR} < 55 \text{ mL/min/1.73 m}^2$), or an allergy to iodine or ICG.

In the operating theatre, after opening of the abdominal cavity, 20 mg of ICG was administered intravenously as single bolus by the anaesthesiologist. The average time between administration of ICG and imaging of the first lesion was 37 minutes. The last lesion was imaged on average 141 minutes post-administration of ICG. First the surgical field was searched for metastases visible by the naked eye. After resection of the primary tumor, uterus and ovaries, the Mini-FLARE™ was used to identify NIR fluorescent signals. When a fluorescent signal was observed, the operating surgeon performed a biopsy or resection of the fluorescent tissue, unless this would jeopardize patient health or success of surgery. In case of non-fluorescence, only macroscopically suspected lesions were resected. Resected specimens were marked as fluorescent or non-fluorescent and were routinely examined by a pathologist for the presence of malignant cells.

INTRAOPERATIVE NEAR-INFRARED FLUORESCENCE IMAGING ● Intraoperative imaging procedures were performed using the Mini-Fluorescence-Assisted Resection and Exploration (Mini-FLARE™) image-guided surgery system, as described earlier [27]. Briefly, the system consists of 2 wavelength isolated light sources: a ‘white’ light source, generating 26,600 lx of 400 to 650 nm light, and a ‘near-infrared’ light source, generating 1.08 mW/cm² of $\approx 760 \text{ nm}$ light. Color video and NIR fluorescence images are simultaneously acquired and displayed in real time using custom optics and software that separate the color video and NIR fluorescence images. A pseudo-colored (lime green) merged

image of the color video and NIR fluorescence images is also displayed. The imaging head is attached to a flexible gooseneck arm, which permits positioning of the imaging head at extreme angles virtually anywhere over the surgical field. For intraoperative use, the imaging head and imaging system pole stand are wrapped in a sterile shield and drape (Medical Technique Inc., Tucson, AZ).

STATISTICAL ANALYSIS ● For statistical analysis, SPSS statistical software package (Version 20.0, Chicago, IL) was used. TBRs were calculated by dividing the fluorescent signal of the tumor by fluorescent signal of surrounding tissue. Patient age was reported in median, standard deviation (SD), and range, and TBR was reported in mean, SD, and range. To compare patient characteristics, independent samples t-test and chi-square tests were used. To compare TBR and background signal between malignant and benign lesions, independent samples t-test was used. $P < 0.05$ was considered significant.

RESULTS

PATIENT CHARACTERISTICS ● Ten patients were included in this study. Figure 1 shows the CONSORT flow diagram for enrollment of patients. Median age was 58 years (range 42-74). Table 1 shows the patient characteristics. Seven patients underwent a staging procedure (70%), and 3 patients underwent a debulking procedure (30%). All staging and debulking procedures were open procedures.

Histological assessment by the pathologist of the resected lesions confirmed the following diagnosis: 6 patients were diagnosed with either ovarian cancer (5) or cancer of the fallopian tube (1), of which the following subtypes were diagnosed: serous (3), clear-cell (1), endometrioid (1), mixed (1); one patient was diagnosed with endometrial cancer (endometrioid type); and 3 patients had benign ovarian tumors. An overview of the final histological diagnoses and FIGO stage is given in Table 1.

METASTATIC LESIONS ● 2 out of the 6 patients with malignant disease of the ovary or fallopian tube, suffered from histologically proven metastatic disease (patients #4 and #5). A total of 8 metastatic lesions, confirmed by the pathologist, were found in these 2 patients (4 lesions in both #4 and #5). Lesions were localized at the pouch of Douglas (N=3), bladder peritoneum (N=2), para iliacal lymphnodes (N=2) and omentum (N=1).

NIR FLUORESCENCE IMAGING ● A total of 21 fluorescent lesions were identified. Fig. 2A shows an example of a clinically suspected lesion, which was NIR fluorescent. This lesion was anatomically located next to the right iliac vein. Fig.

2B shows the *ex vivo* images of the same NIR fluorescent lesion. This lesion was found histologically to be a metastasis of serous adenocarcinoma of the ovary. Fig. 3A and 3B show 2 NIR fluorescent lesions located in the greater omentum of the same patient as presented in Fig. 2, both containing serous adenocarcinoma. All 8 histologically proven malignant metastatic lesions were NIR fluorescent, so detection of metastatic lesions of ovarian cancer with ICG had a sensitivity of 100% in this study (Table 2). The specificity of NIR fluorescence imaging could not be calculated, since lesions that were neither clinically suspect nor fluorescent were not resected.

Clinically none of these 8 malignant and fluorescent lesions had a benign appearance, therefore the use of NIR fluorescence did not lead to the detection of otherwise undetected malignant lesions. In addition 13, on histological assessment, non-malignant lesions were also NIR fluorescent, resulting in a false-positives rate of 62% (Table 2). Of these lesions, 2 were clinically characterized as malignant, 6 as suspicious for malignancy, and 5 as not suspicious for malignancy. Fig. 4 shows an example of a NIR fluorescent lesion that was found to be histologically benign, thus a false-positive lesion. This particular lesion was a calcified lymph node. The localization, clinical appearance, pathology, and TBR for each false-positive lesion are listed in Table 3. Globally these false-positive lesions can be divided into two groups: normal tissue (N=10) and tissue with reactive changes (N=3).

Mean TBR of the fluorescent lesions was 2.0 ± 0.6 . There was no significant difference in TBR between histologically confirmed malignant and benign lesions (2.0 vs 2.0; $P=0.99$). Although the numbers are small, within the group of false-positive lesions a significant difference in TBR ($P = 0.003$) did exist between the histologically normal (1.7 ± 0.4) and reactive tissue (2.7 ± 0.2).

No adverse reactions regarding the use of ICG or NIR fluorescence imaging were seen.

DISCUSSION

In this feasibility study we investigated the use of NIR fluorescence imaging with the clinically available, non-targeted fluorescent tracer ICG in ovarian cancer patients who underwent a surgical staging procedure or cytoreductive surgery. Malignant metastatic lesions were present in 2 out of 10 patients only, but we found that 100% of these histologically proven malignant lesions were fluorescent using this technique. However, there was also a high false-positive rate of 62%.

In cytoreductive surgery, the goal is to remove as much tumor as possible, aiming for complete (no tumor visible after surgery) or leastwise optimal cytoreduction

(residual tumor maximized to 10 mm), because the amount of residual tumor is one of the most important prognostic factors for survival in advanced stage patients. Van Dam *et al.* [14] already showed that with the use of fluorescence imaging using a folate receptor alpha targeting probe (that is over-expressed in 90-95% of ovarian cancer patients), it was possible to identify more tumor deposits than by the naked eye. In our study we could not demonstrate such an added value of NIR fluorescence using the non-specific agent ICG, because all of the fluorescent, histologically malignant lesions were identified with the naked eye.

Treatment decisions in early stage ovarian cancer patients, for instance regarding adjuvant chemotherapy, are based on the presence of occult metastases and the extent of disease found during surgical staging procedures. If staging is not done properly, this could lead to under treatment of the patient. It has been shown that completeness of surgical staging is an independent prognostic factor for overall survival in early stage patients [4]. If the use of NIR fluorescence imaging leads to more accurate detection of (occult) ovarian cancer metastases, more patients could be optimally staged, possibly leading to better treatment decision making and overall survival. In none of the 3 patients with early stage ovarian or fallopian tube cancer who underwent a staging procedure in this study, metastatic disease was found. Therefore, no added value of NIR fluorescence imaging could be demonstrated in this study using ICG. A total of 13 fluorescent lesions were observed in the 7 patients undergoing surgical staging. On pathologic testing, all 13 lesions were benign and thus false-positive. To conclude, NIR fluorescence imaging could not demonstrate added value in staging procedures because no otherwise undetected metastatic disease could be found, but did result in the resection of non-malignant lesions. The intended effect of NIR fluorescence imaging with ICG was based on the EPR effect. Due to tumor-induced angiogenesis, solid tumors exhibit leaky and immature vessels. Because of this macromolecules are able to permeate through the vessels and into tumor tissue where they are retained due to impaired lymph drainage [16]. ICG is not a macromolecule, but behaves like one after binding to serum proteins. This, combined with the rapid clearance from the circulation, makes ICG a potentially good probe for NIR fluorescence imaging of solid tumors. This theory has proven to be true for gastric and breast cancer [18–23]. But it should be noted that all the trials in breast cancer patients were conducted in a pre-operative diagnostic setting and results may differ from intraoperative usage of ICG.

The large number of false-positives found in this study may be due to the lack of specificity of the EPR effect. It is known that the EPR effect is influenced by multiple factors, such as size, presence of necrosis, tumor type, presence of

vascular mediators such as bradykinin or prostaglandins, and location (including primary tumor vs metastatic lesion) of the lesion. Moreover, reactive processes and cancer have parallels in pathophysiological pathways and in vascular mediators. It has been shown that the EPR effect also occurs in inflammatory lesions [25,28,29]. This is in agreement with part of the false-positive lesions identified in the current study. Especially since the EPR effect in reactive tissue is more prominently present hours after injection (coinciding with our imaging window) versus days to weeks after injection in tumor tissue [26].

Several studies describe the intraoperative identification of solid tumors using clinically available, non-targeted fluorescent probes as ICG and methylene blue (MB). These studies report higher TBRs than found in the current study. For example, imaging of colorectal liver metastases using ICG (TBR 7.0) [30], parathyroid adenomas using MB (6.1) [31] and breast cancer using MB (2.4) [32] all showed higher TBRs than the observed 2.0. A possible explanation for this is that in these studies other mechanisms causing accumulation of the fluorescent probe in or around tumor tissue played a role in addition to the possible EPR effect. The EPR effect on its own may not be sufficient in providing high enough TBRs for tumor imaging. Finally, the average TBR of false-positive, benign lesions was just as high as the average TBR of true positive malignant lesions, while the average TBR of reactive benign lesions was even higher than that of malignant lesions. This lack of discriminative power makes NIR fluorescence imaging based on the EPR effect unsuitable for further clinical implementation in ovarian cancer.

CONCLUSIONS

This is the first clinical trial demonstrating the feasibility of intraoperative detection of ovarian cancer metastases using NIR fluorescence imaging and ICG. However, a high number of false-positive lesions that could be explained by the lack of specificity of the EPR effect was found. Moreover, no distinction between malignant, reactive, or benign tissue based on TBR of the different lesions could be made. Therefore, the use of ICG, even when optimized, is not satisfactory for intraoperative NIR fluorescence imaging of ovarian cancer metastases and the need for more tumor-specific targeting agents remains. These results should be confirmed in other solid tumors where intraoperative NIR fluorescence imaging based on the EPR effect is being contemplated.

REFERENCES

- 1 Oncoline, www.oncoline.nl/epithelial-ovariumcarcinoom Accessed 28th August 2014.
- 2 Ferlay J, Shin HR, Bray F, Forman D, Mathers C, Parkin DM (2010) Estimates of worldwide burden of cancer in 2008: GLOBOCAN 2008. *Int J Cancer* 127: 2893-2917. 10.1002/ijc.25516 [doi].
- 3 Jemal A, Bray F, Center MM, Ferlay J, Ward E, Forman D (2011) Global cancer statistics. *CA Cancer J Clin* 61: 69-90. caac.20107 [pii];10.3322/caac.20107 [doi].
- 4 Trimbos B, Timmers P, Pecorelli S, Coens C, Ven K, van der Burg M, Casado A (2010) Surgical staging and treatment of early ovarian cancer: long-term analysis from a randomized trial. *J Natl Cancer Inst* 102: 982-987. djq149 [pii];10.1093/jnci/djq149 [doi].
- 5 Fader AN, Rose PG (2007) Role of surgery in ovarian carcinoma. *J Clin Oncol* 25: 2873-2883. 25/20/2873 [pii];10.1200/JCO.2007.11.0932 [doi].
- 6 Bristow RE, Tomacruz RS, Armstrong DK, Trimble EL, Montz FJ (2002) Survival effect of maximal cytoreductive surgery for advanced ovarian carcinoma during the platinum era: a meta-analysis. *J Clin Oncol* 20: 1248-1259.
- 7 Hoskins WJ, McGuire WP, Brady MF, Homesley HD, Creasman WT, Berman M, Ball H, Berek JS (1994) The effect of diameter of largest residual disease on survival after primary cytoreductive surgery in patients with suboptimal residual epithelial ovarian carcinoma. *Am J Obstet Gynecol* 170: 974-979. S0002937894000906 [pii].
- 8 Griffiths CT (1975) Surgical resection of tumor bulk in the primary treatment of ovarian carcinoma. *Natl Cancer Inst Monogr* 42: 101-104.
- 9 Colombo N, Van GT, Parma G, Amant F, Gatta G, Sessa C, Vergote I (2006) Ovarian cancer. *Crit Rev Oncol Hematol* 60: 159-179. S1040-8428(06)00064-3 [pii];10.1016/j.critrevonc.2006.03.004 [doi].
- 10 Vergote I, De W, I, Tjalma W, Van GM, Decloedt J, van DP (1998) Neoadjuvant chemotherapy or primary debulking surgery in advanced ovarian carcinoma: a retrospective analysis of 285 patients. *Gynecol Oncol* 71: 431-436. S0090-8258(98)95213-1 [pii];10.1006/gyno.1998.5213 [doi].
- 11 Vergote I, Trimbos BJ (2003) Treatment of patients with early epithelial ovarian cancer. *Curr Opin Oncol* 15: 452-455.
- 12 Vahrmeijer AL, Hutteman M, van der Vorst JR, van de Velde CJ, Frangioni JV (2013) Image-guided cancer surgery using near-infrared fluorescence. *Nat Rev Clin Oncol*. nrclinonc.2013.123 [pii];10.1038/nrclinonc.2013.123 [doi].
- 13 Frangioni JV (2003) In vivo near-infrared fluorescence imaging. *Curr Opin Chem Biol* 7: 626-634. S1367593103001091 [pii].
- 14 van Dam GM, Crane LM, Themelis G, Harlaar NJ, Pleijhuis RG, Kelder W, Sarantopoulos A, de Jong JS, Arts HJ, Van Der Zee AG, Bart J, low PS, Ntziachristos V (2011) Intraoperative tumor-specific fluorescence imaging in ovarian cancer by folate receptor-alpha targeting: first in-human results. *Nat Med* 17: 1315-9.
- 15 Schaafsma BE, Mieog JS, Hutteman M, van der Vorst JR, Kuppen PJ, Lowik CW, Frangioni JV, van de Velde CJ, Vahrmeijer AL (2011) The clinical use of indocyanine green as a near-infrared fluorescent contrast agent for image-guided oncologic surgery. *J Surg Oncol* 104: 323-332. 10.1002/jso.21943 [doi].
- 16 Maeda H, Wu J, Sawa T, Matsumura Y, Hori K (2000) Tumor vascular permeability and the EPR effect in macromolecular therapeutics: a review. *J Control Release* 65: 271-284. S0168-3659(99)00248-5 [pii].
- 17 Matsumura Y, Maeda H (1986) A new concept for macromolecular therapeutics in cancer chemotherapy: mechanism of tumor tropic accumulation of proteins and the antitumor agent smancs. *Cancer Res* 46: 6387-6392.
- 18 Alacam B, Yazici B, Intes X, Nioka S, Chance B (2008) Pharmacokinetic-rate images of indocyanine green for breast tumors using near-infrared optical methods. *Phys Med Biol* 53: 837-859. S0031-9155(08)62576-2 [pii];10.1088/0031-9155/53/4/002 [doi].
- 19 Hagen A, Grosenick D, Macdonald R, Rinneberg H, Burock S, Warnick P, Poellinger A, Schlag PM (2009) Late-fluorescence mammography

assesses tumor capillary permeability and differentiates malignant from benign lesions. *Opt Express* 17: 17016-17033. 185849 [pii].

20 Kimura T, Muguruma N, Ito S, Okamura S, Imoto Y, Miyamoto H, Kaji M, Kudo E (2007) Infrared fluorescence endoscopy for the diagnosis of superficial gastric tumors. *Gastrointest Endosc* 66: 37-43. S0016-5107(07)00022-3 [pii];10.1016/j.gie.2007.01.009 [doi].

21 Mataka N, Nagao S, Kawaguchi A, Matsuzaki K, Miyazaki J, Kitagawa Y, Nakajima H, Tsuzuki Y, Itoh K, Niwa H, Miura S (2003) Clinical usefulness of a new infrared videoendoscope system for diagnosis of early stage gastric cancer. *Gastrointest Endosc* 57: 336-342. 10.1067/mge.2003.133 [doi];S0016510703501766 [pii].

22 Ntziachristos V, Yodh AG, Schnall M, Chance B (2000) Concurrent MRI and diffuse optical tomography of breast after indocyanine green enhancement. *Proc Natl Acad Sci U S A* 97: 2767-2772. 10.1073/pnas.040570597 [doi];040570597 [pii].

23 Poellinger A, Burock S, Grosenick D, Hagen A, Ludemann L, Diekmann F, Engelken F, Macdonald R, Rinneberg H, Schlag PM (2011) Breast cancer: early- and late-fluorescence near-infrared imaging with indocyanine green—a preliminary study. *Radiology* 258: 409-416. radiol.10100258 [pii];10.1148/radiol.10100258 [doi].

24 Kosaka N, Mitsunaga M, Longmire MR, Choyke PL, Kobayashi H (2011) Near infrared fluorescence-guided real-time endoscopic detection of peritoneal ovarian cancer nodules using intravenously injected indocyanine green. *Int J Cancer* 129: 1671-1677. 10.1002/ijc.26113 [doi].

25 Fang J, Nakamura H, Maeda H (2011) The EPR effect: Unique features of tumor blood vessels for drug delivery, factors involved, and limitations and augmentation of the effect. *Adv Drug Deliv Rev* 63: 136-151. S0169-409X(10)00090-6 [pii];10.1016/j.addr.2010.04.009 [doi].

26 Maeda H (2012) Vascular permeability in cancer and infection as related to macromolecular drug delivery, with emphasis on the EPR effect for tumor-selective drug targeting. *Proc Jpn Acad Ser B Phys Biol Sci* 88: 53-71. JST.JSTAGE/pjab/88.53 [pii].

27 Mieog JS, Troyan SL, Hutteman M, Donohue KJ, van der Vorst JR, Stockdale A, Liefers GJ, Choi HS, Gibbs-Strauss SL, Putter H, Gioux S, Kuppen PJ, Ashitate Y, Löwik CW, Smit VT, Oketokoun R, Ngo LH, van de Velde CJ, Frangioni JV, Vahrmeijer AL (2011) Towards Optimization of Imaging System and Lymphatic Tracer for Near-Infrared Fluorescent Sentinel Lymph Node Mapping in Breast Cancer. *Ann Surg Oncol* 18: 2483-2491.

28 Maeda H, Fang J, Inutsuka T, Kitamoto Y (2003) Vascular permeability enhancement in solid tumor: various factors, mechanisms involved and its implications. *Int Immunopharmacol* 3: 319-328. S1567-5769(02)00271-0 [pii];10.1016/S1567-5769(02)00271-0 [doi].

29 Maeda H (2013) The link between infection and cancer: tumor vasculature, free radicals, and drug delivery to tumors via the EPR effect. *Cancer Sci* 104: 779-789. 10.1111/cas.12152 [doi].

30 van der Vorst JR, Schaafsma BE, Hutteman M, Verbeek FP, Liefers GJ, Hartgrink HH, Smit VT, Lowik CW, van de Velde CJ, Frangioni JV, Vahrmeijer AL (2013) Near-infrared fluorescence-guided resection of colorectal liver metastases. *Cancer* 119: 3411-3418. 10.1002/cncr.28203 [doi].

31 van der Vorst JR, Schaafsma BE, Verbeek FP, Swijnenburg RJ, Tummers QR, Hutteman M, Hamming JF, Kievit J, Frangioni JV, van de Velde CJ, Vahrmeijer AL (2013) Intraoperative near-infrared fluorescence imaging of parathyroid adenomas with use of low-dose methylene blue. *Head Neck* . 10.1002/hed.23384 [doi].

32 Tummers QR, Verbeek FP, Schaafsma BE, Boonstra MC, van der Vorst JR, Liefers GJ, van de Velde CJ, Frangioni JV, Vahrmeijer AL (2014) Real-time intraoperative detection of breast cancer using near-infrared fluorescence imaging and Methylene Blue. *Eur J Surg Oncol* 40: 850-858. S0748-7983(14)00303-5 [pii];10.1016/j.ejso.2014.02.225 [doi].

TABLE 1 PATIENT AND TUMOR CHARACTERISTICS

Study number	Age	Origin	Histologic type	FIGO stage	Surgical procedure	Metastases found during procedure
1	58	Ovary	Clearcell	1a	Staging	No
2	69	Benign disease	N.A.	N.A.	Staging	No
3	74	Benign disease	N.A.	N.A.	Staging	No
4	73	Ovary	Serous	3c	Cytoreduction	Yes
5	42	Ovary	Serous	2c	Cytoreduction	Yes
6	50	Endometrium	Endometrioid	3a	Staging	No*
7	73	Benign disease	N.A.	N.A.	Staging	No
8	58	Ovary	Endometrioid	1a	Staging	No
9	54	Fallopian Tube	Serous	1a	Staging	No
10	50	Ovary	Serous, Mucinous	2c	Cytoreduction	No**

* Staging was performed because an ovarian metastasis was detected at pathology after an earlier polypectomy procedure

** No biopsies were taken due to the presence of adhesions and tumor spill during the procedure, therefore defining the tumor stage as 11c with a concomitant indication for postoperative chemotherapy

TABLE 2 CHARACTERISTICS LESIONS FOUND WITH ICG NIR FLUORESCENCE IMAGING

	Ovarian / tubal carcinoma N=6		Endometrium carcinoma N=1		Benign N=3		Total N=10	
	Metastatic disease N=2	Non meta-static disease N=4						
NIR fluorescent lesions	8	9	2		2		21	
Concordance histopathology	N	%	N	%	N	%	N	%
True-positive	8	100	0	0	0	0	8	38
False-positive	0	0	9	100	2	100	13	62

TABLE 3 OVERVIEW OF FALSE-POSITIVE LESIONS DETECTED USING ICG

Patient	Localisation	Clinically suspect for malignancy	Pathology	TBR
<i>Tissue with reactive changes</i>				
2	Mesenterium small bowel	Uncertain	Fibrosis and hemorrhages	2.7
3	Mesenterium ileum	Yes	Calcified lymph node	2.9*
6	Ligamentum infundibulum pelvicum left	No	Mature fat and connective tissue, vascular structures, inflammatory infiltrate with giant cell clean-up reaction	2.4
<i>Healthy tissue</i>				
1	Omentum	Yes	Fat and connective tissue	2.1
6	Omentum	Uncertain	Muscle	1.3
8	Peritoneum right	Uncertain	Connective tissue and some tubular structures	1.6
8	Iliaca interna right	Uncertain	Lymph node	1.7
8	Omentum	Uncertain	Muscle	1.6
9	Bladder peritoneum	No	Fat and connective tissue	1.3
9	Rectosigmoid	Uncertain	Fat and connective tissue	1.3
9	Superficial pelvic right	No	Lymph node	1.8
9	Superficial pelvic left	No	Lymph node	2.6
9	High paracolic right	No	Fat and connective tissue	! **

* Image shown in Figure 4

** TBR could not be calculated

FIGURE 1 CONSORT FLOW DIAGRAM FOR PATIENT ENROLMENT



CONSORT 2010 Flow Diagram

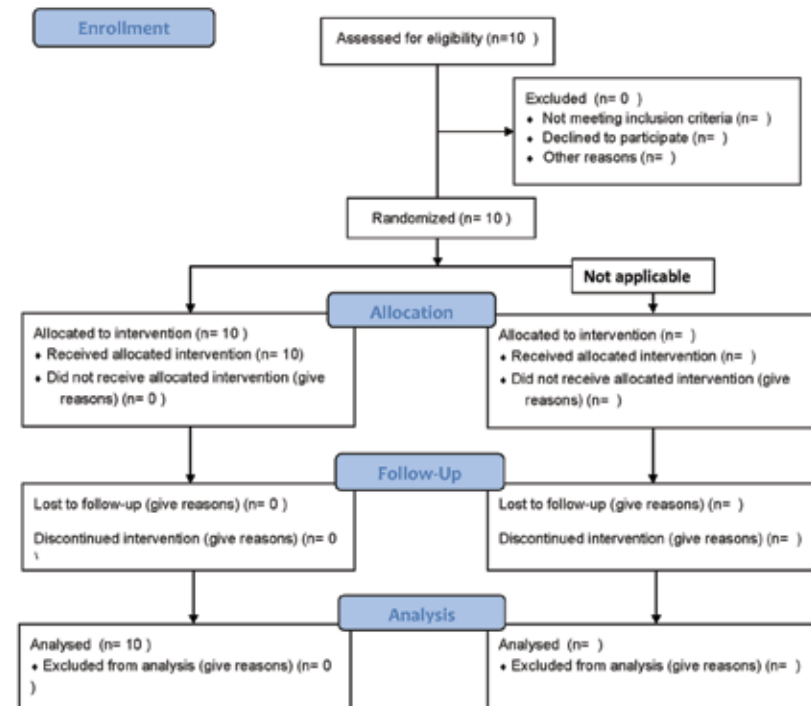
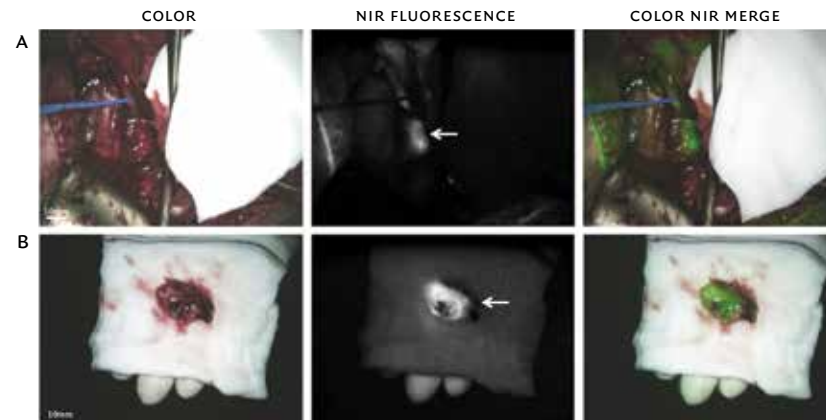
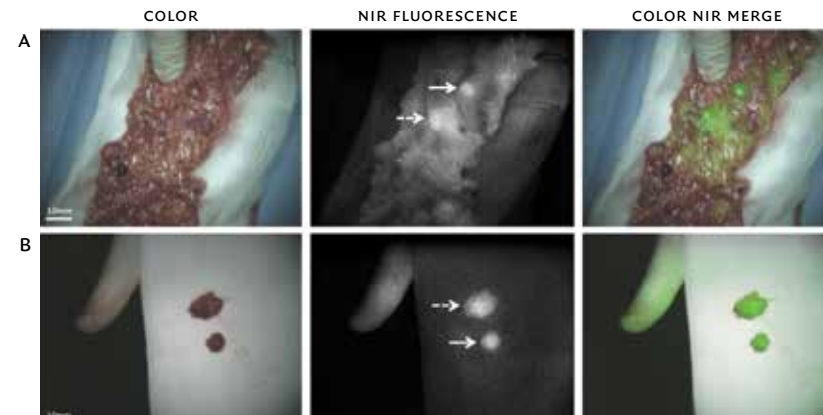


FIGURE 2 IDENTIFICATION OF OVARIAN CANCER METASTASES USING NIR FLUORESCENCE IMAGING



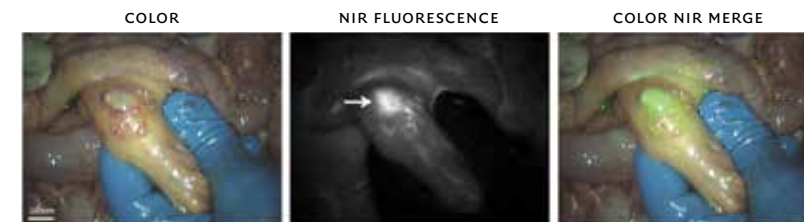
A. Identification of ovarian cancer metastases located in a lymph node next to the right iliac vein (arrow) using NIR fluorescence imaging. The lesion was found histologically to be a metastasis of serous adenocarcinoma
 B. Ex vivo imaging of the same ovarian cancer metastases located in a lymph node next to the right iliac vein (arrow).

FIGURE 3 IDENTIFICATION OF OVARIAN CANCER OMENTAL METASTASES USING NIR FLUORESCENCE IMAGING



A. Identification of 2 ovarian cancer metastases located in the greater omentum (arrow and dashed arrow) using NIR fluorescence imaging.
 B. Imaging of the same two NIR fluorescent lesions removed from the omentum (arrow and dashed arrow). Both lesions were found histologically to be metastases of serous adenocarcinoma.

FIGURE 4 IDENTIFICATION OF OVARIAN CANCER OMENTAL METASTASES USING NIR FLUORESCENCE IMAGING



Identification of a NIR fluorescent lesion located in the mesentery of the intestine. The lesion was classified clinically as a metastasis but was found histologically to be a calcified lymph node.

Chapter 3

In search for optimal targets for intraoperative fluorescence imaging of peritoneal metastasis from colorectal cancer

Biomark Cancer. 2017 Aug 28

CHARLOTTE HOOGSTINS, BENJAMIN WEIXLER, LEONORA BOOGERD, DIEDERIK HÖPPENER, HENDRICA PREVОО, CORNELIS SIER, JACOBUS BURGER, CORNELIS VERHOEF, SHADVHI BHAIROSINGH, ARANTZA FARINA SARASQUETA, JACOBUS BURGГRAAF, ALEXANDER VAHRMEIJER

ABSTRACT

Peritoneal metastasis (PM) occurs in about 10% of patients with colorectal cancer (CRC). Fluorescence imaging can enhance contrast between cancerous and benign tissue, enabling the surgeon to clearly visualize PM during cytoreductive surgery. This study assessed the suitability of different biomarkers as potential targets for tumor-targeted imaging of PM of CRC. Tissue samples from primary tumor and PM from patients with CRC were obtained from the pathology archives and immunohistochemical (IHC) stainings were performed. Overexpression of the epithelial cell adhesion molecule (EPCAM) and carcino-embryonic antigen (CEA) was seen in 100% of PM samples and the expression was strong in >70% of samples. Tyrosine-kinase Met (C-MET) and folate receptor-alpha (FRO) overexpression was seen in 20% of PM samples. For successful application of tumor-targeted intraoperative fluorescence imaging of PM, biomarkers need to be identified. We demonstrated that both EPCAM and CEA are suitable targets for fluorescence imaging of PM in patients with CRC.

INTRODUCTION

Peritoneal metastasis (PM) is frequently seen in patients with colorectal cancer (CRC). Approximately 5% of patients already have PM at the time of diagnosis and another 5% will develop PM during the course of the disease [1]. Until the 1990s PM was considered incurable and treatment consisted of palliative chemotherapy only. In 1993 Sugarbaker revolutionized the management of PM with the introduction of cytoreductive surgery (CRS) followed by hyperthermic intraperitoneal chemotherapy (HIPEC) [2]. During CRS all macroscopic tumor lesions are removed from the peritoneal cavity. Hereafter, a high dose of heated chemotherapy is administered intraperitoneally, hereby maximizing the local effect while systemic exposure is kept to a minimum. Preoperative imaging modalities, including CT, have limited value in the detection of PM [3,4]. Due to the small size and superficial nature of PM lesions, extent of the disease is often underestimated by these modalities [3,4]. As a result, surgical exploration of the abdomen is performed prior to CRS and the peritoneal cancer index (PCI) is assessed during the exploration.

Although morbidity (36%) and mortality (8%) associated with this aggressive treatment is high, patients undergoing CRS and HIPEC have a significantly improved overall survival (22.3 months) compared to patients undergoing standard treatment consisting of only palliative chemotherapy (12.6 months) [5-7]. Survival benefits decrease when a high number of abdominal regions (6 or 7) are affected by PM and when the PCI is >17 [5-7]. Therefore, accurate assessment of the extent of the disease and careful patient selection is of utmost importance. Another prognostic predictor is the completeness of CRS, survival percentage is higher in patients with a macroscopic complete resection compared to patients with macroscopic residual disease [6,8,9]. Thus, clear tumor visualization is pivotal for optimal staging and macroscopically radical resection; as Sugarbaker himself stressed: 'It's what the surgeon doesn't see that kills the patient' [10]. At present, surgeons must rely on inspection with the naked eye and palpation for intraoperative tumor detection.

Near-infrared (NIR, 700-900 nm) fluorescence imaging is a relatively novel imaging modality. This technique is eminently suitable for real-time intraoperative application as the NIR fluorescent signal can be acquired within milliseconds. Moreover NIR fluorescent light is invisible to the human eye and therefore does not permanently alter the surgical field, and can travel up to 1 cm through tissue allowing signal detection below the tissue surface [11-13]. NIR fluorescence imaging can make use of endogenous tissue properties, but

more commonly an exogenous fluorescent contrast agent is administered intravenously. These fluorescent contrast agents can be coupled with targeting moieties that specifically bind to a target, i.e. tumor protein. Using an open or laparoscopic NIR fluorescence imaging device, the target can be detected by the fluorescent signal arising from the contrast agent [14]. The enhanced contrast between cancerous and benign tissue will enable the surgeon to clearly visualize tumor lesions in real-time during surgery. In the case of CRS this will greatly aid in the initial assessment of PM extent, but will also potentially allow an increase of macroscopically radical resections. The first clinical trials with tumor-specific fluorescent contrast agents report successful intraoperative fluorescence imaging of malignant glioma, head and neck, ovarian and lung cancer [15-19]. Studies with ovarian cancer patients are especially interesting, as in this cancer type PM is also frequently seen. Both studies demonstrated that it was possible to visualize PM in ovarian cancer using a folate receptor targeting fluorescent agent [16,19]. Fluorescence imaging led to the detection and subsequent resection of additional tumor lesions that were otherwise not detected.

These results encourage investigation of fluorescence imaging in PM of CRC. Selection of tumor-targeting fluorescent contrast agents suitable for imaging of PM of CRC requires identification of biomarkers with overexpression on PM of CRC. Immunohistochemical (IHC) staining of tumor tissue is a validated and commonly used technique to assess the degree of expression levels of specific biomarkers. The aim of this study is to assess the suitability of various biomarkers for tumor-targeted fluorescence imaging of PM of CRC using IHC. Upregulation of numerous biomarkers in colorectal tumor tissues is described in the literature [20]. Our selection of biomarkers is based on the availability of fluorescence agents and the Target Selection Criteria (TASC)-scoring system for biomarkers for imaging purposes [21]. When expression of a biomarker on a PM is concordant with expression on the primary tumor, staining of the primary tumor could predict PM expression and aid in patient selection. Therefore we also aimed to determine the concordance between biomarker expression on the primary tumor and the corresponding PM.

METHODS

SAMPLE SELECTION ● Tissue samples of all patients diagnosed with CRC who underwent CRS and HIPEC procedure in Erasmus Medical Center between March 2014 and September 2015 (N=36) were reviewed. Formalin-fixed, paraffin-embedded (FFPE) tissue blocks were obtained from the pathology

archives of the Erasmus Medical Center and the primary care facility if the primary tumor was previously resected elsewhere. This study was approved by the Institutional Ethics Committee of the Leiden University Medical Center (LUMC). All samples were handled anonymously and used in accordance with the ethical standards of the local ethics committee and with national Dutch guidelines ('Code for Proper Secondary Use of Human Tissues', Dutch Federation of Medical Scientific Societies).

IMMUNOHISTOCHEMISTRY ● Sections of 4 μm were sliced, collected on Starfrost adhesive slides and dried overnight. Sections were deparaffinized in a series of xylene and rehydrated in decreasing concentrations of ethanol. After rinsing in distilled water slides were incubated in 0.3% H_2O_2 for 20 minutes to block endogenous peroxidase, followed by a washing step in water. Antigen retrieval was performed in EnVision FLEX Target Retrieval Solution, Low pH (DAKO PT Link) for 10 minutes at 95°C.

Antibodies used for IHC staining of carcinoembryonic antigen (CEA), tyrosine-protein kinase Met (C-Met), epithelial cell adhesion molecule (EPCAM) and folate receptor alpha (FR α) were: monoclonal mouse anti-CEACAM5, Clone C1-P83-1 (Santa Cruz sc-23928, 0.5 $\mu\text{g}/\text{ml}$), polyclonal rabbit anti-cMet (Santa Cruz sc-10, 0.5 $\mu\text{g}/\text{ml}$), monoclonal anti-EPCAM, clone MOC31 (Acris Antibodies DM2014A, 0.05 $\mu\text{g}/\text{ml}$) and monoclonal mouse anti-FR α , clone 26B3.F2 (IHC Assay Kit, Biocare Medical 4006K). FR α was staining following manufacturer's instructions. Normal lung tissue was included as positive control for FR α staining, for the other three biomarkers an internal positive control was present. For CEA, C-Met and EPCAM staining, primary antibodies were incubated over night at room temperature, followed by three washes with PBS and incubation with Envision anti-mouse-HRP or Envision anti-rabbit-HRP (DAKO) for 30 minutes at room temperature. After another three washes, antibody binding was visualized using 3,3'-diaminobenzidine for five minutes. Sections were rinsed in deionized water, counterstained with hematoxylin, dehydrated and mounted with pertex. Next to immunohistochemistry, a hematoxylin and eosin (H&E) staining was performed for routine pathological evaluation. All slides were scanned using the Ultra Fast Scanner (Philips, Eindhoven, the Netherlands).

SCORING METHOD ● Biomarker expression for the different biomarkers was assessed in both primary tumor and PM tissue by using an intensity scoring method with a scale ranging from 0 to 3+ (0 for absence of staining; 1+ for weak staining; 2+ for moderate staining; and 3+ for strong staining). This score

was applied to the epithelial and stromal staining. Representative images of these intensity scores are depicted in Figure 1. When various tumor cells within a tumor exhibited different intensity scores (e.g. both 1+ and 2+) the highest score was noted. In addition to the intensity also the percentage of positive staining tumor cells was assessed. Percentages were recorded in quartiles (25%, 50%, 75% and 100%). For the purpose of this study the intensity scores and percentages were combined in a final expression score, calculated using the following formula: Expression score = (Intensity score - 1)*4 + (Percentage of observed expression / 25). This gives a linear score of 0 - 12, with a score of 0 corresponding to absent expression and a score of 12 corresponding to strong (3+) intensity expression in 100% of tumor cells.²² The tumor was considered positive and thus the biomarker suitable for intraoperative fluorescence imaging when the expression score of tumor cells or tumor stroma was ≥ 5 . Strong overexpression was defined as a combined score ≥ 9 , indicating an expression pattern highly suitable for tumor imaging.

Concordance was established when the expression score of the primary tumor matched the expression score of the PM. Evaluation of the IHC staining was performed blinded and independently by two observers. In case of disagreements the staining was discussed to reach consensus amongst the observers. If still no agreement was reached, the relevant staining was evaluated with a third observer, specialized in CRC pathology.

STATISTICAL ANALYSIS ● All statistical analyses were performed using the Statistical Package for the Social Sciences (SPSS® version 23, IBM, Chicago IL, USA) and GraphPad Prism 6 (GraphPad Software Inc., La Jolla, CA, USA). Statistical evaluation of inter-rater reliability was not performed. The correlation between primary tumor and PM was calculated using the Spearman's correlation coefficient (ρ). Perfect correlation was considered as Spearman's correlation coefficient of 1 or -1. Spearman's correlation coefficient values close to or < 0 were considered as poor correlation. A p-value of < 0.05 was considered statistically significant.

RESULTS

Incomplete sets of primary tumor and PM, as a result of inability to obtain a primary tumor sample from another hospital (N=5) or absence of PM in pathology samples (N=8), were discarded from further analysis. A total of 23 sets were included in the staining protocol. During the staining procedure, the sets

containing an empty or broken FFPE block (N=3) were excluded, resulting in a total of 20 sets for the final analysis. Histology of primary tumors was mostly adenocarcinoma (16/20) and mucinous adenocarcinoma in the remaining samples (4/20). For the primary tumor, 20 samples (100%) demonstrated expression of both EpcAM and CEA. Strong expression was seen in almost all cases (95%) for EpcAM and to a lesser extent for CEA (70%). C-Met and FR α expression was positive in a smaller part of primary tumor samples, 15% and 30% respectively. Strong expression was not seen for C-Met and only in 1 sample (5%) for FR α . Stromal expression was only seen in samples stained for CEA, with a positive expression in about half of the samples (45%). For EpcAM and FR α stromal staining was absent and for C-Met stromal staining was seen in most samples (75%) but expression was too low (<5) to qualify the staining as positive (Table 1).

For the PM, 20 samples (100%) demonstrated epithelial expression of EpcAM and CEA staining. The staining was strong in 90% of samples for EpcAM and in 70% of samples for CEA. These percentages are similar to the percentages of the primary tumor. Stromal staining was not seen for EpcAM, however stromal CEA expression was again noted in 45% of samples. Five PM samples had a positive expression for C-Met (25%), including 4 tissues with positive epithelial expression and 1 tissue with stromal expression. The FR α expression was slightly lower, 20%, and limited to epithelial expression. Strong C-Met or FR α expression was not seen in any of the PM samples (Table 1).

Concordance between expression scores of primary tumor and PM was assessed using the Spearman's correlation-coefficient. A significant moderate to strong correlation between primary tumor and PM was seen for the EpcAM (0.688) and FR α (0.803) epithelial expression score and for the C-Met (0.461) stromal expression score. For all other scores, correlation between primary tumor and PM was weak (<0.39). When comparing both the mean tumor and PM score (Table 2), a clear compatibility is seen between the primary tumor and PM expression score.

DISCUSSION

Clear intraoperative tumor visualization using NIR fluorescence imaging could improve both diagnosis and treatment of patients with PM of CRC. NIR fluorescence imaging can be performed during open as well as laparoscopic surgery and can be applied to various oncologic surgeries, making the technique suitable for all centers performing colorectal surgeries. Potential benefits of fluorescence imaging are already reported in patients with PM from ovarian cancer

using an ovarian cancer specific agent [16,19]. Extrapolation of these results to patients with CRC requires identification of tumor targets with overexpression on PM of CRC.

Upregulation of numerous biomarkers in CRC is described in the literature [20]. Suitability of a certain biomarker for fluorescence imaging is not only determined by its upregulation but also influenced by various other factors. In general, an optimal target exhibits strong and homogenous overexpression in a large majority of tumors. In an attempt to objectively assess the suitability of a potential biomarker for tumor targeting, Oosten *et al* proposed the use of the TASC-scoring system [21]. In addition to the previously mentioned factors this system gives scores for extracellular localization of the biomarker, previous use of the biomarker in in-vivo imaging studies, enzymatic activity in or around tumor tissue (which will allow the use of activatable agents) and internalization of the agent. This adds up to a maximum score of 22 points. A biomarker with a score ≥ 18 should be considered as a potential target. When applying this score to biomarkers for CRC, 6 potential targets, including CEA, EpcAM and FR α , for tumor-targeted imaging are identified [23]. The clinical evaluation and use of these potential targets is entirely depending on the availability of imaging agents for these targets. FR α and C-Met targeting clinical agents have been studied in small groups of patients and properties of these agents were found to be suitable for fluorescence imaging [16,19,24]. A fluorescent agent targeting EpcAM is expected to reach the clinic by the end of this year and a fluorescent labelled anti-CEA antibody is currently studied in patients suffering from CRC (NTR5673). In the present study we evaluated the most eligible targets for clinical imaging of CRC. The most frequently expressed biomarkers on PM were EpcAM and CEA. Positive epithelial expression for these biomarkers was seen in all samples and the majority of samples showed strong expression. Expression of C-Met and FR α was seen in only 1 out of 5 PM samples and expression was never strong. Therefore from the evaluated markers, EpcAM seems the most favorable target for intraoperative fluorescence imaging of PM. For CEA, a similar expression pattern is found, although a strong expression is seen less frequent compared to EpcAM. A potential advantage of CEA as imaging target is that apart from expression on the epithelium, CEA is also expressed in the stroma surrounding tumor cells. Stroma is often abundantly present in aggressive tumors and is located at the border, at the invasive front of the tumor, a location particularly suited for NIR fluorescence imaging [25]. From our data C-Met and FR α seem less favorable targets, as expression was not consistently seen in PM and the level of expression was never strong. FR α expression of the primary

tumor did show a significant and strong correlation with the expression of the PM, therefore staining of the primary tumor to predict presence of positive expression in the PM is feasible. Weak correlation coefficients between expression of the primary tumor and PM were seen for most other biomarkers, this is likely a consequence of the small variability between scores, which causes a high likelihood that the same scores are given based on chance. We expect tumor heterogeneity will have an impact on this technique. However, due to the retrospective nature of this study our sample selection was limited to 1 PM sample per patient, which precludes assessment of the effect of tumor heterogeneity.

The biomarkers evaluated in this study are suitable for tumor-targeted fluorescence imaging. Two recently published studies describe fluorescence-guided surgery of PM in CRC patients using the non-targeted dye Indocyanine Green (ICG) [26,27]. As ICG does not specifically target tumor biomarkers, the use of ICG for fluorescence imaging is based on processes that cause aspecific accumulation of the agent in or around the tumor. *Liberale et al* [26] hypothesize that if it is possible to visualize small liver tumors or colorectal liver metastases using ICG, it will also be possible to visualize PM from CRC. However, retention of ICG around liver tumors is largely a consequence of the hepatic clearance of ICG [28,29]. As this process does not apply to PM, accumulation of ICG in PM was likely the result of the increased vascular permeability and reduced drainage in tumor tissue following tumor-induced angiogenesis (the enhanced permeability and retention [EPR] effect) [30,31]. It is very likely that the lack of specificity of the EPR effect precludes successful application for intraoperative imaging.³² Moreover detection of small PM lesions (<2 mm) based on the EPR effect is most likely not possible as these lesions are still avascular eg before the angiogenic switch [33]. Therefore the need for tumor-specific fluorescent agents remains.

We are aware that our study contains several limitations. First, selection of the biomarkers was not fully comprehensive because the selection was also based on availability of fluorescence imaging agents for these biomarkers. Second, the analyzed sample size is relatively small. Nevertheless, the study represents the largest cohort of CRC patients investigated for fluorescence imaging of PM. And third, IHC staining was not performed on adjacent normal colon tissue. For successful image-guided surgery it is essential that the fluorescence ratio between tumor tissue and healthy background tissue (tumor-to-background ratio, TBR) is greater than 2 [11]. The fluorescence ratio is determined by various factors including affinity of the fluorescent agent for the biomarker, clearance from normal tissues and upregulation of biomarker on cancer cells. Concerning upregulation of the biomarker a tumor-to-normal (T/N)

ratio of greater than 10 is generally considered sufficient [34]. Although not specifically addressed in the current study, expression of EPCAM, CEA, C-Met and FR α on normal tissue is well described in the literature and all mentioned biomarkers apart from C-Met have a T/N ratio >10. For C-Met variable T/N ratios were reported, ranging from 0.2 to 50.^{35,36} Equally important is expression on abnormal, non-malignant tissue, i.e. scar tissue or inflamed tissue. This should be assessed, as absent or low expression is warranted to prevent false positive fluorescence. Although false positive fluorescence is undesirable it is not unsurmountable as long as the sensitivity is high, e.g. missing malignant lesions has worse implications than resection of non-malignant lesions. Lastly, the effect of various neoadjuvant treatments on biomarker upregulation in remaining vital tumor cells should be studied.

CONCLUSION

In conclusion, this study provides valuable insights in the optimal target for intraoperative fluorescence imaging of PM from CRC. Positive and generally strong expression of both EPCAM and CEA was found on PM samples, making these biomarkers pre-eminently suitable for fluorescence detection of PM from CRC patients undergoing CRS and HIPEC. A fluorescent agent targeting EPCAM is expected to reach the clinic by the end of this year and a fluorescent labelled anti-CEA antibody is currently studied in patients suffering from CRC (NTR5673). Therefore, the first intraoperative fluorescence imaging trials in PM from CRC using tumor-targeting agents could be approaching soon.

REFERENCES

- 1 Thomassen I, van Gestel YR, Lemmens VE, de Hingh IH. Incidence, prognosis, and treatment options for patients with synchronous peritoneal metastasis and liver metastases from colorectal origin. *Dis Colon Rectum*. 2013;56(12):1373-1380.
- 2 Sugarbaker PH, Zhu BW, Sese GB, Shmookler B. Peritoneal metastasis from appendiceal cancer: results in 69 patients treated by cytoreductive surgery and intraperitoneal chemotherapy. *Dis Colon Rectum*. 1993;36(4):323-329.
- 3 Esquivel J, Chua TC. CT versus intraoperative peritoneal cancer index in colorectal cancer peritoneal metastasis: importance of the difference between statistical significance and clinical relevance. *Ann Surg Oncol*. 2009;16(9):2662-2663; author reply 2264.
- 4 Koh JL, Yan TD, Glenn D, Morris DL. Evaluation of preoperative computed tomography in estimating peritoneal cancer index in colorectal peritoneal metastasis. *Ann Surg Oncol*. 2009;16(2):327-333.
- 5 Verwaal VJ, van Ruth S, de Bree E, et al. Randomized trial of cytoreduction and hyperthermic intraperitoneal chemotherapy versus systemic chemotherapy and palliative surgery in patients with peritoneal metastasis of colorectal cancer. *J Clin Oncol*. 2003;21(20):3737-3743.
- 6 Shen P, Levine EA, Hall J, et al. Factors predicting survival after intraperitoneal hyperthermic chemotherapy with mitomycin C after cytoreductive surgery for patients with peritoneal metastasis. *Arch Surg*. 2003;138(1):26-33.
- 7 Goere D, Souadka A, Faron M, et al. Extent of colorectal peritoneal metastasis: attempt to define a threshold above which HIPEC does not offer survival benefit: a comparative study. *Ann Surg Oncol*. 2015;22(9):2958-2964.
- 8 Sugarbaker PH, Chang D, Koslowe P. Prognostic features for peritoneal metastasis in colorectal and appendiceal cancer patients when treated by cytoreductive surgery and intraperitoneal chemotherapy. *Cancer Treat Res*. 1996;81:89-104.
- 9 Elias D, Quenet F, Goere D. Current status and future directions in the treatment of peritoneal dissemination from colorectal carcinoma. *Surg Oncol Clin N Am*. 2012;21(4):611-623.
- 10 Sugarbaker PH. It's what the surgeon doesn't see that kills the patient. *J Nippon Med Sch*. 2000;67(1):5-8.
- 11 Vahrmeijer AL, Hutteman M, van der Vorst JR, van de Velde CJ, Frangioni JV. Image-guided cancer surgery using near-infrared fluorescence. *Nat Rev Clin Oncol*. 2013;10(9):507-518.
- 12 Chance B. Near-infrared images using continuous, phase-modulated, and pulsed light with quantitation of blood and blood oxygenation. *Ann N Y Acad Sci*. 1998;838:29-45.
- 13 Frangioni JV. In vivo near-infrared fluorescence imaging. *Curr Opin Chem Biol*. 2003;7(5):626-634.
- 14 Keereweer S, Kerrebijn JD, van Driel PB, et al. Optical image-guided surgery--where do we stand? *Mol Imaging Biol*. 2011;13(2):199-207.
- 15 Stummer W, Stocker S, Wagner S, et al. Intraoperative detection of malignant gliomas by 5-aminolevulinic acid-induced porphyrin fluorescence. *Neurosurgery*. 1998;42(3):518-525; discussion 525-516.
- 16 van Dam GM, Themelis G, Crane LM, et al. Intraoperative tumor-specific fluorescence imaging in ovarian cancer by folate receptor-alpha targeting: first in-human results. *Nat Med*. 2011;17(10):1315-1319.
- 17 Kennedy GT, Okusanya OT, Keating JJ, et al. The Optical Biopsy: A Novel Technique for Rapid Intraoperative Diagnosis of Primary Pulmonary Adenocarcinomas. *Ann Surg*. 2015;262(4):602-609.
- 18 Rosenthal EL, Warram JM, de Boer E, et al. Safety and Tumor Specificity of Cetuximab-IRDye800 for Surgical Navigation in Head and Neck Cancer. *Clin Cancer Res*. 2015;21(16):3658-3666.
- 19 Hoogstins CE, Tummers QR, Gaarenstroom KN, et al. A Novel Tumor-Specific Agent for Intraoperative Near-Infrared Fluorescence Imaging: A Translational Study in Healthy Volunteers and Patients with Ovarian Cancer. *Clin Cancer Res*. 2016;22(12):2929-2938.
- 20 Cardoso J, Boer J, Morreau H, Fodde R. Expression and genomic profiling of colorectal cancer. *Biochim Biophys Acta*. 2007;1775(1):103-137.
- 21 van Oosten M, Crane LM, Bart J, van Leeuwen FW, van Dam GM. Selecting Potential Targetable Biomarkers for Imaging Purposes in Colorectal Cancer Using Target Selection Criteria (TASC): A Novel Target Identification Tool. *Transl Oncol*. 2011;4(2):71-82.
- 22 Ren J, Chen QC, Jin F, et al. Overexpression of Rsf-1 correlates with pathological type, p53 status and survival in primary breast cancer. *Int J Clin Exp Pathol*. 2014;7(9):5595-5608.
- 23 Hutteman M, Mieog JS, van der Vorst JR, et al. Intraoperative near-infrared fluorescence imaging of colorectal metastases targeting integrin alpha(v)beta(3) expression in a syngeneic rat model. *Eur J Surg Oncol*. 2011;37(3):252-257.
- 24 Burggraaf J, Kamerling IM, Gordon PB, et al. Detection of colorectal polyps in humans using an intravenously administered fluorescent peptide targeted against c-Met. *Nat Med*. 2015;21(8):955-961.
- 25 Boonstra MC, Prakash J, Van De Velde CJ, et al. Stromal Targets for Fluorescent-Guided Oncologic Surgery. *Front Oncol*. 2015;5:254.
- 26 Liberale G, Vankerckhove S, Caldon MG, et al. Fluorescence Imaging After Indocyanine Green Injection for Detection of Peritoneal Metastases in Patients Undergoing Cytoreductive Surgery for Peritoneal metastasis From Colorectal Cancer: A Pilot Study. *Ann Surg*. 2016;264(6):1110-1115.
- 27 Filippello A, Porcheron J, Klein JP, Cottier M, Barabino G. Affinity of Indocyanine Green in the Detection of Colorectal Peritoneal metastasis. *Surg Innov*. 2017;24(2):103-108.
- 28 van der Vorst JR, Schaafsma BE, Hutteman M, et al. Near-infrared fluorescence-guided resection of colorectal liver metastases. *Cancer*. 2013;119(18):3411-3418.
- 29 de Graaf W, Hausler S, Heger M, et al. Transporters involved in the hepatic uptake of (99m)Tc-mebrofenin and indocyanine green. *J Hepatol*. 2011;54(4):738-745.
- 30 Maeda H, Wu J, Sawa T, Matsumura Y, Hori K. Tumor vascular permeability and the EPR effect in macromolecular therapeutics: a review. *J Control Release*. 2000;65(1-2):271-284.
- 31 Matsumura Y, Maeda H. A new concept for macromolecular therapeutics in cancer chemotherapy: mechanism of tumor tropic accumulation of proteins and the antitumor agent smancs. *Cancer Res*. 1986;46(12 Pt 1):6387-6392.
- 32 Tummers QR, Hoogstins CE, Peters AA, et al. The Value of Intraoperative Near-Infrared Fluorescence Imaging Based on Enhanced Permeability and Retention of Indocyanine Green: Feasibility and False-Positives in Ovarian Cancer. *PLoS One*. 2015;10(6):e0129766.
- 33 Bergers G, Benjamin LE. Tumorigenesis and the angiogenic switch. *Nat Rev Cancer*. 2003;3(6):401-410.
- 34 Segal EI, Low PS. Tumor detection using folate receptor-targeted imaging agents. *Cancer Metastasis Rev*. 2008;27(4):655-664.
- 35 Di Renzo MF, Olivero M, Giacomini A, et al. Overexpression and amplification of the MET/HGF receptor gene during the progression of colorectal cancer. *Clin Cancer Res*. 1995;1(2):147-154.
- 36 Prat M, Narsimhan RP, Crepaldi T, Nicotra MR, Natali PG, Comoglio PC. The receptor encoded by the human c-MET oncogene is expressed in hepatocytes, epithelial cells and solid tumors. *Int J Cancer*. 1991;49(3):323-328.

TABLE 1 BIOMARKER EXPRESSION IN PRIMARY TUMOR AND PERITONEAL METASTASIS

	Primary Tumor (N=20)		Peritoneal Carcinomatosis (N=20)		Primary Tumor (N=20)		Peritoneal Carcinomatosis (N=20)		Primary Tumor (N=20)		Peritoneal Carcinomatosis (N=20)	
	n	%	n	%	n	%	n	%	n	%	n	%
Positive Epithelial Expression	20	100	20	100	20	100	20	100	3	15	4	20
Strong Epithelial Expression	19	95	18	90	14	70	14	70	0	0	0	0
Positive Stromal Expression	0	0	0	0	9	45	9	45	0	0	1	5
Strong Stromal Expression	0	0	0	0	0	0	0	0	0	0	0	0
Total Positive Expression	20	100	20	100	20	100	20	100	3	15	5	25
Total Strong Expression	19	95	18	90	14	70	14	70	0	0	0	0

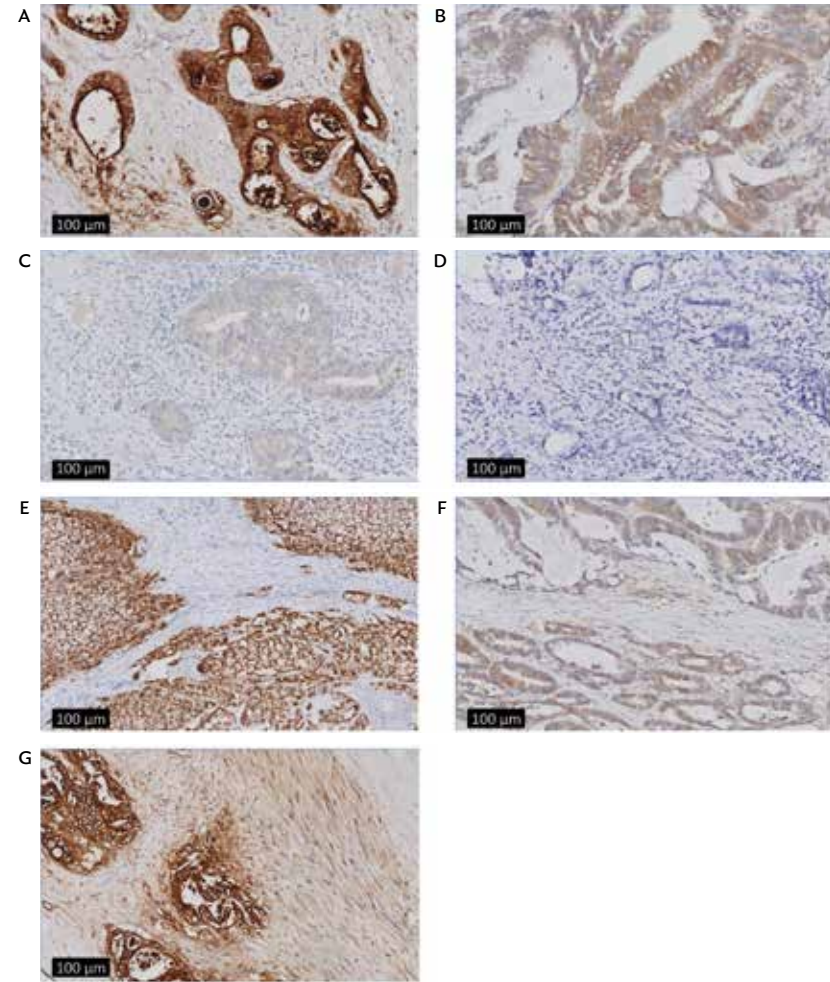
N = number; EPCAM= epithelial cell adhesion molecule; CEA= carcinoembryonic antigen; C-MET= Tyrosine-kinase Met; FRα= folate receptor-alpha

TABLE 2 CONCORDANCE PRIMARY TUMOR AND PERITONEAL METASTASIS

	EPCAM			CEA			C-MET			FRα		
	Primary Tumor Mean (SD) (N=20)	Peritoneal Carcinomatosis Mean (SD) (N=20)	Correlation coefficient ρ	Primary Tumor Mean (SD) (N=20)	Peritoneal Carcinomatosis Mean (SD) (N=20)	Correlation coefficient ρ	Primary Tumor Mean (SD) (N=20)	Peritoneal Carcinomatosis Mean (SD) (N=20)	Correlation coefficient ρ	Primary Tumor Mean (SD) (N=20)	Peritoneal Carcinomatosis Mean (SD) (N=20)	Correlation coefficient ρ
Epithelial Expression Score	11.8 (0.9)	11.6 (1.2)	0.688	10.6 (2.0)	10.6 (2.1)	0.128	3.9 (1.8)	4.1 (2.2)	-0.024	2.2 (3.0)	1.6 (2.3)	0.803
Stromal Expression Score	0.1 (0.3)	0.1 (0.2)	-0.076	3.1 (2.4)	3.1 (2.9)	0.191	1.8 (1.5)	2.3 (1.6)	0.461	0.0 (0.0)	0.1 (0.2)	n/a

N = number; EPCAM= epithelial cell adhesion molecule; CEA= carcinoembryonic antigen; C-MET= Tyrosine-kinase Met; FRα= folate receptor-alpha; n/a= not applicable

FIGURE 1 REPRESENTATIVE EPITHELIAL AND STROMAL STAINING INTENSITIES IN PERITONEAL METASTASIS FROM COLORECTAL CANCER USING IMMUNOHISTOCHEMISTRY (IHC)



Examples of (A) strong 3+ epithelial staining intensity (CEA); (B) moderate 2+ epithelial staining intensity (C-MET); (C) weak 1+ epithelial staining intensity (C-MET); (D) absent epithelial staining (FRα); (E) absent stromal staining (EPCAM); (F) moderate 2+ stromal staining (CEA); (G) moderate 2+ stromal staining (C-MET); CEA= carcinoembryonic antigen; C-MET= Tyrosine-kinase Met; EPCAM= epithelial cell adhesion molecule; FRα= folate receptor-alpha

PART II

CLINICAL TRANSLATION OF

TUMOR-TARGETED AGENTS

Chapter 4

Intraoperative imaging of folate receptor alpha positive ovarian and breast cancer using the tumor specific agent EC17

Oncotarget. 2016 May 31

QUIRIJN TUMMERS*, CHARLOTTE HOOGSTINS*, KATJA GAARENSTROOM, COR DE KROON, MARIETTE VAN POELGEEST, JAAP VUYK, TJALLING BOSSE, VINCENT SMIT, CORNELIS VAN DE VELDE, ADAM COHEN, PHILIP LOW, JACOBUS BURGGRAAF, ALEXANDER VAHRMEIJER

* Shared first authorship

ABSTRACT

INTRODUCTION: Intraoperative fluorescence imaging of the folate-receptor alpha (FR α) could support completeness of resection in cancer surgery. Feasibility of EC17, a FR α -targeting agent that fluoresces at 500 nm, was demonstrated in a limited series of ovarian cancer patients. Our objective was to evaluate EC17 in a larger group of ovarian cancer patients. In addition, we assessed the feasibility EC17 in patients with breast cancer.

METHODS Two-to-three hours before surgery 0.1mg/kg EC17 was intravenously administered to 12 patients undergoing surgery for ovarian cancer and to 3 patients undergoing surgery for biopsy-proven FR α -positive breast cancer. The number of lesions/positive margins detected with fluorescence and concordance between fluorescence and tumor- and FR α -status was assessed in addition to safety and pharmacokinetics.

RESULTS Fluorescence imaging in ovarian cancer patients allowed detection of 57 lesions of which 44 (77%) appeared malignant on histopathology. Seven out of these 44 (16%) were not detected with inspection/palpation. Histopathology demonstrated concordance between fluorescence and FR α - and tumor status. Fluorescence imaging in breast cancer patients, allowed detection of tumor-specific fluorescence signal. At the 500 nm wavelength, autofluorescence of normal breast tissue was present to such extent that it interfered with tumor identification.

CONCLUSIONS FR α is a favorable target for fluorescence-guided surgery as EC17 produced a clear fluorescent signal in ovarian and breast cancer tissue. This resulted in resection of ovarian cancer lesions that were otherwise not detected. Notwithstanding, autofluorescence caused false-positive lesions in ovarian cancer and difficulty in discriminating breast cancer-specific fluorescence from background signal. Optimization of the 500 nm fluorophore, will minimize autofluorescence and further improve intraoperative tumor detection.

INTRODUCTION

Over the past decades multiple imaging modalities have become available for preoperative detection of tumors, staging disease and identifying sentinel lymph nodes [1,2]. However, translation of preoperative obtained images to the surgical theatre can be challenging. Consequently, surgeons largely have to rely on visual inspection and palpation to discriminate between healthy and malignant tissue. As a result, incomplete resection of malignant tissue may occur. In breast cancer surgery, for example, positive resection margins are reported in up to 20% of patients after resection of the primary tumor [3]. In metastasized disease, intraoperative imaging of tumor tissue can be of great advantage. In ovarian cancer for example, clear intraoperative detection of metastatic lesions can improve staging procedures in early stage ovarian cancer (FIGO I and IIa), and facilitate complete or optimal cytoreductive surgery in advanced stage disease (FIGO IIb to IV). Both the prevention of positive margins in solid tumors and the performance of adequate staging and complete/optimal cytoreduction will improve individual patient outcome [4-9]. Hence there is a clear unmet need for intraoperative modalities that can identify tumor tissue with high sensitivity and specificity.

An innovative intraoperative optical imaging technique is fluorescence imaging. Over the past years multiple studies have been performed on tumor imaging, sentinel lymph node (SLN) mapping and identification of vital structures, using fluorescence imaging [10,11].

Optical properties of fluorescent contrast agents are of importance for successful tumor imaging. The wavelength of the fluorescent light largely determines the degree of penetration of photons into the tissue. Photons in the visible light range have a depth penetration limited to a few millimeters and are suitable for detection of superficial targets. Conversely photons in the NIR range (650-900 nm) can travel more than a centimeter through tissue, which also enables detection of targets below the tissue surface [12]. Moreover, the wavelength of the fluorescent light also plays a role in autofluorescence. Autofluorescence is fluorescence arising from intrinsic tissue components after excitation with UV, visible, or NIR radiation of suitable wavelength. To detect cancer cells targeted with an optical contrast agent, the signal of the target-specific fluorescence must be significantly higher than the autofluorescence. The occurrence of autofluorescence is determined by the tissue type and excitation wavelength [13,14].

Biological characteristics of fluorescent contrast agents are essential to achieve target-specific fluorescence imaging. Ideally, a contrast agent binds exclusively to a cancer specific ligand, while being excreted rapidly from the rest of the body. Over the past years, extensive preclinical validation of tumor-specific contrast agents targeting a variety of ligands was reported, however only very few were clinically introduced [15,16]. For this reason, several clinical studies have been performed to explore feasibility of clinical available fluorescent contrast agents like methylene blue (MB) and indocyanine green (ICG) for intraoperative tumor imaging of breast cancer tissue and ovarian cancer tissue [17,18]. These agents do not specifically bind to the tumor, but make use of other mechanisms such as the Enhanced Permeability and Retention (EPR) [19,20] effect and disturbed excretion profiles causing accumulation in or around tumor tissue. Although promising results were described, resection of non-malignant lesions due to false positive fluorescence proved an insurmountable problem in the road to clinical application. Consequently, the need for newly developed contrast agents with highly specific binding to tumor-specific targets remains.

A promising target for image-guided surgery is the folate receptor alpha (FR α). Normally the FR α is expressed only at low levels and due to its location on the apical membrane of epithelial cells it is not accessible for molecules transported by blood [21,22]. In contrast, in many types of epithelial cancers, the FR α is highly expressed. As a result of the loss of cell polarity in cancer, the FR α is easily accessible by blood making it an ideal tumor target. Over 90% of all epithelial ovarian cancers over-express FR α , and in ovarian cancers of serous morphology this percentage is even higher (90-100%) [23-25]. Moreover, expression is not altered by chemotherapy [26,27], allowing use of this target in both primary and interval cytoreductive surgical procedures. In breast cancer, FR α overexpression is reported in 30% of tumors, this percentage is even higher (67%) in tumors with a 'triple-negative' receptor profile [28]. In almost all breast cancer patients, preoperative biopsies are available, allowing characterization of FR α status before surgery to select patients who will benefit from FR α targeted imaging agents.

While multiple preclinical studies have been performed on the imaging of FR α positive tumors [29-31], clinical experience is very limited. Van Dam *et al.* showed feasibility of intraoperative imaging of ovarian cancer metastases using EC17, a FR α targeting contrast agent with fluorescent properties in the visible light spectrum (500 nm). In a limited series of patients undergoing surgery for suspected ovarian cancer, fluorescent tumor tissue was observed

intraoperatively after intravenous administration of EC17 in 3 out of 4 patients with proven ovarian cancer. However, the intra-operative detection of additional tumor lesions due to the use of EC17 and fluorescence imaging was not reported. Moreover, administration of the contrast agents had to be interrupted, although the study could be completed, in several (4 out of 10) patients due to mild adverse events. As a result the initial dose of 0.3 mg/kg was decreased to 0.1 mg/kg, which reduced adverse events while maintaining fluorescent signal. To demonstrate the tolerability and additional value of fluorescence imaging using EC17 in ovarian cancer, evaluation in a larger patient cohort is required. And though the overexpression of the FR α on selected breast cancer cells has been shown, feasibility of fluorescence imaging using EC17 in patients with FR α positive breast cancer has not yet been demonstrated.

Our objective was to evaluate a relatively low dose of EC17 (0.1 mg/kg) in a larger group of ovarian cancer patients and to assess feasibility of intraoperative fluorescence imaging in patients with FR α positive breast cancer.

METHODS

INVESTIGATIONAL AGENT • EC17 (molecular formula: C₄₂H₃₆N₁₀Na₂O₁₀S; On Target Laboratories LLC, West Lafayette, USA) consists of a folate analogue conjugated to 5-fluorescein isothiocyanate (FITC), which is excited between the wavelengths of 465 and 490 nm and fluoresces at wavelengths of 520-530 nm. Before administration, the frozen vials containing 5 mg/mL EC17 in 3 mL water for injection were thawed and diluted in 10 mL sterile saline. Patients received 0.1 mg/kg EC17 intravenously over 10 minutes, 2-3 hours before surgery.

PATIENTS • Patients suspected of early stage epithelial ovarian cancer presenting at the department of Gynecology of the Leiden University Medical Center (LUMC) between February 2014 and September 2014 scheduled to undergo staging surgery or of advanced epithelial ovarian cancer scheduled to undergo cytoreductive surgery, were included in this study. All patients gave written informed consent.

For breast cancer, patients presenting at the department of Surgery of the LUMC between May 2014 and February 2015 planned for, either breast conserving surgery (BCS) or breast ablation, were eligible for participation. After selection, preoperatively obtained biopsies of potentially eligible patients were stained for FR α expression using immunohistochemistry (IHC). FR α expression was assessed by using a membranous scoring method with a scale ranging

from 0 to 3+, as described by O'Shannessy *et al.* [49] A score of 0 corresponded to absence of staining; 1+ equaled faint staining on luminal borders; 2+ equaled moderate staining on apical and sometimes lateral borders and 3+ indicated strong circumferential staining. The tumor was considered positive when more than 10% of malignant cells were positively stained (>0). Assessment of the stained biopsies was performed by a pathologist (VTHBMS or TB), and after presence of FR α positive tumor cells was confirmed, patients were eligible for EC17 administration. All patients gave written informed consent.

Exclusion criteria were age <18, pregnancy (excluded by pregnancy test in woman of childbearing potential), renal impairment (defined as EGFR <50 mL/min/1.73m²), impaired liver function (defined as evidenced by greater than 3x the upper limit of normal (ULN) for ALT, AST, or total bilirubin), or a history of anaphylactic reaction to EC17, insect bites or fluorescein.

CLINICAL TRIAL • The study was approved by the Medical Ethics Committee of the LUMC and was performed in accordance with the laws and regulations of the Netherlands. Suitability of selected patients was further assessed by a medical screening consisting of a medical history, physical examination including vital signs, weight, 12-lead ECG, and routine laboratory assessments.

Before administration of EC17, two IV cannulas were inserted. One IV cannula was used for study drug administration and the cannula in the contralateral arm for PK sampling (Supplementary Methods). After administration, safety assessments (blood pressure, pulse, peripheral oxygen saturation and temperature) and blood collection for pharmacokinetics were performed regularly from just prior to administration up to the end of surgery. A stopping rule was defined in the protocol. In case of treatment-related serious adverse events or results suggesting futility to continue, the trial would be halted or stopped.

SURGICAL PROCEDURE IN OVARIAN CANCER PATIENTS • All surgical procedures were performed by laparotomy through a midline abdominal incision. After opening of the abdominal cavity, the surgical field was searched for the primary tumor and metastases visible by the naked eye or palpation. Thereafter, the Artemis imaging system (see below for details) was used to identify fluorescent signals. When a fluorescent signal was observed, the operating surgeon performed a biopsy or resection of the fluorescent tissue. In case of non-fluorescence, only lesions macroscopically suspect for malignancy were resected. Resected specimens were marked as clinically suspect or not clinically suspect and as fluorescent or non-fluorescent. All resected lesions were examined by a

pathologist for tumor status. In addition, an immunohistochemical (IHC) staining for FR α expression and fluorescence microscopy (Leica DM5500B fluorescence microscope) were performed to assess concordance of fluorescence with tumor and FR α presence and to evaluate binding sites of EC17 (Supplementary Methods).

To assess the number of malignant lesions that were identified by the naked eye and/or fluorescence imaging, stills from intraoperative obtained videos were analyzed by three dedicated gynecologic oncologists, experienced in ovarian cancer surgery. A total of 5 different images were analyzed. Each image was analyzed 3 times (normal, horizontally and vertically flipped), leading to a total of 15 images to be analyzed. First, only color images were used to score the number of observed metastatic lesions. When this was completed, color images supplemented with fluorescence images were scored.

SURGICAL PROCEDURE IN BREAST CANCER ● Patients underwent standard of care breast ablation or BCS both combined with SLN biopsy. The Artemis fluorescence imaging system was used to identify fluorescent signal during surgery and on resected specimens transferred to the pathology department. Intra-operative images of SLNs, the surgical field, resected specimen, and wound bed after resection were obtained. Following standard procedure, the resected specimen was dissected at the pathology department, where images from the dissected tumor were obtained as well. The resected specimens were routinely examined by a pathologist for tumor status. In addition, IHC staining for FR α expression and fluorescence microscopy (Leica DM5500B fluorescence microscope) were performed to evaluate binding site of EC17 (Supplementary Methods).

ARTEMIS FLUORESCENCE IMAGING SYSTEM ● Imaging procedures were performed using the Artemis fluorescence imaging system (Quest Medical Imaging, The Netherlands). The system consists of 3 wavelength isolated light sources: a 'white' light source, and a two different 'near-infrared' light sources. For this study, the camera and light engine were optimized for EC17 to generate 7.5 mW/cm² at 490 nm light. Color video and fluorescence images are simultaneously acquired on separate sensors and displayed in real time using custom optics and software showing the separate the color video and NIR fluorescence images. A pseudo-colored (lime green) merged image of the color video and fluorescence images is also displayed. The intensities of the light sources could be controlled from the Artemis software. The camera can be attached to a freely

moveable arm head. For intraoperative use, the camera and freely moveable arm were wrapped in a sterile shield and drape (Medical Technique Inc., Tucson, AZ).

Statistical and Image Analysis: SPSS statistical software package (Version 20.0, Chicago, IL) was used. Patient characteristics were reported in median, standard deviation (SD), and range. PK parameters (AUC, C_{MAX}, T_{MAX}) were statistically summarized including number of subjects, mean, standard deviation (SD), median, minimum and maximum. Plasma drug concentrations were plotted versus time per individual using both a linear and log y-axis. Additionally, concentration versus time curves were plotted as a spaghetti plot with the median added.

Fluorescent signal in tumor and background was quantified using ImageJ (version 1.49b; a public domain, Java-based image processing program developed at the National Institute of Health). Regions of interest (ROI) were drawn with ImageJ on the stored images to quantify fluorescent signal in arbitrary units [AU]. Tumor to background ratios (TBRs) were calculated by dividing the fluorescent signal of the tumor by fluorescent signal of surrounding tissue. To compare TBR and background signal between malignant and benign lesions independent samples t-test was used. TBR was reported in mean, SD, and range.

RESULTS

PATIENT CHARACTERISTICS ● A total of 13 ovarian cancer patients were included. Surgery was cancelled in 1 patient due to deterioration of the medical condition of the patient prior to surgery. Thus 12 ovarian cancer patients received EC17 and underwent open surgery; a tabular overview of the patient characteristics, FIGO status and histology of the tumor type is given in Table 1. Six patients underwent a primary cytoreductive procedure, 4 patients an interval cytoreductive procedure and 2 patients a staging procedure.

For breast cancer, a total of 53 potentially eligible breast cancer patients were selected for characterization of FR α status on preoperatively obtained biopsies. Samples of six patients stained positive for FR α (11%). Of the 6 patients, 2 patients eventually did not meet the inclusion criteria and 1 patient declined participation. Three patients were included in the study and their characteristics are provided in Table 2.

SAFETY ● All patients received 0.1 mg/kg EC17 over 10 minutes, and no infusion was intermitted or stopped. Infusion of EC17 was associated with mild, self-limiting hypersensitivity reactions in 7 out of 15 patients. The symptoms consisted

of abdominal discomfort, itching throat and sneezing (for a summary list of treatment related adverse events, see Table S1). One patient vomited after EC17 administration and received ondansetron 8 mg intravenously, followed by the planned surgical procedure. There were no clinical relevant changes in blood pressure or pulse rate compared to baseline.

INTRAOPERATIVE FLUORESCENCE IMAGING ● Intraoperative fluorescence imaging in ovarian cancer patients allowed clear detection of ovarian cancer lesions. Figure 1 shows an example of fluorescent ovarian cancer metastases. In total, 57 fluorescent lesions that were identified during surgery were resected. Of these resected lesions 44 (77%) appeared to be malignant on histopathology. Seven (16%) of these 44 lesions were not detected by visual inspection with the naked eye or palpation either because they appeared benign or because they were missed during inspection due to small size (<10 mm) and flat nature. These lesions were only removed because these could be identified using fluorescence imaging. Mean TBR was 7.0 ± 1.2 . Fluorescence imaging was successful up to about 5.5 hours after EC17 administration, which was the longest time interval measured between administration and the end of a surgical procedure.

Histopathology demonstrated clear concordance between fluorescence and FR α - and tumor status. Fluorescence microscopy showed clear membranous and cytoplasmic accumulation of EC17 in tumor cells (Figure 2).

The (ex-vivo) assessment of the stills obtained from the videos made during the surgical procedure showed that on average (SD) 23.3 (\pm 11.9) lesions per still were identified with the naked eye. When the stills were supplemented with the fluorescence image, 39.6 (\pm 22.7) lesions per still were identified, a 70% increase.

In total, 3 false-negative lesions were identified. These lesions were all metastases in the greater omentum. The lesions were considered suspicious for malignancy by the surgeons, but showed no intraoperative fluorescence signal from the outside (Figure 3A). However, upon dissection of the omentum on the backtable, strong fluorescent signal was identified (Figure 3B), suggesting that the intraoperative non-fluorescence was caused by the lack of tissue penetration at 500 nm wavelength.

Thirteen out of the 57 (23%) fluorescent lesions appeared benign. Five of these false positive lesions were identified as normal fallopian tube tissue on histopathological evaluation, showing FR α expression. These lesions were thus expected to bind EC17, and were resected anyway as part of the standard surgical procedure. Six lesions were structures mainly containing collagen, which is known to cause autofluorescence at 500 nm. Mean TBR of the false-positives

was 5.4 ± 1.0 . There was no significant difference in TBR between true-positives and false-positives (7.0 vs. 5.4; $P = 0.47$). Characteristics of false positive and false negative lesions are provided in Table 3.

Also in breast cancer, tumor-specific fluorescence signal was observed. Median TBR was 2.3 (range 2.1 – 6.2). However, autofluorescence of normal breast tissue was present to such extent that it interfered with tumor identification. Figure 4 shows fluorescent signal in breast cancer tissue and in normal, autofluorescent breast tissue. Fluorescence microscopy showed clear membranous and cytoplasmic accumulation of EC17 in tumor cells (Figure 5). In addition, high background fluorescent signal was observed, which is in concordance with images obtained with the intraoperative Artemis imaging system.

In one patient with breast cancer, a tumor-positive SLN was found on histopathological evaluation. This SLN however was not detected with fluorescence imaging. After HE and FR α staining, the metastasis appeared to be in the center of the SLN, and was therefore not detected due to lack of tissue penetration.

PHARMACOKINETICS ● The maximal concentration for each dose was obtained directly after the end of the infusion and declined thereafter with a half-life of 86.8 minutes.

DISCUSSION

Intraoperative imaging of tumor tissue may improve patient outcome by enhanced identification and subsequent resection of tumor tissue. Fluorescence guided surgery using the FR α specific contrast agents EC17 allowed real time identification of both ovarian- and breast cancer cells. In ovarian cancer, the intraoperative use of fluorescence imaging resulted in the resection of 16% more malignant lesions compared to inspection with the naked eye and/or palpation only. Visual identification was improved on stills made from intraoperative videos, supporting the notion that fluorescent imaging improves detection even when other techniques like palpation are not available.

The biophysical properties of imaging agents are of paramount importance for successful tumor identification. Ideally, high fluorescence signal is observed in malignant lesions, while normal or healthy tissue shows minimal fluorescence because of a low binding constant and fast excretion of the imaging agent after initial biodistribution. The size of the compound greatly influences this profile. Currently monoclonal antibodies, antibody fragments, such as single-chain (scFv) of fab fragments, small peptides or structure-inherent targeting

fluorophores are used for tumor-specific imaging [32-36]. The biodistribution, excretion and binding profile of EC17 shows several great advantages in imaging. The maximum concentration (C_{MAX}) of EC17 is observed directly after the end of administration and is followed by a rapid excretion from the blood. While fluorescence signal of the tumor is observed up to more than 5 hours after administration of the compound. This short terminal half-life in blood, strong tumor specific signal and low background signal allows tumor imaging from 2 hours post dosing and during a relative long time.

Around 75% of patients with ovarian cancer present with advanced stage [37] of the disease. Multiple studies have shown that the amount of residual disease is the most important prognostic factor for survival in ovarian cancer patients. As a result of these studies, consensus exists that all attempts should be made to achieve complete cytoreduction i.e. complete removal of all macroscopically visible tumor tissue [4,6,8,38,39]. In this study, real-time visualization of malignant lesions using fluorescence imaging during surgery led to the detection of 14% additional malignant lesions. This may improve cytoreduction and hereby patient outcome. The effect of the addition of intraoperative fluorescence imaging on survival was already shown by Stummer *et al.* in patients with brain glioma. They demonstrated that fluorescence imaging with 5-ALA not only leads to more complete resections but also to improved progression free survival [5]. For ovarian cancer more prospective research is necessary to establish the effect on overall survival.

When patients present with clinically early stage ovarian cancer, a staging procedure is recommended. During this procedure, biopsies of suspicious lesions are taken, supplemented with, 'blind' biopsies from predefined locations. Ultimate goal is to identify metastatic lesions whenever present in order to give adequate treatment i.e. systemic chemotherapy. Visualizing metastatic lesions by fluorescence imaging may optimize staging procedures, while less 'blind' biopsies have to be taken. This could facilitate discrimination between true early stage ovarian cancer and more advanced stage with occult tumor spread. Especially in minimal-invasive surgery, when tactile information (palpation) of lesions cannot be obtained, fluorescence imaging could be of additional value.

In breast cancer, up to 20% of patients have positive resection margins after resection of the primary tumor [3]. Visualizing tumor cells during surgery could lower the risk of an incomplete resection as identification of a positive margin can result in direct resection of residual tumor tissue. Although this will probably not influence overall survival, as patient with positive resection margins are currently treated with a re-resection or more intensive radiotherapy, significantly

lower healthcare costs and burden to the patient could result. To investigate this concept, both FR α positive breast cancer patients treated with BCS and breast ablation were included in the current feasibility study. However, for future applicability of fluorescence imaging in breast cancer surgery, the most added value is to be expected in BCS. Moreover, a significant number of patients with breast carcinoma is pre-treated with neoadjuvant systemic chemotherapy to reduce the primary tumor to facilitate BCS instead of radical mastectomy [40]. Although pre-treatment with systemic therapy does not result in an increased number of positive resection margins [41], recognition of vital tumor tissue can be challenging. As FR α status is not changed by chemotherapy [42,27], fluorescence imaging could be of added value in these challenging cases.

In literature, FR α positive breast cancer lesions are described in up to 30% of patient [43-45]. In our series however, only 11% of the obtained biopsies stained positive for FR α . No explanation was found for this lower expression level. A high number of normal breast tissue stained weak positive for FR α , mainly located at the apical surface of epithelial cells and at myoepithelial cells. This finding has been described previously [43,45], and does not necessarily cause a pitfall for FR α as target for fluorescence guided surgery, because the myoepithelium is not accessible for blood carried contrast agents.

Several limitations of the described technique and contrast agent were caused by the optical properties of the contrast agent. EC17 fluoresces at 488 nm, which does not allow identification of lesions located beneath the surface. In 3 patients with ovarian cancer, the greater omentum was suspected for malignancy, but only showed fluorescence after dissection of the tissue and this clearly showed the low tissue penetration of the photons emitted by EC17. We identified 23% false-positive lesions in the patients with ovarian cancer. The non-malignant lesions that fluoresced in this study were in particular collagen-containing structures, from which it known that they can show autofluorescence in the visible light spectrum [14,46].

All the above-mentioned limitations could be overcome by conjugating the folate analog to a fluorophore that fluoresces in the NIR spectrum. This allows identification of structures located deeper beneath the surface due to a lower absorption coefficient, and causes less autofluorescence of normal tissue [47]. For surface detection of malignant cells, as in breast cancer, depth penetrating is less important, but currently the autofluorescent signal prevented clinical decision-making. Figure S1 shows fluorescence imaging at 500 nm and 800 nm of breast tissue containing a tumor. These tissue specimens, from patients that were not treated with an exogenous contrast agent as EC17, are thus suitable

to demonstrate background fluorescence. At 500 nm high background fluorescence is observed, while at 800 nm no background fluorescence signal is seen (Supplementary Methods). This illustrates the need for tumor-specific contrast agents in the NIR spectrum. Currently, our research group is performing a first-in-human clinical trial in ovarian cancer patients using the FR α specific near-infrared contrast agent OTL38. Preclinical tests comparing OTL38 with EC17 have demonstrated superiority of OTL38 in sensitivity and brightness [48].

In conclusion, administration of EC17 was reasonably well-tolerated and produced clear fluorescent signals in ovarian and breast cancer tissue. This allowed resection of 16% more ovarian cancer lesions. Notwithstanding, autofluorescence of benign, predominantly collagen-containing tissues led to detection of a significant proportion of false positive lesions in ovarian cancer. Further, autofluorescence resulted in difficulty in discriminating breast cancer tissue specific fluorescence from background fluorescence. We conclude that FR α is a favorable tumor-specific target, but EC17 lacks full set of requirements for fluorescence-guided surgery in FR α -positive ovarian and breast cancer, especially because of auto-fluorescence and insufficient penetration depth. Replacing the 500 nm fluorophore by a fluorophore in the NIR spectrum could likely further improve optical properties and thereby clinical relevance of fluorescence-guided surgery.

REFERENCES

- Frangioni JV. In vivo near-infrared fluorescence imaging. *Curr.Opin.Chem.Biol.* 2003; 626-634.
- Weissleder R and Pittet MJ. Imaging in the era of molecular oncology. *Nature.* 2008; 580-589.
- Pleijhuis RG, Graafland M, de VJ, Bart J, de Jong JS, and van Dam GM. Obtaining adequate surgical margins in breast-conserving therapy for patients with early-stage breast cancer: current modalities and future directions. *Ann.Surg.Oncol.* 2009; 2717-2730.
- Chang SJ, Bristow RE, and Ryu HS. Impact of complete cytoreduction leaving no gross residual disease associated with radical cytoreductive surgical procedures on survival in advanced ovarian cancer. *Ann.Surg.Oncol.* 2012; 4059-4067.
- Stummer W, Pichlmeier U, Meinel T, Wiestler OD, Zanella F, and Reulen HJ. Fluorescence-guided surgery with 5-aminolevulinic acid for resection of malignant glioma: a randomised controlled multicentre phase III trial. *Lancet Oncol.* 2006; 392-401.
- Bristow RE and Berek JS. Surgery for ovarian cancer: how to improve survival. *Lancet.* 2006; 1558-1560.
- Bristow RE, Tomacruz RS, Armstrong DK, Trimble EL, and Montz FJ. Survival effect of maximal cytoreductive surgery for advanced ovarian carcinoma during the platinum era: a meta-analysis. *J.Clin.Oncol.* 2002; 1248-1259.
- Vergote I, Trope CG, Amant F, Kristensen GB, Ehlen T, Johnson N, Verheijen RH, van der Burg ME, Lacave AJ, Panici PB, Kenter GG, Casado A, Mendiola C, et al. Neoadjuvant chemotherapy or primary surgery in stage IIIc or IV ovarian cancer. *N.Engl.J.Med.* 2010; 943-953.
- Hoskins WJ, McGuire WP, Brady MF, Homesley HD, Creasman WT, Berman M, Ball H, and Berek JS. The effect of diameter of largest residual disease on survival after primary cytoreductive surgery in patients with suboptimal residual epithelial ovarian carcinoma. *Am.J.Obstet.Gynecol.* 1994; 974-979.
- Handgraaf HJ, Verbeek FP, Tummers QR, Boogerd LS, van de Velde CJ, Vahrmeijer AL, and Gaarenstroom KN. Real-time near-infrared fluorescence guided surgery in gynecologic oncology: a review of the current state of the art. *Gynecol.Oncol.* 2014; 606-613.
- Vahrmeijer AL, Hutteman M, van der Vorst JR, van de Velde CJ, and Frangioni JV. Image-guided cancer surgery using near-infrared fluorescence. *Nat.Rev.Clin.Oncol.* 2013; 507-518.
- Patterson MS, Chance B, and Wilson BC. Time resolved reflectance and transmittance for the non-invasive measurement of tissue optical properties. *Appl.Opt.* 1989; 2331-2336.
- Weissleder R and Ntziachristos V. Shedding light onto live molecular targets. *Nat.Med.* 2003; 123-128.
- Monici M. Cell and tissue autofluorescence research and diagnostic applications. *Biotechnol. Annu.Rev.* 2005; 227-256.
- van Dam GM, Themelis G, Crane LM, Harlaar NJ, Pleijhuis RG, Kelder W, Sarantopoulos A, de Jong JS, Arts HJ, van der Zee AG, Bart J, Low PS, and Ntziachristos V. Intraoperative tumor-specific fluorescence imaging in ovarian cancer by folate receptor-alpha targeting: first in-human results. *Nat.Med.* 2011; 1315-1319.
- Burggraaf J, Kamerling IM, Gordon PB, Schrier L, de Kam ML, Kales AJ, Bendiksen R, Indrevoll B, Bjerke RM, Moestue SA, Yazdanfar S, Langers AM, Swaerd-Nordmo M, et al. Detection of colorectal polyps in humans using an intravenously administered fluorescent peptide targeted against c-Met. *Nat.Med.* 2015; 955-961.
- Tummers QR, Verbeek FP, Schaafsma BE, Boonstra MC, van der Vorst JR, Liefers GJ, van de Velde CJ, Frangioni JV, and Vahrmeijer AL. Real-time intraoperative detection of breast cancer using near-infrared fluorescence imaging and Methylene Blue. *Eur.J.Surg.Oncol.* 2014; 850-858.
- Tummers QR, Hoogstins CE, Peters AA, de Kroon CD, Trimbos JB, van de Velde CJ, Frangioni JV, Vahrmeijer AL, and Gaarenstroom KN. The Value of Intraoperative Near-Infrared Fluorescence Imaging Based on Enhanced Permeability and Retention of Indocyanine Green: Feasibility and False-Positives in Ovarian Cancer. *PLoS.One.* 2015; e0129766-
- Maeda H, Wu J, Sawa T, Matsumura Y, and Hori K. Tumorvascular permeability and the EPR

- effect in macromolecular therapeutics: a review. *J.Control Release*. 2000; 271-284.
- 20 Matsumura Y and Maeda H. A new concept for macromolecular therapeutics in cancer chemotherapy: mechanism of tumor tropic accumulation of proteins and the antitumor agent smancs. *Cancer Res*. 1986; 6387-6392.
- 21 low PS, Henne WA, and Doorneweerd DD. Discovery and development of folic-acid-based receptor targeting for imaging and therapy of cancer and inflammatory diseases. *Acc.Chem. Res*. 2008; 120-129.
- 22 Vergote IB, Marth C, and Coleman RL. Role of the folate receptor in ovarian cancer treatment: evidence, mechanism, and clinical implications. *Cancer Metastasis Rev*. 2015;
- 23 Kalli KR, Oberg AL, Keeney GL, Christianson TJ, low PS, Knutson KL, and Hartmann LC. Folate receptor alpha as a tumor target in epithelial ovarian cancer. *Gynecol.Oncol*. 2008; 619-626.
- 24 O'Shannessy DJ, Somers EB, Smale R, and Fu YS. Expression of folate receptor-alpha (FRA) in gynecologic malignancies and its relationship to the tumor type. *Int.J.Gynecol.Pathol*. 2013; 258-268.
- 25 Parker N, Turk MJ, Westrick E, Lewis JD, low PS, and Leamon CP. Folate receptor expression in carcinomas and normal tissues determined by a quantitative radioligand binding assay. *Anal. Biochem*. 2005; 284-293.
- 26 Crane LM, Arts HJ, van OM, Low PS, van der Zee AG, van Dam GM, and Bart J. The effect of chemotherapy on expression of folate receptor-alpha in ovarian cancer. *Cell Oncol.(Dordr.)*. 2012; 9-18.
- 27 Despierre E, Lambrechts S, Leunen K, Berteloot P, Neven P, Amant F, O'Shannessy DJ, Somers EB, and Vergote I. Folate receptor alpha (FRA) expression remains unchanged in epithelial ovarian and endometrial cancer after chemotherapy. *Gynecol.Oncol*. 2013; 192-199.
- 28 O'Shannessy DJ, Somers EB, Maltzman J, Smale R, and Fu YS. Folate receptor alpha (FRA) expression in breast cancer: identification of a new molecular subtype and association with triple negative disease. *Springerplus*. 2012; 22-
- 29 Liu TW, Stewart JM, Macdonald TD, Chen J, Clarke B, Shi J, Wilson BC, Neel BG, and Zheng G. Biologically-targeted detection of primary and micro-metastatic ovarian cancer. *Theranostics*. 2013; 420-427.
- 30 Vaitilingam B, Chelvam V, Kularatne SA, Poh S, Ayala-Lopez W, and low PS. A folate receptor-alpha-specific ligand that targets cancer tissue and not sites of inflammation. *J.Nucl.Med*. 2012; 1127-1134.
- 31 Kennedy MD, Jallad KN, Thompson DH, Ben-Amotz D, and low PS. Optical imaging of metastatic tumors using a folate-targeted fluorescent probe. *J.Biomed.Opt*. 2003; 636-641.
- 32 Altintas I, Kok RJ, and Schifferers RM. Targeting epidermal growth factor receptor in tumors: from conventional monoclonal antibodies via heavy chain-only antibodies to nanobodies. *Eur.J.Pharm.Sci*. 2012; 399-407.
- 33 Choi HS, Gibbs SL, Lee JH, Kim SH, Ashitate Y, Liu F, Hyun H, Park G, Xie Y, Bae S, Henary M, and Frangioni JV. Targeted zwitterionic near-infrared fluorophores for improved optical imaging. *Nat.Biotechnol*. 2013; 148-153.
- 34 Hyun H, Park MH, Owens EA, Wada H, Henary M, Handgraaf HJ, Vahrmeijer AL, Frangioni JV, and Choi HS. Structure-inherent targeting of near-infrared fluorophores for parathyroid and thyroid gland imaging. *Nat.Med*. 2015; 192-197.
- 35 Oliveira S, Heukers R, Sornkom J, Kok RJ, and van Bergen En Henegouwen PM. Targeting tumors with nanobodies for cancer imaging and therapy. *J.Control Release*. 2013; 607-617.
- 36 Rosenthal EL, Warram JM, de BE, Chung TK, Korb ML, Brandwein-Gensler M, Strong TV, Schmalbach CE, Morlandt AB, Agarwal G, Hartman YE, Carroll WR, Richman JS, et al. Safety and Tumor Specificity of Cetuximab-IRDye800 for Surgical Navigation in Head and Neck Cancer. *Clin.Cancer Res*. 2015; 3658-3666.
- 37 Fader AN and Rose PG. Role of surgery in ovarian carcinoma. *J.Clin.Oncol*. 2007; 2873-2883.
- 38 Bristow RE, Tomacruz RS, Armstrong DK, Trimble EL, and Montz FJ. Survival effect of maximal cytoreductive surgery for advanced ovarian carcinoma during the platinum era: a meta-analysis. *J.Clin.Oncol*. 2002; 1248-1259.
- 39 Hoskins WJ, McGuire WP, Brady MF, Homesley HD, Creasman WT, Berman M, Ball H, and Berek JS. The effect of diameter of largest residual disease on survival after primary cytoreductive surgery in patients with suboptimal residual epithelial ovarian carcinoma. *Am.J.Obstet. Gynecol*. 1994; 974-979.
- 40 Barranger E, Antomarchi J, Chamorey E, Cavrot C, Flipo B, Follana P, Peyrottes I, Chapellier C, Ferrero JM, and Ibrai T. Effect of Neoadjuvant Chemotherapy on the Surgical Treatment of Patients With Locally Advanced Breast Cancer Requiring Initial Mastectomy. *Clin.Breast Cancer*. 2015;
- 41 Soucy G, Belanger J, Leblanc G, Sideris L, Drolet P, Mitchell A, Leclerc YE, Dufresne MP, Beaudet J, and Dube P. Surgical margins in breast-conservation operations for invasive carcinoma: does neoadjuvant chemotherapy have an impact? *J.Am.Coll.Surg*. 2008; 1116-1121.
- 42 Crane LM, Arts HJ, van OM, low PS, Van Der Zee AG, van Dam GM, and Bart J. The effect of chemotherapy on expression of folate receptor-alpha in ovarian cancer. *Cell Oncol.(Dordr.)*. 2012; 9-18.
- 43 O'Shannessy DJ, Somers EB, Maltzman J, Smale R, and Fu YS. Folate receptor alpha (FRA) expression in breast cancer: identification of a new molecular subtype and association with triple negative disease. *Springerplus*. 2012; 22-
- 44 van Driel PB, van de Giessen M, Boonstra MC, Snoeks TJ, Keereweer S, Oliveira S, van de Velde CJ, Lelieveldt BP, Vahrmeijer AL, Lowik CW, and Dijkstra J. Characterization and evaluation of the artemis camera for fluorescence-guided cancer surgery. *Mol.Imaging Biol*. 2015; 413-423.
- 45 Zhang Z, Wang J, Tacha DE, Li P, Bremer RE, Chen H, Wei B, Xiao X, Da J, Skinner K, Hicks DG, Bu H, and Tang P. Folate receptor alpha associated with triple-negative breast cancer and poor prognosis. *Arch.Pathol.Lab Med*. 2014; 890-895.
- 46 Monici M, Basile V, Romano G, Evangelisti L, Lucarini L, Attanasio M, Bertini E, Fusi F, Gensini GF, and Pepe G. Fibroblast autofluorescence in connective tissue disorders: a future tool for clinical and differential diagnosis? *J.Biomed. Opt*. 2008; 054025-
- 47 Weissleder R and Ntziachristos V. Shedding light onto live molecular targets. *Nat.Med*. 2003; 123-128.
- 48 De JE, Keating JJ, Kularatne SA, Jiang J, Judy R, Predina J, Nie S, Low P, and Singhal S. Comparison of Folate Receptor Targeted Optical Contrast Agents for Intraoperative Molecular Imaging. *Int.J.Mol.Imaging*. 2015; 469047-
- 49 O'Shannessy DJ, Yu G, Smale R, Fu YS, Singhal S, Thiel RP, Somers EB, and Vachani A. Folate receptor alpha expression in lung cancer: diagnostic and prognostic significance. *Oncotarget*. 2012; 414-425.

TABLE 1 DEMOGRAPHIC AND BASELINE CHARACTERISTICS OF OVARIAN CANCER PATIENTS

Patient ID	Age	Surgical procedure	Diagnosis	FIGO stage	Metastases identified	Tumor FRα+	Fluorescence imaging successful
1	71	Primary debulking	Serous adenocarcinoma	3c	Yes	Yes	Yes
2	51	Primary debulking	Endometrioid type adenocarcinoma	3b	Yes	Yes	Yes
3	59	Staging	Endometrioid type adenocarcinoma	2c	No	Yes	Yes
4	61	Interval debulking	Serous adenocarcinoma of endometrium	4	Yes	Yes	Yes
5	64	Primary debulking	Borderline serous adenocarcinoma	3b	Non-invasive implants	Yes	Yes
6	71	Primary debulking	Serous adenocarcinoma	3c	Yes	Yes	Yes
7	71	Primary debulking	Serous adenocarcinoma	3b	Yes	Yes	Yes
8	78	Interval debulking	Serous adenocarcinoma	3c	Yes	Yes	Yes
9	57	Interval debulking	Serous adenocarcinoma	3c	Yes	Yes	Yes
10	52	Interval debulking	Serous adenocarcinoma	4	Yes	Yes	Yes
11	42	Primary debulking	Mucinous adenocarcinoma	3c	Yes	No	No
12	73	Staging	Endometrioid type adenocarcinoma	2b	No	Yes	Yes

TABLE 2 DEMOGRAPHIC AND BASELINE CHARACTERISTICS OF BREAST CANCER PATIENTS

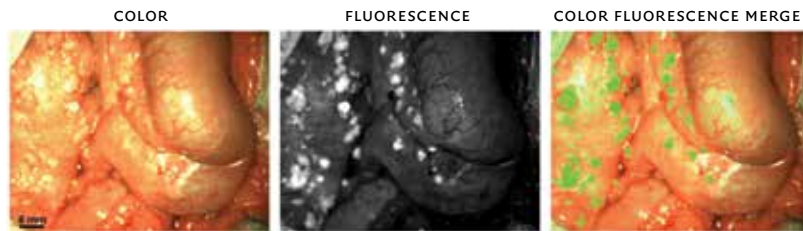
Patient ID	Age	Surgical procedure	Diagnosis	Tumor size in mm	ER status	PR Status	HER2 Status	SLN meta-stasis	Tumor FRα+	Fluorescence imaging successful
1	54	BCS	IBC NST	19	Neg	Neg	Neg	Yes, 9mm	Yes	Yes*
2	61	BCS	Metaplastic carcinoma	42	Neg	Neg	Neg	No	Yes	Yes
3	53	Mastectomy	IBC NST	23	Pos	Pos	Neg	No	Yes	Yes

BCS = Breast Conserving Surgery; IBC = infiltrative breast cancer; NST = No Special Type
 * Tumor successfully identified in resection specimen. SLN metastasis not identified due to lack of tissue penetration.

TABLE 3 CHARACTERISTICS OF FALSE POSITIVE AND FALSE NEGATIVE FLUORESCENT LESIONS IN OVARIAN CANCER

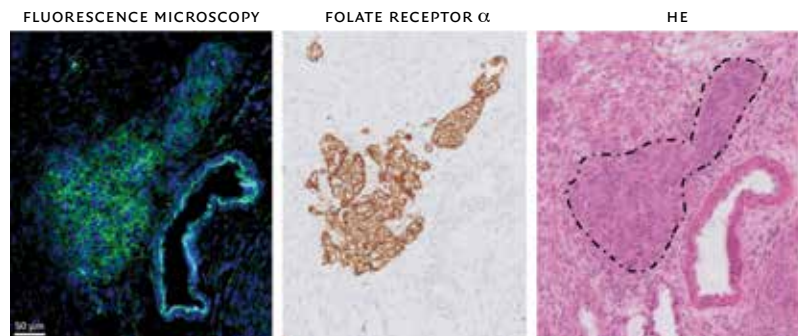
Patient ID	Location lesion	False positive or negative	Probable cause
1	Fallopian tube	False positive	FRα expression
2	Iliac lymph node	False positive	FRβ expression activated macrophages
2	Ligamentum rotundum	False positive	Autofluorescence collagen containing structure
4	Omentum	False negative	Inadequate penetration depth
5	Leiomyoma Uterus	False positive	Autofluorescence collagen containing structure
5	Leiomyoma Uterus	False positive	Autofluorescence collagen containing structure
5	Omentum biopsy	False positive	Unknown
7	Omentum	False negative	Inadequate penetration depth
8	Omentum	False negative	Inadequate penetration depth
8	Fallopian tube	False positive	FRα expression
10	Fallopian tube	False positive	FRα expression
12	Cervix	False positive	Autofluorescence collagen containing structure
12	Myometrium uterus	False positive	Autofluorescence collagen containing structure
12	Fallopian tube	False positive	FRα expression
12	Infundibulopelvic ligament	False positive	Autofluorescence collagen containing structure
12	Ovary (contralateral)	False positive	FRα expression

FIGURE 1 IDENTIFICATION OF OVARIAN CANCER METASTASES USING FLUORESCENCE IMAGING



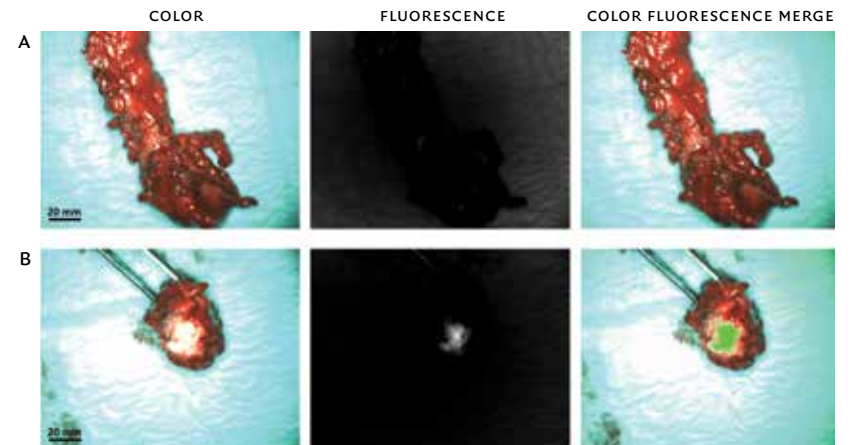
Identification of ovarian cancer metastases located on the intestine and mesentery using fluorescence imaging. Biopsies of lesions were found histologically to be metastases of serous adenocarcinoma.

FIGURE 2 HISTOPATHOLOGICAL EVALUATION OF FLUORESCENCE SIGNAL IN OVARIAN CANCER



Fluorescence signal is indicated with green, blue color represents cell nuclei stained with DAPI. Fluorescence microscopy showed clear membranous and cytoplasmic accumulation of EC17 in tumor cells. The fluorescent signal is located on all sites that stain positive for FR α expression, which is the anatomical site that appears to be a metastasis of serous ovarian adenocarcinoma on hematoxylin and eosin staining (dashed circle).

FIGURE 3 FALSE-NEGATIVE FLUORESCENT SIGNAL CAUSED BY A LACK OF DEPTH PENETRATION



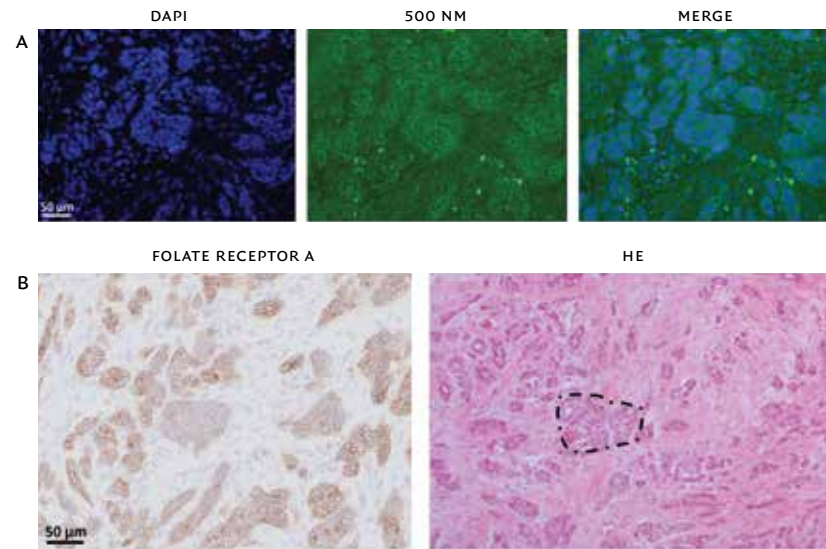
A. Example of a metastasized greater omentum, which was clinical suspicious, but showed no fluorescence signal from the outside.
B. After dissecting the omentum, strong fluorescent signal was identified. This observation shows the lack of tissue penetration at 500nm.

FIGURE 4 IDENTIFICATION OF BREAST CANCER METASTASES USING FLUORESCENCE IMAGING



Identification of a bisected primary breast cancer lesion using fluorescence imaging (dashed arrows). The arrow indicated autofluorescence signal from normal breast tissue. The tumor was found histologically to be an infiltrating breast cancer of no special type.

FIGURE 5 HISTOPATHOLOGICAL EVALUATION OF FLUORESCENCE SIGNAL IN BREAST CANCER



A. Fluorescence microscopy showed clear membranous and cytoplasmic accumulation of EC17 in tumor cells. Blue color represents cell nuclei stained with DAPI, fluorescence signal is indicated with green. Also a relatively high diffusely fluorescent background signal is seen, which is in concordance with the fluorescence images obtained with the intraoperative imaging system. B. Immunohistological staining for FR α expression shows a FR α positive infiltrating breast cancer of no special type (example in dashed circle). Clear concordance is observed between fluorescent signal and FR α positive malignant lesions.

Chapter 5

A novel tumor-specific agent for intraoperative near-infrared fluorescence imaging: a translational study in healthy volunteers and patients with ovarian cancer

Clin Cancer Res. 2016 Jun 15

CHARLOTTE HOOGSTINS, QUIRIJN TUMMERS, KATJA GAARENSTROOM, COR DE KROON, BAPTIST TRIMBOS, TJALLING BOSSE, VINCENT SMIT, JAAP VUYK, CORNELIS VAN DE VELDE, ADAM COHEN, PHILIP LOW, JACOBUS BURGGRAAF, ALEXANDER VAHRMEIJER

ABSTRACT

PURPOSE Completeness of cytoreductive surgery is a key prognostic factor for survival in patients with ovarian cancer. The ability to differentiate clearly between malignant and healthy tissue is essential for achieving complete cytoreduction. Using current approaches, this differentiation is often difficult and can lead to incomplete tumor removal. Near-infrared fluorescence imaging has the potential to improve the detection of malignant tissue during surgery, significantly improving outcome. Here, we report the use of OTL38, a near-infrared (796 nm) fluorescent agent that binds folate receptor alpha, that is expressed in >90% of epithelial ovarian cancers.

EXPERIMENTAL DESIGN We first performed a randomized, placebo-controlled study in 30 healthy volunteers. Four single increasing doses of OTL38 were delivered intravenously. At fixed times following drug delivery, tolerability and blood/skin pharmacokinetics were assessed. Next, using the results of the first study, three doses were selected and administered to 12 patients who had epithelial ovarian cancer and were scheduled for cytoreductive surgery. We measured tolerability and blood pharmacokinetics, as well as the ability to detect the tumor using intraoperative fluorescence imaging.

RESULTS Intravenous infusion of OTL38 in 30 healthy volunteers yielded an optimal dosage range and time window for intraoperative imaging. In 12 patients with ovarian cancer, OTL38 accumulated in folate receptor alpha-positive tumors and metastases, enabling the surgeon to resect an additional 29% of malignant lesions that were not identified previously using inspection and/or palpation.

CONCLUSIONS This study demonstrates that performing real-time intraoperative near-infrared fluorescence imaging using a tumor-specific agent is feasible and potentially clinically beneficial.

INTRODUCTION

The completeness of surgical tumor removal is an important factor for determining the survival of patients with a solid tumor. Despite advances in preoperative imaging techniques, during surgery the surgical oncologist must rely primarily upon inspection and/or palpation to identify the tumor tissue; however, these methods are often inadequate [1-3].

Ovarian cancer has the highest mortality rate of all gynecological cancers [4]. The surgical treatment of advanced-stage ovarian cancer (i.e., International Federation of Gynecology and Obstetrics stage IIb through stage IV) typically consists of cytoreductive surgery combined with systemic chemotherapy. Several studies have shown that the amount of residual tumor that remains following cytoreductive surgery is the most important prognostic indicator of survival [5-9]. Thus, because imaging modalities that improve tumor identification during surgery can increase the number and thoroughness of metastatic lesions resected during cytoreductive surgery, they can significantly improve patient outcome.

Near-infrared (NIR) fluorescence imaging is an innovative technique that can be used to detect tumor lesions during surgery [10]. NIR fluorescence is invisible to the human eye, but can be detected in the millisecond range using a dedicated imaging system. Because the imaging system can be toggled on and off rapidly, this approach allows the surgeon to identify malignant tissue in real time without altering the surgical field. In addition, NIR light can penetrate tissue on the order of centimeters, allowing the surgeon to delineate targets underneath the tissue surface [11, 12]. Despite its high potential in clinical applications, NIR fluorescence in surgical oncology has been used primarily with nonspecific agents previously available for clinical use. For example, indocyanine green is retained either in or around tumor tissue due to impaired secretion or increased vascular permeability and decreased lymphatic drainage; however, indocyanine green does not bind specifically to cancer tissue [13, 14]. This lack of specificity results in a high rate of intraoperative false positive images in patients with ovarian cancer [15]. Thus, fluorescent agents that specifically target cancer-specific targets are highly desired.

Folate receptor alpha (FR α) is a promising target, as it is robustly expressed on a variety of cancers of epithelial origin, including >90% of epithelial ovarian cancers [16-18]. Moreover, FR α is expressed at relatively low levels in healthy tissue, where it is expressed primarily at the apical membrane of polarized epithelial cells, including fallopian tube and endometrial tissue [16, 19, 20]. Thus,

when targeted with a fluorescent agent, background fluorescence will be low in healthy tissue, making this protein an ideal candidate target for fluorescence-guided ovarian cancer surgery. Importantly, because chemotherapy does not affect the expression of FR α , this protein can be targeted in both primary and interval cytoreductive surgical procedures [21, 22].

The potential of using a folate analog coupled to a dye that fluoresces outside of the NIR spectrum (e.g., folate-FITC) was demonstrated previously in a small patient series, yielding a positive fluorescence signal in three out of four patients with ovarian cancer [23]. Although this study showed the feasibility of detecting fluorescently labeled tumor deposits in real time, the approach did not allow the surgeon to detect lesions beneath the tissue surface. In addition, we found that using folate-FITC in both ovarian cancer and breast cancer produces high autofluorescence in healthy tissue (data not shown). This finding underscores the need for agents that fluoresce in the NIR spectrum.

OTL38 is a folate analog conjugated to a NIR fluorescent dye (excitation at 776 nm, emission at 796 nm); OTL38 has high specificity and affinity for FR α . Here, we first examined the tolerability, pharmacokinetics, and tissue and blood distribution of increasing doses of OTL38 in healthy volunteers. Based upon these results, we then determined the optimal dosage range and the imaging time window. We then used these parameters in a study in patients with epithelial ovarian cancer in order to determine the correlation between fluorescence detection and histopathology of the resected lesions. We also determined whether the detection of tumors using the traditional surgical view was improved with the addition of fluorescence imaging.

MATERIALS AND METHODS

STUDY DESIGN ◉ The primary objective of the study in healthy volunteers was to assess the tolerability and pharmacokinetics (in plasma and skin) of a single intravenous dose of OTL38; in addition, the results were used to determine the optimal dosage range and time window for performing intraoperative imaging in the subsequent study in patients with ovarian cancer. For the patient study, the objectives were to assess the tolerability and pharmacokinetics of OTL38, the efficacy with respect to intraoperative detection of ovarian cancer lesions, and the practical feasibility of the technique. The results were used to determine the optimal dose for intraoperative imaging. Because both studies were exploratory in nature, sample size was not based on a formal calculation

of statistical power. In the first study, tolerability and pharmacokinetics of a single intravenous dose of OTL38 were used as the endpoints. These same endpoints were used in the patient study; in addition, we also measured the efficacy of OTL38 in the intraoperative detection of ovarian cancer by measuring the following endpoints: TBR (tumor-to-background ratio), defined as the ratio between the fluorescent signal in the tumor tissue and the fluorescent signal in the tissue surrounding the tumor; concordance between the pathology results with respect to the presence of cancer and the imaging assessment; the number and location of FR α -positive, cancerous lesions identified the usual visual and/or tactile approaches with or without fluorescence imaging; and the surgeons' evaluation of the practical application of the technique. Data of all subjects participating in the studies was included in the analyses if the data could meaningfully contribute to the objectives of the studies.

For the study in healthy volunteers, we included 30 subjects who were 18-65 years of age and were considered healthy based on medical screening. For the patient study, we included twelve patients who had a high suspicion of epithelial ovarian cancer or a tissue-based diagnosis of epithelial ovarian cancer and were scheduled for primary or interval cytoreductive surgery. The main exclusion criteria were current pregnancy, history of anaphylactic reactions, impaired renal function (defined as EGFR <50 ml/min/1.73 m²), and impaired liver function (defined as ALT, AST, or total bilirubin levels that exceeded 3x the established upper limit of normal).

The study in healthy volunteers was a randomized, placebo-controlled design in which subjects were randomized to receive a single intravenous dose of 0.025, 0.05, 0.1, or 0.2 mg/kg OTL38 or placebo. The randomization code was generated by a study-independent statistician using SAS 9.1.3 for Windows (SAS Institute Inc., Cary, NC). The randomization code was made available for data analysis only after the study was completed. At fixed time points following administration, blood samples were collected and used to measure pharmacokinetics and to perform routine laboratory tests. Adverse events, ECG, and vital signs were recorded. The fluorescent signal in superficial skin was measured using the Artemis imaging system at fixed time points following intravenous administration of OTL38 or placebo (Fig. 1). After a dose cohort was completed, all data collected up to 24 hours following each dose were reviewed prior to increasing the dose. In the event of an unacceptable tolerability profile (based on the nature, frequency, and intensity of adverse events, as judged by the investigator), the dose was not increased. Subjects were assigned to a dosing group

based on the order in which they enrolled in the study. The study was performed in a double-blind fashion; thus, the investigator, staff, subjects, sponsor, and monitor were blinded with respect to the treatment until the end of the study. The placebo and OTL38 were formulated and packaged identically. The randomization list was made available only to the pharmacist who prepared the study drug, the individual who was responsible for sample bioanalysis, and the statisticians and programmers who prepared the blinded summaries, graphs, and listings to support the dosing decisions.

The patient study was a single ascending dose, open label exploratory study. The patient study was not randomized, and all patients received the active drug. Assignment to the dosage groups was based on the order in which the patients enrolled in the study. The patients received a one-hour intravenous infusion of OTL38 2-3 hours prior to the start of surgery. A dose-escalating scheme with planned doses of 0.025, 0.05, and 0.1 mg/kg (and the possibility to decrease the dose to 0.0125 mg/kg) was used. Dose escalation was terminated in the event of an unacceptable tolerability profile. Tolerability assessment (blood pressure, pulse, peripheral oxygen saturation, respiratory rate, ECG, temperature, and skin assessments) and blood collection for pharmacokinetics and routine laboratory tests were performed at regular intervals starting just prior to administration and lasting until 24 hours post-dosing. Adverse events and the concomitant use of other medications were recorded. Cytoreductive surgery generally included the removal of the uterine adnexa, uterus, and infracolic omentum, as well as resection of all macroscopic tumors, where possible. All surgical procedures were open procedures performed by an experienced gynecological oncologist using a midline abdominal incision. First, the primary tumor and metastases were identified in the surgical field using standard visual and tactile methods. Thereafter, the Artemis imaging system was used to identify NIR-fluorescent lesions. All tumor tissue identified by visual/tactile methods and NIR fluorescence was resected, provided it was both surgically feasible and clinically useful. Each resected lesion was marked on a case report form as being either fluorescent or non-fluorescent and as being either clinically suspected of malignancy or not (Fig. S1). All resected lesions were examined for tumor status by an experienced pathologist. A positive tumor that was fluorescent was considered a true positive; a negative lesion that was fluorescent was considered a false positive; and a positive tumor that was non-fluorescent was considered a false negative. In addition, we performed immunohistochemistry to demonstrate FR α and FR β expression coupled with fluorescence microscopy in order to evaluate OTL38 binding (Supplementary Materials and Methods).

INVESTIGATIONAL PRODUCT ● OTL38 (chemical formula: C₆₁H₆₃N₉Na₄O₁₇S₄; molecular weight: 1414.42 Da) consists of a folate analog conjugated to an NIR fluorescent dye. OTL38 (>96% purity) was obtained from On Target Laboratories (West Lafayette, IN). The drug was synthesized and manufactured at Aptuit (Harrisonville, MO) in compliance with Good Manufacturing Practices (Fig. S2). OTL38 was stored in frozen form at -20°C in vials containing 6 mg OTL38 free acid in 3 ml water. Before administration, the frozen vials were thawed, vortexed, and then diluted with 0.9% NaCl or 5% dextrose for intravenous infusion. OTL38 was diluted in either 20 ml or 220 ml and was infused over 10 or 60 minutes. Placebo consisted of a similar volume of 0.9% NaCl or 5% dextrose.

INTRAOPERATIVE NEAR-INFRARED FLUORESCENCE IMAGING SYSTEM ● Imaging was performed using the Artemis fluorescence imaging system (Quest Medical Imaging, Middenmeer, NL) [24]. The system consists of three wavelength-isolated light sources, including a 'white' light source and two separate near-infrared light sources. For this study, the camera and light engine were optimized for use with OTL38; specifically, they were designed to generate 7.5 mW/cm² at 760-nm light. Color video and fluorescence images were acquired simultaneously using separate sensors and were displayed in real time using custom-built optics and software, thereby displaying color video and NIR fluorescence images separately. A pseudo-colored (lime green) merged image of the color video and fluorescence images was also generated. The intensity of the light source was controlled using the Artemis software. The camera was attached to a freely moveable arm. During surgery, the camera and moveable arm were enclosed in a sterile shield and drape (Medical Technique Inc., Tucson, AZ).

ETHICS COMMITTEE APPROVAL ● Both studies were performed in accordance with the tenets established by the Helsinki Declaration of 1975 (as amended in Tokyo, Venice, Hong Kong, Somerset West, Edinburgh, Washington, and Seoul), ICH-GCP guidelines, and the laws and regulations of the Netherlands. In addition, both studies were approved by a certified medical ethics review board. All subjects provided written informed consent prior to the start of any study-related procedures. The healthy volunteer study and ovarian cancer patient study were registered in the European Clinical Trials Database under numbers 2013-004774-10 and 2014-002352-12, respectively; publicly accessible via the CCMO register (https://www.toetsingonline.nl/to/ccmo_search.nsf/Searchform?OpenForm).

PRACTICAL EVALUATION ◉ Directly following the surgical procedure, the surgeon was asked to complete a questionnaire regarding the practical application of the technique during the surgical procedure (Supplementary Materials and Methods).

VISUAL DETECTION ◉ Color and fluorescence images of seven representative surgical views of patients with confirmed ovarian cancer were captured from the videos recorded using the Artemis imaging system. Intra-observer variability was assessed by including a matching color and fluorescence image set twice (one set was a horizontal mirror image of the original), resulting in a total of eight sets of matching color and fluorescence images that were printed in full color; representative images are shown in Fig. 2. Three experienced gynecological oncologists were asked to mark clinically suspect lesions directly on the color images; they were then asked to mark clinically suspected lesions on the matching fluorescence images. Visual detection was performed *ex vivo* because intraoperative assessment of the number of lesions was not feasible.

PHARMACOKINETICS ANALYSIS ◉ The bioanalysis was performed using validated methodologies in compliance with good clinical laboratory practices at Analytical Biochemical Laboratory (Assen, the Netherlands). In brief, OTL38 was extracted from human K2EDTA plasma samples and urine samples using off-line solid-phase extraction, followed by analysis using liquid chromatography-mass spectrometry (APL-4000, Attodyne Inc., Toronto, Ontario, Canada). The assay's lower limit of quantification (LLOQ) and upper limit of quantification (ULOQ) were 2.00 and 500 ng/ml, respectively. The coefficient of variability for intra-day and inter-day plasma LLOQ and urine LLOQ was 8.2% and 13.3%, respectively.

STATISTICAL ANALYSIS ◉ SPSS statistical software package (version 20.0, IBM Corp., Armonk, NY) was used for statistical analyses. The individual OTL38 concentration-time profiles were analyzed using non-compartmental methods. The obtained PK parameters (i.e., AUC, C_{MAX} , and T_{MAX}) were summarized per treatment group, including the number of subjects, mean values, standard deviation (SD), median values, and minimum and maximum values. The fluorescence signal in the skin (healthy volunteers) or tumor and background tissue (patients) was quantified using ImageJ (version 1.49b, National Institutes of Health, Bethesda, MD; <http://imagej.nih.gov/ij/>). Using ImageJ, a region of interest (ROI) was drawn on the images and used to quantify the fluorescence

signal in arbitrary units (AU). TBR was calculated by dividing the fluorescence signal of the tumor by the fluorescence signal of the surrounding tissue. To compare the TBR values and fluorescence background signals between malignant and benign (i.e., false positive) lesions and between different dose groups, an independent samples Student's t-test was performed. TBR is reported as the mean, SD, and range. Patient characteristics are reported as the median, SD, and range. Tumor deposits that were marked on the color and fluorescence images were counted. To compare the number of deposits between the color and fluorescence images, a paired Student's t-test was performed.

RESULTS

CLINICAL TRIAL IN HEALTHY VOLUNTEERS ◉ This study included a total of 30 subjects (18 females and 12 males) 18-64 years of age with a BMI of 18-30 kg/m² (see Fig. S3 for the CONSORT flow diagram).

TOLERABILITY ◉ OTL38 at 0.025mg/kg diluted in 20 ml 0.9% NaCl infused for 10 or 60 minutes caused moderate hypersensitivity in two out of the four subjects receiving this dose. These reactions were not classic allergic reactions, as they were not accompanied by an increase in tryptase or IGE, nor did they involve the complement system (see Data File S1). Subsequent studies using dynamic light scattering and scanning electron microscopy revealed that these reactions may have been due to aggregation of the OTL38 compound in the 0.9% NaCl solution. This aggregation was reduced considerably when OTL38 was diluted in 5% dextrose and when the infusion volume was increased. Because OTL38 did not aggregate measurably when diluted to 7.5 μ M in 5% dextrose, the study was restarted at the lowest dose with OTL38 dissolved in 220 ml 5% dextrose; this volume was infused for a period of 60 minutes.

Infusion of 0.025, 0.05, and 0.1 mg/kg OTL38 diluted in 5% dextrose was associated with mild adverse events that disappeared gradually during and/or after the infusion. These adverse events were dose-dependent and suggestive of hypersensitivity (e.g., abdominal discomfort, nausea, and pruritus), but did not require intervention. All adverse events are listed in Table S1. At the 0.2 mg/kg dose, some subjects developed adverse events of moderate severity, which required the temporary interruption of the infusion or the administration of an antihistamine (e.g., 1-2 mg clemastine intravenously). Overall, more than 80% of these adverse events were mild in severity, and all other adverse events were moderate in severity. Despite the development of adverse events, the infusion

of OTL38 at 0.025-0.2 mg/kg did not cause clinically meaningful changes relative to baseline with respect to laboratory values, ECG, or vital signs.

PHARMACOKINETICS ● The maximum blood plasma concentration was achieved with each dose immediately at the end of the infusion and declined thereafter with a half-life of 2-3 hours (Fig. S4). Table S2 summarizes the most important pharmacokinetics (PK) parameters in each treatment group.

OTL38 excreted in the urine (expressed as a percentage of the dose administered) increased with increasing dose, and the highest level was approximately 11% for the highest dose (0.2 mg/kg). It is therefore reasonable to assume that the relatively low recovery is due in part to the lower limit of detection for OTL38 in urine.

PHARMACOKINETICS IN SUPERFICIAL TISSUE ● Figure 1 shows example images obtained using the Artemis imaging system. Although OTL38 was cleared from the plasma 2-3 hours after intravenous infusion, our analysis of the fluorescence signal in the skin revealed that fluorescence increased initially, remained increased for six hours, and then decreased with a half-life of approximately 15 hours (Fig. 1).

CLINICAL TRIAL IN PATIENTS WITH OVARIAN CANCER ● Fourteen patients initially enrolled in this study. However, because the study drug was temporarily unavailable, one patient could not participate, another patient withdrew from the study. Thus, a total of 12 patients 49-77 years of age with a BMI of 20-41 kg/m² received OTL38 (see Fig. S5 for the CONSORT flow diagram). The surgical procedure, histology, differentiation grade, and International Federation of Gynecology and Obstetrics (FIGO) stages are summarized in Table 1.

DOSE ESCALATION ● Patients 1, 2, and 3 received a starting dose of 0.025 mg/kg. After we reviewed the safety and efficacy data, the dose was increased to 0.05 mg/kg in the next three patients. However, when the 3 patients 4, 5, and 6 received this higher dose, the number and severity of symptoms (primarily consisting of abdominal discomfort, nausea, and pruritus) increased. In addition, TBR appeared to decrease. Therefore, the dose was decreased to 0.0125 mg/kg for the next three patients (patients 7, 8, and 9), yielding fewer, less severe symptoms, as well as an increase in TBR. Nevertheless, even at this lowest dose, mild, self-limiting adverse events were reported. After reviewing the safety and

efficacy data collected using all three doses, 0.0125 mg/kg was chosen as the optimal dose for the expansion cohort (patients 10, 11, and 12). In retrospect, this lower dose was a good choice, as adverse symptoms were minimal and TBR was maximal. Table S3 and Fig. S6 summarize the TBR results.

OTHER ADVERSE EVENTS ● One patient who received a dose of 0.0125 mg/kg OTL38 developed a case of post-operative hospital-acquired pneumonia and coughing-induced wound dehiscence. These complications were considered unrelated to OTL38 administration. The complete list of all adverse events recorded in the patients is provided in Table S4. Administration of OTL38 itself did not lead to any obvious changes in laboratory values, ECG, vital signs, or temperature.

PHARMACOKINETICS ● The PK profile of OTL38 in patient blood was similar to the profile measured in the healthy volunteers. Specifically, with each dose, the maximum concentration was achieved at the end of the infusion. After stopping the infusion, plasma concentration decreased with a half-life of 2-3 hours (Fig. S4).

INTRAOPERATIVE NEAR-INFRARED FLUORESCENCE IMAGING ● Lesions could be detected clearly after OTL38 administration. The optimal camera exposure time was dependent on OTL38 dose, with lower doses requiring longer exposure times. At higher doses, the longer exposure time led to saturated images; however, in all cases it was possible to use a sufficiently brief exposure time in order to obtain real-time images. Figure 3 shows an example of fluorescent lesions that were subsequently confirmed as ovarian cancer metastases on histopathology. A total of 83 fluorescent lesions were resected during the surgeries; 62 of these lesions were confirmed as malignant on histopathology (i.e., true positives). Strikingly, 18 (29%) of these true positive lesions were not detected using standard inspection and/or palpation methods. Mean TBR was 4.4 (SD: 1.46, range: 1.7-9.8), and TBR generally decreased with increasing doses, likely due to increased background signal. TBR was constant throughout the surgical procedure, and fluorescence could be detected for at least six hours after infusion. Importantly, using NIR fluorescence enabled us to detect malignant lesions up to 8 mm below the tissue surface, showing the added value of using light in the NIR spectrum (Movie S1).

HISTOPATHOLOGY OF RESECTED LESIONS ● No malignant disease was found in 21 of the 83 fluorescent lesions, corresponding to a false positive rate of 23%. These false positive lesions were observed primarily in lymph nodes, representing 52% of all false positive lesions (Table S5). Additional staining experiments and a closer examination of these lymph nodes revealed that activated macrophages, accumulated in the sinuses of the lymph node, express folate receptor beta (FR β), which is also a binding target for OTL38. Our immunofluorescence experiments revealed that the fluorescence signal co-localized with FR β staining (Fig. 4). Other false positive results arose due to the expression of FR α on the apical membrane of non-cancerous epithelial cells in the uterus and fallopian tubes, which are routinely resected during cytoreductive surgery. The mean TBR of the false positive lesions was 5.4 (SD: 2.0, range: 1.8-9.3), which did not differ sufficiently from true positive lesions (mean: 4.4, range: 1.7-9.8) to allow us to differentiate between false positive and true positive lesions based solely on TBR. We observed only two false negative lesions. Finally, fluorescence microscopy revealed the accumulation of OTL38 in the membrane and cytoplasm of FR α -expressing tumor cells (for representative images, see Fig. 5).

VISUAL DETECTION ● The examination of tumor deposits based on color images obtained from the intraoperative videos allowed us to identify an average of 8.3 (SD: 5.4, range: 1-18) lesions per image. In contrast, performing the same assessment using the matching NIR fluorescence images allowed us to identify an average of 17.6 (SD: 10.8, range: 5-45) lesions per image, reflecting a more than two-fold improvement in our ability to detect tumor lesions (Fig. 2).

PRACTICAL EVALUATION ● The use of fluorescence imaging did not interfere with the surgeon's ability to perform cytoreductive surgery, and the majority of participating surgeons reported that they found the technique to be useful (Supplementary Materials and Methods).

DISCUSSION

Here, we report the successful use of the first tumor-specific NIR fluorescence based-imaging agent to target FR α in ovarian cancer, significantly increasing removal of tumor lesions.

In healthy volunteers, OTL38 caused moderate hypersensitivity; however, these reactions were easily managed. Given their symptomology, these reactions were likely pseudoallergic, a finding that has been described previously by

Szebeni with respect to radiocontrast media [25]. Moreover, investigating the cause of this hypersensitivity led to the development of procedures designed to minimize or eliminate this reaction in our subsequent study with cancer patients. This was likely related to aggregation of OTL38 rather than a classic allergic response to the drug, suggesting that the severity may be reduced further by modifying the drug's formulation. Regardless, even these reactions were not severe enough to preclude the administration of a single dose of OTL38.

In healthy volunteers, the agent was essentially cleared from the plasma within 2-3 hours of intravenous delivery; however, a stable signal remained visible in the skin for at least six hours after dosing. This information was extremely valuable for determining the optimal time window for intraoperative imaging in patients, in which a favorable TBR was required during the surgical procedure. Our assessment of TBR at all doses revealed that the TBR of fluorescent lesions was maintained throughout the surgical procedure (i.e., 2-6 hours after dosing). However, because the fluorescent lesions were resected during surgery, we were unable to track the TBR of individual lesions over time.

A sufficiently high TBR is needed in order to optimally detect the tumor; in our study, a TBR of approximately 4.4 allowed the clear detection of tumor deposits. Higher doses (non-quenched) of OTL38 may translate into higher TBR, assuming linear binding of the agent to the tumor and background tissue. However, because the tumor contains a fixed number of receptors, it is conceivable that even with a low dose, the majority of FR α molecules in the tumor tissue will be bound by the agent. Therefore, higher doses will not necessarily increase the tumor-specific signal but might lead to increased nonsaturable, non-specific background binding, resulting in a less favorable TBR at higher doses. Indeed, the highest dose used in this study (0.05 mg/kg) resulted in a high background signal and lower TBR value, whereas the lowest dose tested (0.0125 mg/kg) yielded the highest TBR and—most importantly—the mildest symptoms. To obtain the best imaging results, the exposure times differed between the different dosing groups; thus, the lowest dose (0.0125 mg/kg) required the longest exposure time (75 ms). Nevertheless, even this relatively longer exposure time enabled us to perform real-time imaging.

When translated to our patient cohort, the optimal dose of OTL38 (i.e., 0.0125 mg/kg) enabled the surgeons to successfully identify malignant lesions with reasonably high sensitivity and specificity. Moreover, 29% of all resected malignant lesions would have gone undetected without the aid of fluorescence-based imaging. Unfortunately, the relatively low number of patients precluded our ability to calculate the specificity and sensitivity of the technique. Moreover,

our inability to study true negatives precluded a clear assessment of specificity. Nevertheless, both the *in situ* and *ex vivo* visual detection of lesions were clearly improved by the use of fluorescence-based imaging. With respect to *in situ* detection, 29% more lesions were resected. However, even this increase may underestimate the total number of lesions that could be detected during surgery, as resection is dependent upon several factors other than detection. Lastly, our *ex vivo* visual detection was performed using still images, as it was not feasible to count lesions during surgery. Although this approach is commonly used and yields useful information, it may be considered suboptimal, as three-dimensional and tactile information is lost.

Although epithelial ovarian cancer cells overexpress FR α , this receptor is also expressed—albeit to a lesser extent—at the apical membrane of various non-cancerous epithelial cells. During surgery, we noted mild, homogenous fluorescence of the uterus and the fallopian tubes, and biopsy revealed FR α expression in these non-malignant tissues, consistent with previous reports [17, 26]. The fluorescence signal in these tissues was homogenous and was clearly distinguishable from the fluorescence measured in the tumor deposits.

In the majority of our patients, we detected brightly fluorescent lymph nodes, and only a small number of these lymph nodes actually contained ovarian cancer metastases. The fluorescence measured in the non-cancerous lymph nodes was likely due to OTL38 binding to activated macrophages, which express FR β [27-30]. On the other hand, the formation of OTL38 aggregates and non-specific uptake by lymph nodes is unlikely, as dissolving the agent at 7.5 μ M in 5% dextrose did not lead to the formation of measurable aggregates. Indeed, given that only three of the 12 patients received the highest dose (0.05 mg/kg), corresponding to a molarity slightly higher than 7.5 μ M (9.5-11.8 μ M OTL38), the presence of aggregates in the infusion solution is highly unlikely. In addition, to further minimize the likelihood of aggregate formation in the circulation, the solution was infused for 60 minutes. Although this apparent false positive fluorescence in the lymph nodes could be considered a drawback of this imaging agent, activated macrophages may actually be tumor-associated macrophages that play a role in preparing the tumor environment for metastasis [31-33]. This notion is supported by our finding that FR β -expressing macrophages were also found in primary tumors as well as in lymph nodes that did contain metastasized tumor cells (Fig. S7). Until the precise role of FR β -expressing macrophages in the lymph nodes is determined, lymph nodes should be resected solely on the basis of standard clinical assessments.

The use of fluorescent light in the near-infrared spectrum allowed us to detect lesions beneath the tissue surface, which is a major improvement over agents that use light outside the NIR spectrum [23, 34, 35]. For example, in our study malignant lesions were visible up to 11 cm below the tissue surface. In addition, most biological tissues have extremely low autofluorescence when excited by light in the NIR spectrum [36, 37]. OTL38 also has several advantageous pharmacokinetic properties, including long residence time in the tumor and relatively rapid clearance from plasma; these properties provide the surgeon with a long window of time in which the tumor lesions can be detected. Unlike fluorescent antibodies—which have a much longer terminal half-life—OTL38 can be administered shortly before surgery [38].

Although more tumor deposits can be visualized and resected using intraoperative fluorescence imaging with OTL38 compared to conventional methods, more prospective research is necessary to establish the effect on overall survival. In addition, the diagnostic accuracy of fluorescence imaging with OTL38 should be further assessed in a larger patient group.

In conclusion, we provide the first evidence that a specific intraoperative NIR imaging agent can be used to increase the efficacy of tumor removal in patients with ovarian cancer. Our approach to clinical translation using both healthy subjects and patients in the same Phase I protocol allowed us to rapidly determine the optimal dose, formulation, and time window for intraoperative imaging, thereby greatly increasing the level of cytoreduction achieved in patients with ovarian cancer.

REFERENCES

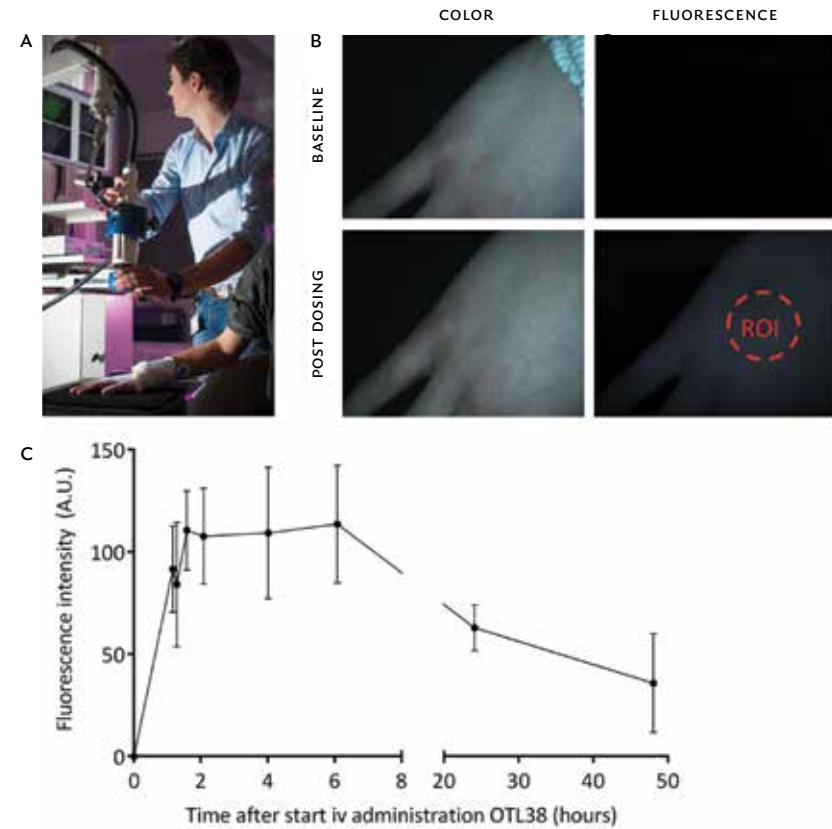
- 1 Frangioni JV. In vivo near-infrared fluorescence imaging. *Curr Opin Chem Biol* 2003;7:626-34.
- 2 Weissleder R, Pittet MJ. Imaging in the era of molecular oncology. *Nature* 2008;452:580-9.
- 3 Lim MC, Seo SS, Kang S, Kim SK, Kim SH, Yoo CW, et al. Intraoperative image-guided surgery for ovarian cancer. *Quant Imaging Med Surg* 2012;2:114-7.
- 4 Ferlay J, Soerjomataram I, Dikshit R, Eser S, Mathers C, Rebelo M, et al. Cancer incidence and mortality worldwide: sources, methods and major patterns in GLOBOCAN 2012. *Int J Cancer* 2015;136:E359-E386.
- 5 Chang SJ, Bristow RE, Ryu HS. Impact of complete cytoreduction leaving no gross residual disease associated with radical cytoreductive surgical procedures on survival in advanced ovarian cancer. *Ann Surg Oncol* 2012;19:4059-67.
- 6 Vergote I, Trope CG, Amant F, Kristensen GB, Ehlen T, Johnson N, et al. Neoadjuvant chemotherapy or primary surgery in stage IIIc or IV ovarian cancer. *N Engl J Med* 2010;363:943-53.
- 7 Bristow RE, Tomacruz RS, Armstrong DK, Trimble EL, Montz FJ. Survival effect of maximal cytoreductive surgery for advanced ovarian carcinoma during the platinum era: a meta-analysis. *J Clin Oncol* 2002;20:1248-59.
- 8 Hoskins WJ, McGuire WP, Brady MF, Homesley HD, Creasman WT, Berman M, et al. The effect of diameter of largest residual disease on survival after primary cytoreductive surgery in patients with suboptimal residual epithelial ovarian carcinoma. *Am J Obstet Gynecol* 1994;170:974-9.
- 9 Bristow RE, Berek JS. Surgery for ovarian cancer: how to improve survival. *Lancet* 2006;367:1558-60.
- 10 Vahrmeijer AL, Hutterman M, van der Vorst JR, van de Velde CJ, Frangioni JV. Image-guided cancer surgery using near-infrared fluorescence. *Nat Rev Clin Oncol* 2013;10:507-18.
- 11 Frangioni JV. In vivo near-infrared fluorescence imaging. *Curr Opin Chem Biol* 2003;7:626-34.
- 12 Chance B. Near-infrared (NIR) optical spectroscopy characterizes breast tissue hormonal and age status. *Acad Radiol* 2001;8:209-10.
- 13 Maeda H, Wu J, Sawa T, Matsumura Y, Hori K. Tumor vascular permeability and the EPR effect in macromolecular therapeutics: a review. *J Control Release* 2000;65:271-84.
- 14 Matsumura Y, Maeda H. A new concept for macromolecular therapeutics in cancer chemotherapy: mechanism of tumorotropic accumulation of proteins and the antitumor agent smancs. *Cancer Res* 1986;46:6387-92.
- 15 Tummers QR, Hoogstins CE, Peters AA, de Kroon CD, Trimbos JB, van de Velde CJ, et al. The Value of Intraoperative Near-Infrared Fluorescence Imaging Based on Enhanced Permeability and Retention of Indocyanine Green: Feasibility and False-Positives in Ovarian Cancer. *PLoS One* 2015;10:e0129766.
- 16 O'Shannessy DJ, Somers EB, Smale R, Fu YS. Expression of folate receptor-alpha (FRA) in gynecologic malignancies and its relationship to the tumor type. *Int J Gynecol Pathol* 2013;32:258-68.
- 17 Parker N, Turk MJ, Westrick E, Lewis JD, Low PS, Leamon CP. Folate receptor expression in carcinomas and normal tissues determined by a quantitative radioligand binding assay. *Anal Biochem* 2005;338:284-93.
- 18 Kalli KR, Oberg AL, Keeney GL, Christianson TJ, Low PS, Knutson KL, et al. Folate receptor alpha as a tumor target in epithelial ovarian cancer. *Gynecol Oncol* 2008;108:619-26.
- 19 Vergote IB, Marth C, Coleman RL. Role of the folate receptor in ovarian cancer treatment: evidence, mechanism, and clinical implications. *Cancer Metastasis Rev* 2015;34:41-52.
- 20 Low PS, Henne WA, Doorneweerd DD. Discovery and development of folic-acid-based receptor targeting for imaging and therapy of cancer and inflammatory diseases. *Acc Chem Res* 2008;41:120-9.
- 21 Crane LM, Arts HJ, van OM, Low PS, van der Zee AG, van Dam GM, et al. The effect of chemotherapy on expression of folate receptor-alpha in ovarian cancer. *Cell Oncol (Dordr)* 2012;35:9-18.
- 22 Despierre E, Lambrechts S, Leunen K, Berteloot P, Neven P, Amant F, et al. Folate receptor alpha (FRA) expression remains unchanged in epithelial ovarian and endometrial cancer after chemotherapy. *Gynecol Oncol* 2013;130:192-9.
- 23 van Dam GM, Themelis G, Crane LM, Harlaar NJ, Pleijhuis RG, Kelder W, et al. Intraoperative tumor-specific fluorescence imaging in ovarian cancer by folate receptor-alpha targeting: first in-human results. *Nat Med* 2011;17:1315-9.
- 24 van Driel PB, van de Giessen M, Boonstra MC, Snoeks TJ, Keereweer S, Oliveira S, et al. Characterization and evaluation of the artemis camera for fluorescence-guided cancer surgery. *Mol Imaging Biol* 2015;17:413-23.
- 25 Szebeni J. Complement activation-related pseudoallergy: a new class of drug-induced acute immune toxicity. *Toxicology* 2005;216:106-21.
- 26 Wu M, Gunning W, Ratnam M. Expression of folate receptor type alpha in relation to cell type, malignancy, and differentiation in ovary, uterus, and cervix. *Cancer Epidemiol Biomarkers Prev* 1999;8:775-82.
- 27 Shen J, Hilgenbrink AR, Xia W, Feng Y, Dimitrov DS, Lockwood MB, et al. Folate receptor-beta constitutes a marker for human proinflammatory monocytes. *J Leukoc Biol* 2014;96:563-70.
- 28 O'Shannessy DJ, Somers EB, Wang LC, Wang H, Hsu R. Expression of folate receptors alpha and beta in normal and cancerous gynecologic tissues: correlation of expression of the beta isoform with macrophage markers. *J Ovarian Res* 2015;8:29.
- 29 Puig-Kroger A, Sierra-Filardi E, Dominguez-Soto A, Samaniego R, Corcuera MT, Gomez-Aguado F, et al. Folate receptor beta is expressed by tumor-associated macrophages and constitutes a marker for M2 anti-inflammatory/regulatory macrophages. *Cancer Res* 2009;69:9395-403.
- 30 Kurahara H, Takao S, Kuwahata T, Nagai T, Ding Q, Maeda K, et al. Clinical significance of folate receptor beta-expressing tumor-associated macrophages in pancreatic cancer. *Ann Surg Oncol* 2012;19:2264-71.
- 31 Smith HA, Kang Y. The metastasis-promoting roles of tumor-associated immune cells. *J Mol Med (Berl)* 2013;91:411-29.
- 32 Joyce JA, Pollard JW. Microenvironmental regulation of metastasis. *Nat Rev Cancer* 2009;9:239-52.
- 33 Lewis CE, Pollard JW. Distinct role of macrophages in different tumor microenvironments. *Cancer Res* 2006;66:605-12.
- 34 Keereweer S, van Driel PB, Snoeks TJ, Kerrebijn JD, Baatenburg de Jong RJ, Vahrmeijer AL, et al. Optical image-guided cancer surgery: challenges and limitations. *Clin Cancer Res* 2013;19:3745-54.
- 35 Weissleder R, Ntziachristos V. Shedding light onto live molecular targets. *Nat Med* 2003;9:123-8.
- 36 Monici M. Cell and tissue autofluorescence research and diagnostic applications. *Biotechnol Annu Rev* 2005;11:227-56.
- 37 Monici M, Basile V, Romano G, Evangelisti L, Lucarini L, Attanasio M, et al. Fibroblast autofluorescence in connective tissue disorders: a future tool for clinical and differential diagnosis? *J Biomed Opt* 2008;13:054025.
- 38 Rosenthal EL, Warram JM, de BE, Chung TK, Korb ML, Brandwein-Gensler M, et al. Safety and Tumor Specificity of Cetuximab-IRDye800 for Surgical Navigation in Head and Neck Cancer. *Clin Cancer Res* 2015;21:3658-66.

TABLE 1 SURGERY AND TUMOR CHARACTERISTICS OF OVARIAN CANCER PATIENTS

Patient ID	Surgical procedure	Diagnosis	FIGO stage	Grade	Metastases identified	Tumor FRA positive	Fluorescence imaging successful
1	Interval debulking	Serous adenocarcinoma	4	III	Yes	Yes	Yes
2	Interval debulking	Serous adenocarcinoma	4	III	Yes	Yes	Yes
3	Interval debulking	Serous adenocarcinoma	3c	III	Yes	Yes	Yes
4	Interval debulking	Serous adenocarcinoma	4	III	Yes	Yes	Yes
5	Interval debulking	Serous adenocarcinoma	3c	III	Yes	Yes	Yes
6	Primary debulking	Mucinous adenocarcinoma	3b	Unknown	Yes	Yes	Yes
7	Debulking recurrent disease	Endometrioid carcinoma	3b	II	Yes	Yes	Yes
8	Primary debulking	Serous adenocarcinoma	3c	III	Yes	Yes	Yes
9	Debulking recurrent disease	Clear cell carcinoma	3	I	Yes	Yes	Yes
10	Interval debulking	Mucinous adenocarcinoma	3c	Unknown	Yes	Yes	Yes
11	Debulking recurrent disease	Endometrioid carcinoma	3c	III	Yes	Yes	Yes
12	Interval debulking	Adenocarcinoma†	3c	III	Yes	Yes	Yes

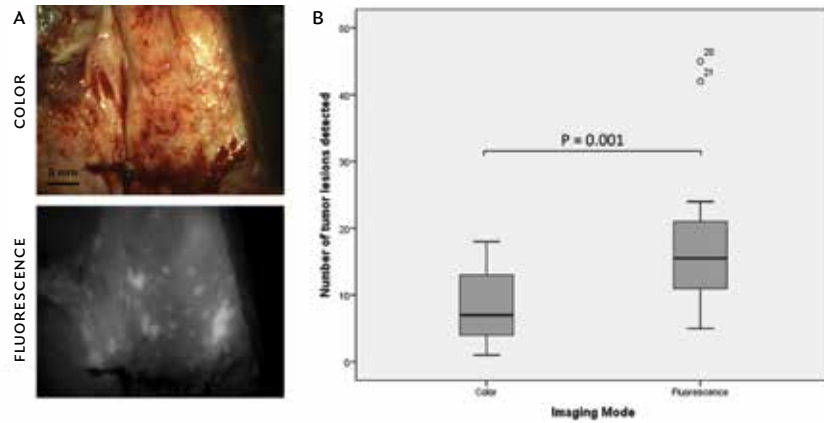
FIGO, International Federation of Gynecology and Obstetrics; FRA, folate receptor alpha
 † Further classification was not possible due to prior chemotherapy

FIGURE 1 FLUORESCENCE MEASUREMENTS IN THE SKIN OF HEALTHY VOLUNTEERS



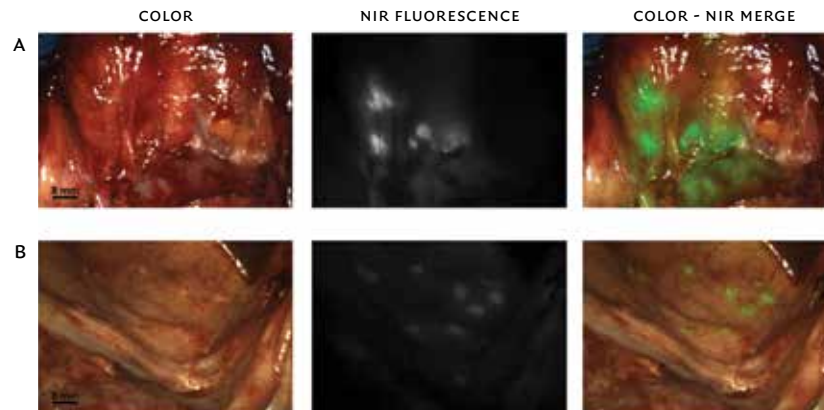
A. A researcher measuring skin fluorescence using the Artemis imaging system.
 B. Color (left column) and fluorescence (right column) images of a healthy volunteer at baseline (upper row) and after receiving a dose of OTL38 (lower row). Note that a bright fluorescent signal is detected after dosing, and fluorescence intensity can be measured within a region of interest (ROI) (dashed circle).
 C. Fluorescence intensity (measured in arbitrary units) in an ROI over time (in hours). The fluorescence signal reached peak levels at approximately 2 hours and was stable for up to 6 hours, then decreased over the following 48 hours.

FIGURE 2 VISUAL DETECTION OF TUMOR DEPOSITS EX VIVO



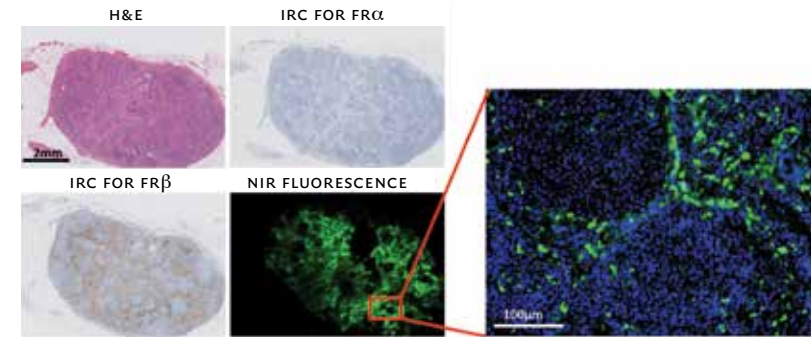
A. Representative color (upper panel) and fluorescence (lower panel) images used to quantify the visual detection of tumor deposits.
 B. Box plot summarizing the number of tumor lesions detected based on the matched color and fluorescence images.

FIGURE 3 INTRAOPERATIVE DETECTION OF OVARIAN CANCER METASTASES USING FLUORESCENCE-BASED IMAGING



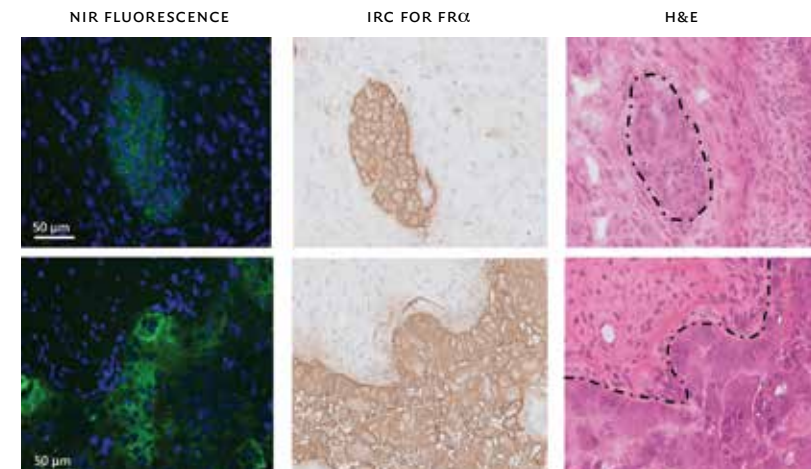
A-B. Color (left column), fluorescence (middle column), and merged (right column) images of retroperitoneal lymph nodes containing metastases of ovarian cancer (A) and superficial peritoneal metastases of ovarian cancer (B).

FIGURE 4 HISTOPATHOLOGICAL EVALUATION AND FLUORESCENCE SIGNAL OF A FALSE POSITIVE LYMPH NODE



The images show a fluorescent lymph node (bottom right panel) that did not contain ovarian cancer metastases on hematoxylin and eosin (H&E) staining (upper left panel) and was negative for $FR\alpha$ immunostaining (upper right panel). Immunostaining for $FR\beta$ showed positive staining in the sinuses, but not in the follicles (lower left panel). The magnified image at the right shows that the fluorescence pattern was localized to the sinuses, consistent with $FR\beta$ staining.

FIGURE 5 HISTOPATHOLOGICAL EVALUATION AND FLUORESCENCE SIGNAL IN OVARIAN CANCER



Representative samples from two different patients. Fluorescence microscopy (left column) shows clear membranous and cytoplasmic accumulation of OTL38 in tumor cells. The fluorescence signal is indicated in green, and the nuclei were counterstained with DAPI (blue). The fluorescence pattern is consistent with $FR\alpha$ expression measured using immunohistochemistry (middle column), which corresponds to the anatomical site containing a serous ovarian adenocarcinoma metastasis visible on hematoxylin and eosin (H&E) staining (right column, dashed outline).

Chapter 6

Feasibility of Folate Receptor-targeted Intraoperative Fluorescence Imaging during Staging Procedures for Early Ovarian Cancer

European Journal of Gynaecological Oncology,
publication pending

CHARLOTTE HOOGSTINS, LEONORA BOOGERD, KATJA GAARENSTROOM,
COR DE KROON, JOCHGUM BELTMAN, BAPTIST TRIMBOS, TJALLING BOSSE,
JAAP VUYK, PHILIP LOW, JACOBUS BURGGRAAF, ALEXANDER VAHRMEIJER

ABSTRACT

OBJECTIVES Completeness of staging is an independent prognostic factor for survival in surgical staging procedures for early ovarian cancer. Near-infrared (NIR) fluorescence imaging has the potential to improve the intraoperative assessment of metastatic spread and thus completeness of staging. Feasibility of folate receptor alpha (FR α) targeted fluorescence imaging using OTL38, a folate analogue conjugated to an NIR fluorescent dye, has been previously demonstrated in advanced ovarian cancer. We hypothesized that in early ovarian cancer, fluorescence imaging using OTL38 could lead to more accurate detection of (occult) ovarian cancer metastases, allowing gynecologic surgeons to take targeted rather than blind biopsy samples.

METHODS / MATERIALS Six patients scheduled to undergo a staging procedure for suspected early stage ovarian cancer, received an intravenous infusion of 0.0125 mg/kg OTL38 2-3 hours prior to surgery. We assessed tolerability, pharmacokinetics and the feasibility of intraoperative NIR fluorescence detection of ovarian cancer lesions. Feasibility was evaluated using histopathological analysis, tumor-to-background ratio and number of false positive and negative lesions.

RESULTS Distinction between a malignant and benign primary tumor was possible with OTL38 based fluorescence imaging. In addition, 9 fluorescent lesions, all lymph node (LN) clusters, were detected intraoperatively. Tumor cells were not demonstrated in any of the biopsy samples taken during staging procedures, including the fluorescent lesions. Therefore all fluorescent LNs were false positives.

CONCLUSIONS Metastatic lesions were not present in the patients with confirmed early ovarian cancer; hence the anticipated added value of NIR fluorescence imaging could not be demonstrated in this study. Fluorescence imaging led to resection of non-malignant LNs, as comprehensive lymph node dissection should be pursued in surgical staging procedures, this should not impede application of OTL38. Importantly, fluorescence imaging allowed distinction between a malignant and benign primary tumor and had no false negatives.

INTRODUCTION

In ovarian cancer distinction is made between early and advanced stage disease. Both surgical procedure and the need for (neo) adjuvant treatment differ between stages. In advanced ovarian cancer (FIGO 11b-IV) a cytoreductive procedure is performed. During this procedure complete cytoreduction of all cancer lesions is the primary goal, as the amount of residual tumor negatively impacts survival [1, 2]. In early ovarian cancer (FIGO 1-11a) a surgical staging procedure is performed. During surgical staging biopsy samples of clinically suspected areas are obtained. These are supplemented with biopsy samples of predefined areas, which are typical locations of ovarian cancer metastases. These include pelvic and para-aortic lymph nodes (LNs), right hemi-diaphragm, paracolic gutters, pelvic sidewalls, ovarian fossa, bladder peritoneum and recto-uterine pouch. The purpose of these 'blind biopsies' is to determine whether there is occult microscopic metastatic spread. In case of metastatic spread patients are upstaged and thus require additional treatment, i.e. chemotherapy. When the ovarian cancer has not metastasized and is true early stage, resection of the primary tumor is adequate and chemotherapy can be omitted [3-5]. Consequently, clear intraoperative assessment of the presence of metastatic spread is of utmost importance during staging procedures.

Near-infrared (NIR) fluorescence imaging is a relatively novel imaging modality, which makes use of invisible fluorescent light to enhance contrast between target and background tissue. Various favorable optical properties, i.e. fast acquisition time, low autofluorescence and penetration depths up to 1cm, make NIR fluorescence imaging eminently suitable for intraoperative application [6-8]. In oncologic surgery, NIR fluorescence imaging can enable surgeons to clearly distinguish malignant from benign tissue [9, 10]. This commonly requires the administration of an exogenous fluorescent contrast agent. Preferably these agents specifically target biomarkers that are overexpressed on tumor cells.

The folate receptor alpha (FR α) is a biomarker that is strongly expressed on >90% of epithelial ovarian cancers, while expression on healthy tissues is low [11-13]. This prompted the development of FR α targeting agents for fluorescence imaging of ovarian cancer. These agents, EC17 (fluoresces outside the NIR spectrum) and OTL38 (fluoresces within the NIR spectrum), were studied in ovarian cancer patients in previous clinical trials [14-16]. Feasibility of FR α targeted fluorescence imaging was demonstrated, as the use of these agents allowed gynecologic surgeons to visualize and resect more ovarian cancer lesions. Regrettably the use of OTL38 also had a drawback as in 23% of resected

fluorescent lesions, histopathology could not confirm the presence of tumor cells [15]. This false positive fluorescence was mainly seen in LNS. Activated macrophages in the sinuses of LNS express folate receptor beta (FR β), which also appeared to be a target for OTL38 [17-19].

Nevertheless, in advanced ovarian cancer the use of intraoperative NIR fluorescence imaging led to better visualization of cancer lesions and consequent resection of 29% additional lesions that were not detected with visual inspection. We hypothesized that application of NIR fluorescence imaging in early ovarian cancer could lead to more accurate detection of (occult) ovarian cancer metastases and could allow gynecologic surgeons to take targeted rather than blind biopsy samples. As completeness of surgical staging is an independent prognostic factor for overall survival, this study could provide a significant step towards improving surgical staging and consequently tailored treatment in early stage ovarian cancer patients.

METHODS

INVESTIGATIONAL PRODUCT ● OTL38 (chemical formula: C₆₁H₆₃N₉Na₄O₁₇S₄; molecular weight: 1414.42 Da) consists of a folate analogue conjugated to an NIR fluorescent dye. OTL38 (>96% purity) was obtained. The drug was synthesized and manufactured in compliance with Good Manufacturing Practices. OTL38 was stored in frozen form at -20°C in vials containing 6 mg OTL38 free acid in 3 mL water. Before administration, the frozen vials were thawed, vortexed, and then diluted in 220 mL 5% dextrose for intravenous infusion. Patients received a 1-hour intravenous infusion of 0.0125 mg/kg OTL38 2-3 hours before the start of surgery. This dose and the time interval between dosing and surgery were deemed optimal in a previous study[15],

STUDY DESIGN ● The objectives of the study were to assess tolerability, pharmacokinetics (PK) and the feasibility of intraoperative NIR fluorescence detection of ovarian cancer lesions using a single intravenous dose of OTL38. Tolerability assessment (blood pressure, pulse, peripheral oxygen saturation, respiratory rate, ECG, temperature, and skin assessments) and blood collection for PK and routine laboratory tests were performed at fixed time points starting shortly before administration and lasting up to 24 hours after dosing. Adverse events and the concomitant use of other medications were recorded. Feasibility was assessed by measuring the following endpoints: tumor-to-background ratio (ratio between fluorescent signal of the tumor and fluorescent signal of

the background); co-localization of tumor cells on hematoxylin & eosin (H&E) and FR α staining on immunohistochemistry (IHC) with fluorescence; the number of additional cancerous lesions detected with NIR fluorescence imaging; and number of false positive and negative lesions. As this study was exploratory in nature, the sample size was not based on statistical considerations.

ETHICS COMMITTEE APPROVAL ● The study was approved by a certified medical ethics review board (Medical Ethics Committee of Leiden University Medical Center [LUMC]) and was performed in accordance with the laws and regulations on drug research in humans in the Netherlands. All patients provided written informed consent prior to the start of any study-related procedures. The study was registered in the European Clinical Trials Database under numbers 2014-002352-12; publicly accessible via the CCMO register (https://www.toetsingonline.nl/to/ccmo_search.nsf/Searchform?OpenForm).

PATIENTS ● We included 6 patients who had a clinical suspicion of early stage epithelial ovarian cancer and were scheduled for a laparoscopic or open surgical staging procedure. Potential patients were selected from the multidisciplinary consent meeting of the LUMC department of Gynecology between December 2015 and July 2016. The main exclusion criteria were current pregnancy, history of anaphylactic reactions, impaired renal function (defined as EGFR <50 mL/min/1.73 m²), and impaired liver function (defined as alanine aminotransferase, aspartate aminotransferase, or total bilirubin levels that exceeded three times the established upper limit of normal).

INTRAOPERATIVE NIR FLUORESCENCE IMAGING SYSTEM ● Imaging was performed using an NIR fluorescence imaging system [20]. Both systems consist of three wavelength-isolated light sources, including a 'white' light source and two separate NIR light sources. Color video and fluorescence images were acquired simultaneously using separate sensors and were displayed in real time using custom-built optics and software, thereby displaying color video and NIR fluorescence images separately. A pseudo-colored (lime green) merged image of the color video and fluorescence images was also generated. During open surgery, the camera and moveable arm were enclosed in a sterile shield and drape. During laparoscopic surgery a sterilized laparoscope and light cable were used.

SURGICAL STAGING PROCEDURE ● Surgical staging generally included hysterectomy, bilateral salpingo-oophorectomy and infracolic omentectomy. Biop-

sies were taken from all suspect lesions and from the following predefined areas: pelvic and para-aortic LNS; right hemidiaphragm; paracolic gutters; pelvic side walls; ovarian fossa; bladder peritoneum; and recto-uterine pouch. Surgical procedures were open procedures or laparoscopic performed by an experienced gynecologic oncologist. First, suspected lesions were identified in the surgical field using standard visual and, in case of open surgery, tactile methods. Thereafter, the imaging system was used to identify NIR-fluorescent lesions. All suspect lesions identified by visual/tactile methods and NIR fluorescence were resected, when surgically feasible. All resected suspect lesions and biopsy samples, were marked on a case report form as being either fluorescent or non-fluorescent and as being either clinically suspected of malignancy or not.

HISTOPATHOLOGY EVALUATION ● An experienced pathologist examined all resected lesions for tumor status. A tumor positive lesion that was fluorescent was considered a true positive; a tumor negative lesion that was fluorescent was considered a false positive; and a tumor positive lesion that was non-fluorescent was considered a false negative. To assess the origin and relative strength of fluorescence signal, formalin-fixed, paraffin-embedded (FFPE) samples were assessed using a closed box imager. In addition, we performed immunohistochemistry (IHC) to demonstrate FR α , FR β and CD68 (a pan macrophage marker) expression in FFPE sections. Lastly a series of six successive sections were stained alternately with H&E and cytokeratin, in accordance with sentinel LN ultra-staging protocol. For assessment of fluorescent signal arising from OTL38 in sections, a flatbed scanner was used.

PHARMACOKINETICS ANALYSIS ● The bioanalysis was performed using validated methodologies in compliance with good clinical laboratory practices at an analytical biochemical laboratory. In brief, OTL38 was extracted from human K2EDTA plasma samples using off-line solid-phase extraction, followed by analysis using liquid chromatography/mass spectrometry. The assay's lower limit of quantification (LLOQ) and upper limit of quantification (ULOQ) were 2.00 and 500 ng/mL, respectively. The coefficient of variability for intra-day and inter-day plasma LLOQ was 8.2%.

STATISTICAL ANALYSIS ● SPSS statistical software package (version 23.0) was used for statistical analyses. Patient characteristics are reported as the median, SD, and range. The fluorescence signal in the tumor and background tissue was quantified using ImageJ (version 1.49b, NIH, Bethesda, MD; <http://imagej>).

nih.gov/ij/). Using ImageJ, a region of interest (ROI) was drawn on the images and used to quantify the fluorescence signal in arbitrary units (AU). Tumor-to-background ratio (TBR) was calculated by dividing the fluorescence signal of the tumor by the fluorescence signal of the surrounding healthy tissue. To compare the TBR values and fluorescence background signals between malignant and benign (i.e., false positive) lesions and between different dose groups, an independent samples student t-test was performed. TBR is reported as the mean, SD, and range. The individual OTL38 PK profiles were analyzed using noncompartmental methods.

RESULTS

GENERAL ● Six patients, with a mean age of 58 (SD 8.2, range 43-66) with a clinical suspicion of early ovarian cancer were included. Characteristics of the surgical procedures and tumor histopathology are summarized in Table 1. In four patients a laparoscopic staging was initiated, in one patient the laparoscopy was converted to a laparotomy because of massive adhesions. The remaining 2 patients underwent an open procedure using a midline abdominal incision. In 4 patients the primary tumor, i.e. adnexa, had already been resected during a prior procedure, in the other patients the primary tumor was still in situ. Following intraoperative frozen section analysis, the staging procedure was abandoned in two patients. In one patient the staging was halted after the primary tumor was found to be benign. In the other patient the staging was converted to a debulking procedure as a consequence of macroscopic gross disease outside the pelvis. In the remaining 4 patients a staging procedure was performed, in 1 patient staging was incomplete as biopsy samples from right paracolic gutter and the right hemi-diaphragm were not obtained.

ADVERSE EVENTS ● In 2/6 patients symptoms suggestive of hypersensitivity (e.g., dysphonia and pruritus) occurred during OTL38 infusion. These symptoms were mild in severity and self-limiting. No serious adverse events or deaths related to OTL38 occurred during the study period. Administration of OTL38 did not lead to any apparent changes in laboratory values, ECG, vital signs, or temperature.

PHARMACOKINETICS ● The maximum blood plasma concentration of OTL38 was achieved at the end of the infusion and subsequently declined with an elimination half-life of 2 -3 hours, similar to earlier results [15].

INTRAOPERATIVE IMAGING ● In two patients the primary tumor, i.e. adnexa, was still in situ, in one patient the tumor was fluorescent (TBR 4.5) while in the other patient fluorescence was not detected (Figure 1A-B). The fluorescent tumor was subsequently confirmed as an ovarian malignancy on frozen section, while the non-fluorescent tumor proved to be a benign mucinous cystadenoma.

In three out of the four patients who underwent a staging procedure fluorescent lesions were detected intraoperatively. A total of 9 fluorescent lesions, all LN clusters, were resected during surgery (Figure 1C). Mean TBR was 4.4 (SD 3.3, median 3.6, range 1.8-10.8). Apart from LNS, fluorescence was not detected elsewhere.

ROUTINE HISTOPATHOLOGY ● In addition to fluorescent lesions, biopsy samples of clinically suspect lesions and of predefined areas were analyzed on histopathology. Apart from the fluorescent primary tumor, tumor cells were not demonstrated in any of the biopsy samples, including the samples of fluorescent lesions. Therefore all fluorescent suspected metastatic lesions were false positives. As none of the non-fluorescent lesions contained tumor cells on histopathology either, false negative fluorescence was not seen.

LYMPH NODE HISTOPATHOLOGY ● All resected LNS (N=38), including LNS that demonstrated false positive fluorescence were assessed. FR α expression was not seen in any of the LNS. Moderate to strong FR β expression was seen in 29 LNS, the remaining LNS had absent or weak FR β expression. Fluorescence signal of the LNS, measured using the Pearl Imager, was significantly higher in the LNS with strong to moderate FR β expression ($p < 0.001$) (Figure 2). The pattern of FR β staining was concordant with the pattern of CD68 staining in all LNS with the main expression in the sinuses of the LNS (Figure 3). This typical pattern, with sparing of the follicles, was also seen on flatbed fluorescence scanning. This confirms co-localization of the fluorescence signal with the FR β expressing macrophages. Additional serial sectioning and cytokeratin staining did not lead to the detection of (micro)metastases.

DISCUSSION

NIR fluorescence imaging has the potential to detect (small) metastatic lesions that are not visible with the naked eye. This could facilitate discrimination between true early stage and occult advanced stage ovarian cancer. NIR

fluorescence imaging could also optimize staging procedures in ovarian cancer, as targeted rather than blind biopsies can be taken, which is especially relevant in laparoscopic staging procedures, where tactile information is lacking. The use of OTL38, a NIR fluorescent FR α targeting agent, was studied in 6 patients that were scheduled to undergo a staging procedure for suspected early stage ovarian cancer. Distinction between a malignant and a benign primary tumor was possible with OTL38 based fluorescence imaging. As metastases were not present in any of these patients, the added value of OTL38 was limited in this study. In fact, apart from the primary tumor, fluorescence signal was only detected in LNS that did not contain metastases.

These false positive LNS were detected intraoperatively in half of the patients. Because this may have implications for the applicability of OTL38 in staging procedures for ovarian cancer, we studied all resected LNS in detail. In none of the LNS FR α expression was present, whereas FR β expression was seen in the majority of the LNS. LNS with strong to moderate overexpression of FR β had significantly higher fluorescent signal, while fluorescent signal in LNS with weak or absent FR β expression was very low or absent. This supports the notion that false positive fluorescence is caused by OTL38 binding to FR β -expressing macrophages in the LNS. Another indication for this concept is the distinct resemblance of staining pattern of FR β with the staining pattern of CD68, a pan-macrophage marker. Alternatively, fluorescence signal arising from LNS could also be due to small metastases that were missed during routine pathology. As the presence of tumor cells is assessed on a limited number of sections stained with H&E staining, it is possible that smaller metastasis can remain undetected. To increase the likelihood of detection of tumor cells, we performed serial sectioning and alternating H&E and cytokeratin staining of sections on all resected LNS. This detailed assessment is too time-consuming for implementation in routine practice [21]. Application of this assessment to all LNS resected during this study did not lead to the detection of additional metastases. Therefore, the false positive fluorescence in LNS is most likely a consequence of FR β expressing macrophages in the LNS rather than missed metastases.

In addition, the FR β overexpressing, CD68 positive macrophages we found in the LNS are likely tumor-associated macrophages (TAMS). The role of TAMS is controversial, as evidence exists for their involvement in pro- as well as anti-tumor processes. However, most recent evidence indicates that macrophages, both in the primary and metastatic sites, adopt a protumoral phenotype [22, 23]. In metastatic sites, TAMS prepare the site by promoting the extravasation, survival, and persistent growth of metastatic cells. A study by Go *et al.*

demonstrated that the density of TAMS in LNS was increased in micrometastasis, moreover a high density of TAMS was significantly associated with malignant LNS [24]. In this light, resection of tumor-negative LNS that contain TAMS identified by FR β -mediated fluorescence may even be beneficial. In fact, this may explain why resection of large numbers of negative LNS leads to survival benefits.

Accurate detection of metastatic spread in early stage ovarian cancer is important as treatment decisions are based on the extent of disease found during surgical staging. If metastases are present but not detected during staging procedures, under-treatment of the patient will occur. Moreover, completeness of surgical staging is an independent prognostic factor for overall survival in early stage ovarian cancer patients [3]. Although fluorescence imaging led to the detection of false positive lesions, true positives do not seem to be missed with NIR fluorescence imaging. High sensitivity is essential in staging procedures, as missing malignant lesions has worse implications than resection of non-malignant lesions [25]. In addition, a positive correlation between the number of resected lymph nodes during a staging procedure and overall survival is established in early stage ovarian cancer patients and this positive effect remains when large numbers of conventionally 'negative' nodes are resected [26, 27].

To conclude, the anticipated added value of NIR fluorescence imaging using OTL38 could not be demonstrated in staging procedures for early stage ovarian cancer, as metastatic lesions were not present in any of the patients in this small series. Fluorescent imaging using OTL38 did contribute to the resection of seemingly non-malignant LNS due to the targeting of FR β on TAMS. However, as comprehensive lymph node sampling should be pursued in surgical staging procedures, this should not impede application of OTL38. Importantly, fluorescence imaging using OTL38 allowed distinction between a malignant and benign primary tumor and had high sensitivity, which justifies further research in a larger patient group.

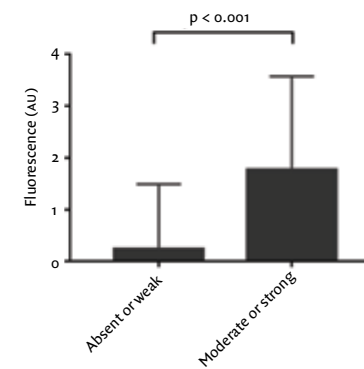
REFERENCES

- 1 Chang SJ, Bristow RE, Ryu HS. Impact of complete cytoreduction leaving no gross residual disease associated with radical cytoreductive surgical procedures on survival in advanced ovarian cancer. *Ann Surg Oncol.* 2012;19(13):4059-67.
- 2 Vergote I, Trope CG, Amant F, Kristensen GB, Ehlen T, Johnson N, et al. Neoadjuvant chemotherapy or primary surgery in stage IIIC or IV ovarian cancer. *N Engl J Med.* 2010;363(10):943-53.
- 3 Trimbos B, Timmers P, Pecorelli S, Coens C, Ven K, van der Burg M, et al. Surgical staging and treatment of early ovarian cancer: long-term analysis from a randomized trial. *J Natl Cancer Inst.* 2010;102(13):982-7.
- 4 Trimbos JB, Vergote I, Bolis G, Vermorken JB, Mangioni C, Madronal C, et al. Impact of adjuvant chemotherapy and surgical staging in early-stage ovarian carcinoma: European Organisation for Research and Treatment of Cancer-Adjuvant ChemoTherapy in Ovarian Neoplasm trial. *J Natl Cancer Inst.* 2003;95(2):113-25.
- 5 Zanetta G, Rota S, Chiari S, Bonazzi C, Bratina G, Torri V, et al. The accuracy of staging: an important prognostic determinant in stage I ovarian carcinoma. A multivariate analysis. *Ann Oncol.* 1998;9(10):1097-101.
- 6 Vahrmeijer AL, Hutteman M, van der Vorst JR, van de Velde CJ, Frangioni JV. Image-guided cancer surgery using near-infrared fluorescence. *Nat Rev Clin Oncol.* 2013;10(9):507-18.
- 7 Chance B. Near-infrared images using continuous, phase-modulated, and pulsed light with quantitation of blood and blood oxygenation. *Ann NY Acad Sci.* 1998;838:29-45.
- 8 Frangioni JV. In vivo near-infrared fluorescence imaging. *Curr Opin Chem Biol.* 2003;7(5):626-34.
- 9 Keereweer S, Kerrebijn JD, van Driel PB, Xie B, Kaijzel EL, Snoeks TJ, et al. Optical image-guided surgery--where do we stand? *Mol Imaging Biol.* 2011;13(2):199-207.
- 10 Handgraaf HJ, Verbeek FP, Tummers QR, Boogerd LS, van de Velde CJ, Vahrmeijer AL, et al. Real-time near-infrared fluorescence guided surgery in gynecologic oncology: a review of the current state of the art. *Gynecol Oncol.* 2014;135(3):606-13.
- 11 Parker N, Turk MJ, Westrick E, Lewis JD, Low PS, Leamon CP. Folate receptor expression in carcinomas and normal tissues determined by a quantitative radioligand binding assay. *Anal Biochem.* 2005;338(2):284-93.
- 12 O'Shannessy DJ, Somers EB, Smale R, Fu YS. Expression of folate receptor-alpha (FRA) in gynecologic malignancies and its relationship to the tumortype. *Int J Gynecol Pathol.* 2013;32(3):258-68.
- 13 Kalli KR, Oberg AL, Keeney GL, Christianson TJ, Low PS, Knutson KL, et al. Folate receptor alpha as a tumor target in epithelial ovarian cancer. *Gynecol Oncol.* 2008;108(3):619-26.
- 14 van Dam GM, Themelis G, Crane LM, Harlaar NJ, Pleijhuis RG, Kelder W, et al. Intraoperative tumor-specific fluorescence imaging in ovarian cancer by folate receptor-alpha targeting: first in-human results. *Nat Med.* 2011;17(10):1315-9.
- 15 Hoogstins CE, Tummers QR, Gaarenstroom KN, de Kroon CD, Trimbos JB, Bosse T, et al. A Novel Tumor-Specific Agent for Intraoperative Near-Infrared Fluorescence Imaging: A Translational Study in Healthy Volunteers and Patients with Ovarian Cancer. *Clin Cancer Res.* 2016;22(12):2929-38.
- 16 Tummers QR, Hoogstins CE, Gaarenstroom KN, de Kroon CD, van Poelgeest MI, Vuyk J, et al. Intraoperative imaging of folate receptor alpha positive ovarian and breast cancer using the tumor specific agent EC17. *Oncotarget.* 2016;7(22):32144-55.
- 17 Shen J, Hilgenbrink AR, Xia W, Feng Y, Dimitrov DS, Lockwood MB, et al. Folate receptor-beta constitutes a marker for human proinflammatory monocytes. *J Leukoc Biol.* 2014;96(4):563-70.
- 18 O'Shannessy DJ, Somers EB, Wang LC, Wang H, Hsu R. Expression of folate receptors alpha and beta in normal and cancerous gynecologic tissues: correlation of expression of the beta isoform with macrophage markers. *J Ovarian Res.* 2015;8:29.
- 19 Puig-Kroger A, Sierra-Filardi E, Dominguez-Soto A, Samaniego R, Corcuera MT, Gomez-Aguado F, et al. Folate receptor beta is expressed by tumor-associated macrophages and constitutes a marker for M2 anti-inflammatory/regulatory macrophages. *Cancer Res.* 2009;69(24):9395-403.
- 20 van Driel PB, van de Giessen M, Boonstra MC, Snoeks TJ, Keereweer S, Oliveira S, et al. Characterization and evaluation of the artemis camera for fluorescence-guided cancer surgery. *Mol Imaging Biol.* 2015;17(3):413-23.
- 21 Weaver DL. Pathology evaluation of sentinel lymph nodes in breast cancer: protocol recommendations and rationale. *Mod Pathol.* 2010;23 Suppl 2:S26-32.
- 22 Biswas SK, Allavena P, Mantovani A. Tumor-associated macrophages: functional diversity, clinical significance, and open questions. *Semin Immunopathol.* 2013;35(5):585-600.
- 23 Noy R, Pollard JW. Tumor-associated macrophages: from mechanisms to therapy. *Immunity.* 2014;41(1):49-61.
- 24 Go Y, Tanaka H, Tokumoto M, Sakurai K, Toyokawa T, Kubo N, et al. Tumor-Associated Macrophages Extend Along Lymphatic Flow in the Pre-metastatic Lymph Nodes of Human Gastric Cancer. *Ann Surg Oncol.* 2016;23 Suppl 2:S230-5.
- 25 Trimbos JB. Surgical treatment of early-stage ovarian cancer. *Best Pract Res Clin Obstet Gynaecol.* 2016.
- 26 Chan JK, Urban R, Hu JM, Shin JY, Husain A, Teng NN, et al. The potential therapeutic role of lymph node resection in epithelial ovarian cancer: a study of 13918 patients. *Br J Cancer.* 2007;96(12):1817-22.

TABLE 1 CHARACTERISTICS OF THE SURGICAL PROCEDURES AND TUMOR HISTOPATHOLOGY

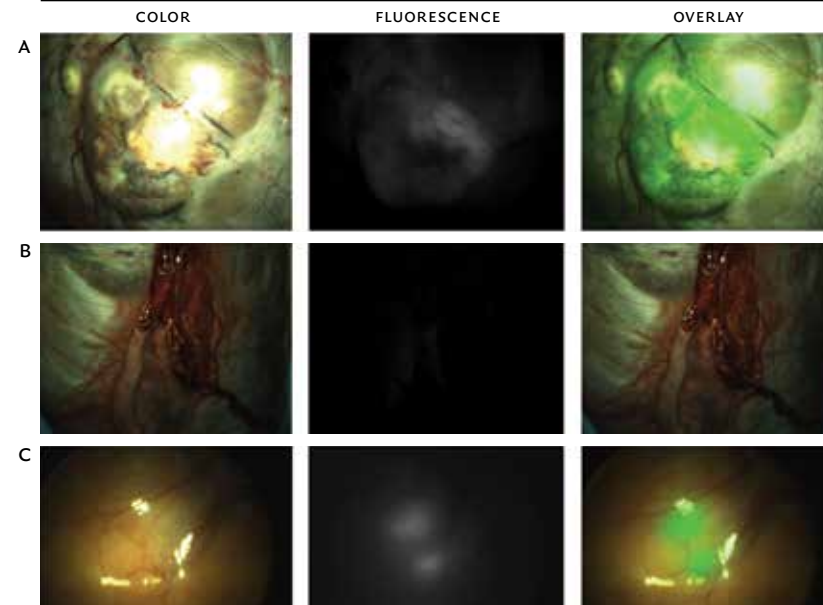
ID	Primary tumor in situ	Diagnosis (stage)	Surgical procedure	Result surgical procedure	Intraoperative fluorescence
1	No	Endometrioid adenocarcinoma (IA)	Laparotomy	Complete staging	Yes False positive LNS
2	Yes	Mucinous cystadenoma (n.a.)	Laparotomy	Resection primary tumor	No Concordant with benign tumor
3	No	Mucinous borderline tumor (IA)	Laparoscopy	Complete staging	No Concordant with absence of metastases
4	Yes	Endometrioid adenocarcinoma (IIIA)	Laparotomy	Complete primary debulking	Yes Concordant with malignant tumor
5	No	Serous adenocarcinoma (IA)	Laparoscopy	Complete staging	Yes False positive LNS
6	No	Serous adenocarcinoma (IA)	Laparoscopy	Incomplete staging	Yes False positive LNS

FIGURE 1 INTRAOPERATIVE FLUORESCENCE



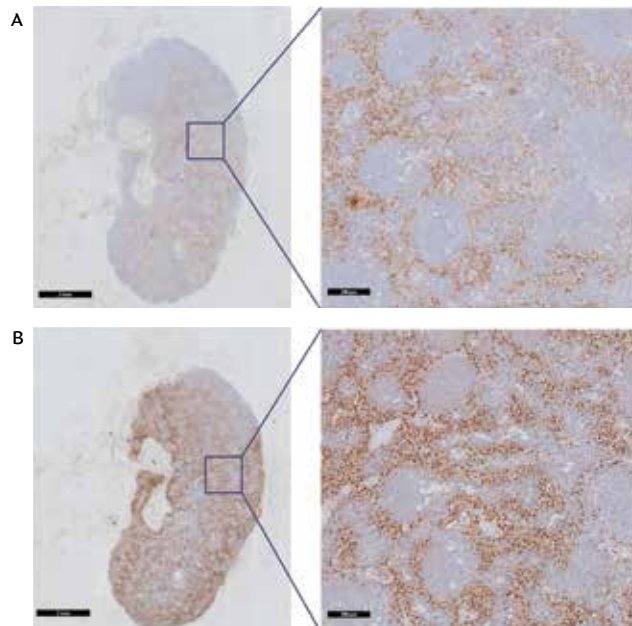
Fluorescence in lymph nodes is significantly ($p < 0.001$) related to the expression of the FR β .

FIGURE 2 LYMPH NODE FLUORESCENCE RELATED TO FOLATE RECEPTOR BETA STAINING INTENSITY



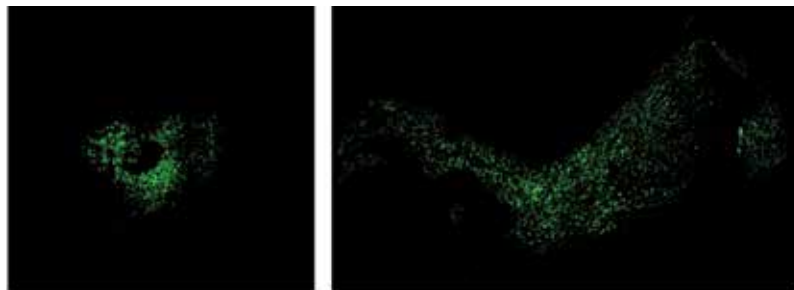
A. Clear fluorescence arising from an endometrioid adenocarcinoma
 B. Absence of fluorescence in a benign mucinous cystadenoma
 C. Two fluorescent lymph nodes that did not contain metastases (false positive)

FIGURE 3 IMMUNOHISTOCHEMICAL STAINING OF A FALSE POSITIVE LYMPH NODE



Sections of a fluorescent lymph node that did not contain metastasis stained for A) FR β and B) pan macrophage marker CD68, demonstrating a resembling staining pattern with the main expression in the, macrophage containing, sinuses of the lymph node.

FIGURE 4 FLUORESCENCE SIGNAL OF A FALSE POSITIVE LYMPH NODE.



The images show fluorescent lymph nodes with a fluorescence pattern localized to the sinuses, consistent with FR β staining.

Chapter 7

Image-guided surgery in patients with pancreatic cancer: first results of a clinical trial using SGM-101, a novel carcinoembryonic antigen-targeting, near-infrared fluorescent agent

Ann Surg Oncol. 2018 Jul 26

CHARLOTTE HOOGSTINS*, LEONORA BOOGERD*, BABS SIBINGA MULDER, SVEN MIEOG, RUTGER JAN SWIJNENBURG, CORNELIS VAN DE VELDE, ARANTZA FARINA SARASQUETA, BERT BONSING, BERENICE FRAMERY, ANDRÉ PÈLEGRIN, MARIAN GUTOWSKI, FRANÇOISE CAILLER, JACOBUS BURGGRAAF, ALEXANDER VAHRMEIJER

* shared first authorship

ABSTRACT

BACKGROUND Near-infrared (NIR) fluorescence is a promising novel imaging technique that can aid in intraoperative demarcation of pancreatic cancer (PDAC) and thus increase radical resection rates. We studied SGM-101, a novel, fluorescent-labeled anti-carcinoembryonic antigen (CEA) antibody. In this phase 1 study we aimed to assess the tolerability and feasibility of intraoperative fluorescence tumor imaging using SGM-101 in patients undergoing a surgical exploration for PDAC.

METHODS Twelve patients were injected intravenously with 5, 7.5 or 10 mg SGM-101 at least 48 hours prior to undergoing surgery for PDAC. Tolerability assessments were performed at regular intervals after dosing. The surgical field was imaged using the Quest NIR imaging system. Concordance between fluorescence and tumor presence on histopathology was studied.

RESULTS SGM-101 specifically accumulated in CEA expressing primary tumors and peritoneal and liver metastases, allowing real-time intraoperative fluorescence imaging. The mean tumor-to-background ratio (TBR) was 1.6 in primary tumors and 1.7 in metastatic lesions. One false positive lesion was detected (CEA-expressing intraductal papillary mucinous neoplasm). False negativity was seen twice as a consequence over overlaying blood or tissue that blocked the fluorescent signal.

DISCUSSION The use of a fluorescent-labeled anti-CEA antibody was safe and feasible for the intraoperative detection of both primary PDAC and metastases. These results warrant further research to determine the impact of this technique on clinical decision-making and overall survival.

INTRODUCTION

Surgical resection is the only possible curative treatment for patients with pancreatic ductal adenocarcinoma (PDAC). Differentiation between tumoral and non-tumoral tissue is often difficult during PDAC surgery and this can lead to incomplete cancer removal, exemplified by high percentages of irradical resections [1-3]. As survival time doubles in patients with a microscopically radical resection [4], enhanced intraoperative visualization of PDAC is crucial to increase radical resection rates and improve patient outcomes.

Image-guided surgery using near-infrared (NIR) fluorescence is a novel imaging technique that can aid in real-time demarcation of tumors during surgery [5]. To detect tumors using NIR fluorescence imaging, a fluorescent contrast agent is administered and the distribution of the agent is visualized using a dedicated imaging system. At first, the fluorescence-imaging field focused predominantly on indocyanine green (ICG), a non-specific imaging agent, as ICG is available for clinical use. Exploiting the hypothesized passive accumulation of ICG in tumor cells, a study in PDAC was performed [6]. The results were unfavorable, as sufficient contrast between the tumor and surrounding pancreatic tissue was not achieved. Currently, the fluorescence-imaging field focusses mainly on tumor-specific agents (e.g. antibodies or ligands that are conjugated to a fluorophore) that molecularly target biomarkers expressed by tumor cells. Recently, clinical trials (including one randomized controlled trial) with these tumor-specific fluorescent agents in other cancer types demonstrated feasibility and potential clinical benefits of image-guided surgery [7-9]. However, tumor-specific agents for fluorescence imaging of PDAC have not been investigated.

A number of targetable biomarkers seem highly potential for specific fluorescence imaging of PDAC: Integrin $\alpha v \beta 6$, carcinoembryonic antigen (CEA), epithelial growth factor receptor (EGFR), and urokinase plasminogen activator receptor (UPAR)[10]. CEA is a glycoprotein produced by gastrointestinal tissue that is overexpressed in many cancer types, including pancreatic ductal adenocarcinoma [11,12]. Antibodies directed towards CEA-overexpressing tumors for various therapeutic applications have been successfully tested in trials [13-15]. Moreover, imaging studies using PET and radiolabelled anti-CEA antibodies demonstrate high tumor uptake and good contrast [16,17].

SGM-101 is a novel fluorescent (700 nm) labeled anti-CEA antibody for clinical application. In a PDAC orthotopic mouse models using BxPC3 cells, different fluorescent labeled anti-CEA antibodies allowed clear tumor delineation [18-20].

Our aim was to assess the tolerability and feasibility of intraoperative fluorescence tumor imaging using SGM-101 in patients undergoing a surgical exploration for PDAC.

METHODS

STUDY DESIGN ● The study was an open label, single ascending dose, exploratory study in 12 patients approved by a certified medical ethics review board (clinicaltrials.gov ID: NCT02973672). The primary objective of the study was to assess SGM-101 with respect to tolerability and performance in the intraoperative detection of PDAC lesions. Due to the exploratory nature of the study, sample size was not based on a formal calculation of statistical power. A dose-escalating scheme with intravenous doses of 5, 7.5 and 10 mg administered 48 or 96 hours prior to surgery was used based on our pre-clinical data [18]. We included patients with elevated plasma CEA levels (>3 ng/mL), who had a clinical diagnosis of PDAC and were scheduled for surgical exploration. Exclusion criteria were pregnancy, history of allergic reactions, impaired renal function, plasma CEA >300 ng/mL and diagnosis of another malignancy within the last 5 years. Tolerability assessment (adverse events, ECG, blood pressure, pulse, peripheral oxygen saturation, respiratory rate and temperature) and routine laboratory tests and urine collection for urinalysis were performed at regular intervals starting just prior to administration and lasting until 12 hours after dosing. On the day of surgery and the first postoperative day measurements were repeated. Follow-up visits coinciding with clinical care took place at the day of discharge and the first outpatient clinic visit. Adverse events and the concomitant use of other medications were recorded throughout the study period. All surgical procedures were open procedures, the surgical field was explored using standard visual and tactile methods, complemented with ultrasound based on the surgeon's preference. Subsequently, the fluorescence imaging system was used to identify NIR-fluorescent lesions. All lesions identified by visual/tactile methods and/or NIR fluorescence were resected, given it was surgically feasible and clinically relevant. Each resected lesion was marked on a case report form as fluorescent or non-fluorescent and as clinically suspected of malignancy or not. Following resection, fluorescence imaging of the resected specimen (before and after slicing) was performed at the pathology department. The slice containing the peak fluorescence signal was imaged using the Pearl imager and corresponding software (LI-COR, Lincoln, NE, USA). The fluorescence signal in tumor and background tissue (tumor-to-background ratio's [TBR]) was

quantified using ImageJ (version 1.49b, NIH, Bethesda, MD, USA; <http://imagej.nih.gov/ij/>) on TIFF images (8 bits) subtracted from intraoperative videos. Tumor status was correlated with intraoperative fluorescent assessment. A fluorescent lesion that was tumor positive was considered a true positive; a fluorescent lesion that was tumor negative was considered a false positive; and a non-fluorescent lesion that was tumor positive was considered a false negative. In addition, immunohistochemistry (IHC) was performed to demonstrate CEA expression. To correlate SGM-101 presence with tumor status and CEA expression on a microscopic level, sections were scanned using the Odyssey imager (LI-COR). TBR is reported as the mean, SD, and range. Patient characteristics are reported as the median, SD, and range.

INVESTIGATIONAL PRODUCT ● SGM-101 (molecular weight: 148,6 kDa) consists of an anti-CEA chimeric monoclonal antibody covalently bound to the fluorophore BM-104 (excitation 686 nm and emission 704 nm). Approximately 30-40% of the antibody is unconjugated, the average number of fluorophores per antibody is between 1 and 2. SGM-101 was manufactured in compliance with Good Manufacturing Practice (GMP) by Novasep (Gosselies, Belgium). The drug was supplied by Surgimab (Montpellier, France) as a sterile solution for injection in an amber glass vials containing 10 mg SGM-101 in 10 mL and stored in frozen form at -20°C. Before administration, the frozen vials were thawed and diluted in 100mL 0,9% NaCl and infused over 30 minutes.

IMAGING SYSTEM ● Imaging was performed using the Artemis and Spectrum fluorescence imaging systems (Quest Medical Imaging, Middenmeer, the Netherlands) [21]. Both systems consist of three wavelength-isolated light sources, including a 'white' light source and two separate NIR light sources. For this study, the CY5,5 filter setting (fluorescent range 680 ± 30 nm) was used. Color video and fluorescence images were acquired simultaneously by separate sensors and were displayed in real time using custom-built optics and software, thereby displaying color video and NIR fluorescence images separately. A pseudo-colored (lime green) merged image of the color video and fluorescence images was also generated. The gain and exposure time settings were controlled using the Quest software, an average gain setting of 25 was used and exposure time was varied between 60 and 120 ms according to the clinical situation. The camera was attached to a freely moveable arm. During surgery, the camera and moveable arm were enclosed in a sterile shield and drape (Medical Technique Inc., Tucson, AZ, USA).

RESULTS

GENERAL ● We included twelve patients; demographics and details on surgical procedure are summarized in Table 1.

DOSE ESCALATION ● As the increase from 5 mg to 7.5 mg did not result in an increase in TBR, the interval between administration and surgery was prolonged to 96 hours, while the dose remained equal at 7.5 mg for the following cohort. The longer interval between administration and surgery resulted in an improvement of TBR. Hence for the last dose level, the dose was increased to 10 mg while the longer interval was retained. TBR results are summarized in Figure 1.

SAFETY DATA ● One patient (208) experienced mild, self-limiting abdominal discomfort and diarrhea on the day of SGM-101 administration (dose 7.5mg), although unlikely related to SGM-101, causality could not be excluded. In the remaining patients, adverse events related to SGM-101 were not seen. Following the surgical procedure four severe adverse events were noted. These events were all related to the surgical procedure or to disease progression.

PRIMARY TUMOR ● In one patient (206), the surgical procedure was abandoned before the primary tumor was visualized following detection of occult liver metastases. In the remaining eleven patients, the primary tumor was always visualized with fluorescence imaging (TBR 1.6 [SD: 0.37; range: 1.3-2.3]) (Figure 2 and Table 1). Tumor specimens were not available in case the surgical procedure was abandoned due to unresectability or metastases. Consequently, ex vivo fluorescence measurements and correlation of fluorescence signal and histopathology were assessed in seven primary tumors. Assessment of one slice containing peak fluorescence per resection specimen with the Pearl demonstrated a mean TBR of 3.2 (SD: 0.79; range: 1.7-4.1) (Table 1). Six primary tumors were confirmed as adenocarcinomas on histopathology. IHC for CEA revealed moderate to strong CEA overexpression (Table 1). Odyssey scans of the fluorescence signal in the primary tumor sections showed concordance with tumor cells on histopathology (Figure 2). The tumor remaining was an intraductal papillary mucinous neoplasm (IPMN) with low grade dysplasia. As this is a pre-malignant condition, fluorescence signal was deemed false positive. Moderate CEA expression in 10-50% of IPMN lesional cells was present, explaining the fluorescence.

OTHER LESIONS ● In three patients liver and/or peritoneal metastases were identified (in both modalities) during surgery, while in only one patient (209) a possible liver metastasis (3 mm) was seen on cross-sectional imaging (CT-scan); all metastatic lesions were fluorescent (TBR 1.7 [SD: 0.42; range: 1.2-2.3]) (Figure 3). IHC for CEA revealed moderate to strong CEA overexpression (Table 1). A total of eight clinically suspect, non-fluorescent lesions were resected. In two patients this non-fluorescent tissue contained malignancy: suspected tumor ingrowth in the common hepatic artery (TBR 1.3; 204), and a suspected, 1 cm aorta-caval lymph node (TBR 1.1; 207).

On frozen section analysis, the biopsy of the ingrowth in the common hepatic artery demonstrated adenocarcinoma (i.e., false negative). Frozen section analysis precluded further ex vivo assessment of this biopsy material. The non-fluorescent lymph node contained a metastasis and was also considered a false negative. Remarkably, ex vivo imaging using the Pearl demonstrated localization of fluorescence and IHC staining demonstrated CEA expression.

DISCUSSION

We assessed the safety and feasibility of intraoperative fluorescence imaging of PDAC using SGM-101 in 12 patients. Administration of doses between 5 and 10 mg SGM-101 appeared safe, as the occurrence of possibly related adverse event was limited to 1 subject. Moreover, administration of SGM-101 did not result in changes in safety measurements, including vital signs, ECG and routine chemistry, hematology and coagulation laboratory tests.

Intraoperative fluorescence imaging of PDAC was feasible as fluorescence could be detected at primary tumors as well as liver and peritoneal metastases. This demonstrates that despite suboptimal intrinsic characteristics of PDAC, including poor vascularization, SGM-101 is able to reach and bind the CEA-expressing tumor cells. However, TBRs in this study were more modest than in other tumor types, 1.6 in primary tumors and 1.7 in metastases. This could also be explained by the histopathology of pancreatic adenocarcinoma with solitary ducts of tumor cells within pre-existent normal pancreatic tissue and a remarkable desmoplastic stroma, which could make the fluorescence pattern sparser as compared to other tumor types. Lastly, SGM-101 fluoresces around 700 nm, this 'far red' part of the spectrum is associated with more autofluorescence of the surrounding background.

Overlaying tissue and blood in the surgical field likely caused both cases of intraoperative false negativity in this study. The maximal depth of penetration of a fluorescence signal is around 1 cm below the tissue surface²². Consequently, more deeply seated tumors will not be detectable using fluorescence imaging. Moreover, absorption of fluorescence signal by blood can negatively impact the detection of the fluorescence signal [23]. Thus, it may be beneficial to combine fluorescence with other modalities, such as radionuclides or photo-acoustic imaging, to increase detection of deeply seated or covered tumors. For example, a study with administration of (111)In-girentuximab-IRDye800CW has been initiated in patients with clear cell renal cell carcinoma. An ex vivo study with his agent already demonstrated that uptake in tumor tissue can be visualized using both radionuclide and fluorescence imaging [24]. The advantage of a radionuclide is not only that it allows increased penetration depth, but it also allows pre-operative scanning.

Based on both preclinical and clinical studies, CEA was chosen as a suitable target for fluorescence imaging of PDAC. The present study confirmed its potential as target for intraoperative fluorescence imaging. PDAC is characterized by several genetic mutations such as KRAS (90%), CDK2NA (90%), TP53 (75%–90%), SMAD4/DPPAC4 (50%)[25]. Hence various other targets are expressed on PDAC including Integrin $\alpha v \beta 6$, EGFR, and UPAR10. Once results from other clinical studies using different tumor-specific agents become available, it is likely that a cocktail of selected agents will be employed in a personalized manner to increase the yield of fluorescence imaging. In addition, the targeting of tumor stroma could be pursued to increase sensitivity. As PDAC is composed of abundant desmoplastic stroma located at the invasive front of the tumor, this tumor is particularly suited for stroma targeting [26].

By demonstrating that both primary tumors and small metastases can be visualized using intraoperative fluorescence imaging, this study provides the first step towards implementing fluorescence-guided PDAC surgery. However, larger clinical studies are needed to assess if this technique allows evaluation of resectability and margins assessment (including vascular involvement) and whether this will ultimately translate into improved overall survival. Moreover, several challenges need to be addressed before fluorescence imaging can be implemented in a broader surgical practice: funding and awareness are required to initiate phase III multicenter trials; regulatory hurdles for approval of both imaging agents and imaging systems need to be overcome; and standardization of imaging systems is required to ensure accurate and reproducible results [27].

To the best of our knowledge, this study is the first to describe a tumor-specific imaging agent for intraoperative fluorescence imaging of PDAC. The use of a fluorescent-labeled anti-CEA antibody was safe and feasible for the detection of primary tumors as well as metastases. These results underline the great potential of image-guided surgery, yet more prospective research is necessary to establish the effect on clinical decision making and overall survival.

CONCLUSION

The use of a fluorescent-labeled anti-CEA antibody was safe and feasible for the intraoperative detection of both primary PDAC and metastases. These results warrant further research to determine the impact of this technique on clinical decision-making and overall survival.

REFERENCES

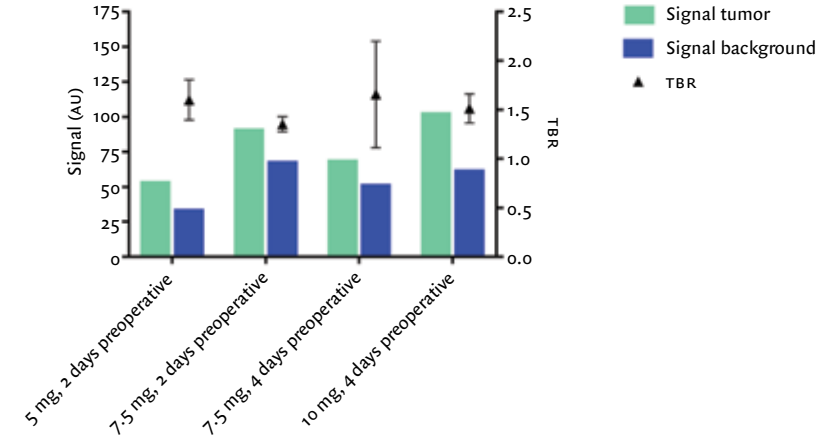
- 1 Merkow RP, Bilimoria KY, Bentrem DJ, et al. National assessment of margin status as a quality indicator after pancreatic cancer surgery. *Ann Surg Oncol*. 2014;21(4):1067-1074.
- 2 Chang DK, Johns AL, Merrett ND, et al. Margin clearance and outcome in resected pancreatic cancer. *J Clin Oncol*. 2009;27(17):2855-2862.
- 3 Esposito I, Kleeff J, Bergmann F, et al. Most pancreatic cancer resections are R1 resections. *Ann Surg Oncol*. 2008;15(6):1651-1660.
- 4 Garcea G, Dennison AR, Pattenden CJ, Neal CP, Sutton CD, Berry DP. Survival following curative resection for pancreatic ductal adenocarcinoma. A systematic review of the literature. *JOP*. 2008;9(2):99-132.
- 5 Vahrmeijer AL, Hutteman M, van der Vorst JR, van de Velde CJ, Frangioni JV. Image-guided cancer surgery using near-infrared fluorescence. *Nat Rev Clin Oncol*. 2013;10(9):507-518.
- 6 Hutteman M, van der Vorst JR, Mieog JS, et al. Near-infrared fluorescence imaging in patients undergoing pancreaticoduodenectomy. *Eur Surg Res*. 2011;47(2):90-97.
- 7 Rosenthal EL, Warram JM, de Boer E, et al. Safety and Tumor Specificity of Cetuximab-IRDye800 for Surgical Navigation in Head and Neck Cancer. *Clin Cancer Res*. 2015;21(16):3658-3666.
- 8 Stummer W, Pichlmeier U, Meinel T, et al. Fluorescence-guided surgery with 5-aminolevulinic acid for resection of malignant glioma: a randomised controlled multicentre phase III trial. *Lancet Oncol*. 2006;7(5):392-401.
- 9 Hoogstins CE, Tummers QR, Gaarenstroom KN, et al. A Novel Tumor-Specific Agent for Intraoperative Near-Infrared Fluorescence Imaging: A Translational Study in Healthy Volunteers and Patients with Ovarian Cancer. *Clin Cancer Res*. 2016;22(12):2929-2938.
- 10 de Geus SW, Boogerd LS, Swijnenburg RJ, et al. Selecting Tumor-Specific Molecular Targets in Pancreatic Adenocarcinoma: Paving the Way for Image-Guided Pancreatic Surgery. *Mol Imaging Biol*. 2016;18(6):807-819.
- 11 Nap M, Mollgard K, Burtin P, Fleuren GJ. Immunohistochemistry of carcino-embryonic antigen in the embryo, fetus and adult. *Tumour Biol*. 1988;9(2-3):145-153.
- 12 Hammarstrom S. The carcinoembryonic antigen (CEA) family: structures, suggested functions and expression in normal and malignant tissues. *Semin Cancer Biol*. 1999;9(2):67-81.
- 13 Bacac M, Fauti T, Sam J, et al. A Novel Carcinoembryonic Antigen T-Cell Bispecific Antibody (CEA TCB) for the Treatment of Solid Tumors. *Clin Cancer Res*. 2016;22(13):3286-3297.
- 14 Sahlmann CO, Homayounfar K, Niessner M, et al. Repeated adjuvant anti-CEA radioimmunotherapy after resection of colorectal liver metastases: Safety, feasibility, and long-term efficacy results of a prospective phase 2 study. *Cancer*. 2017;123(4):638-649.
- 15 Duggan MC, Jochems C, Donahue RN, et al. A phase I study of recombinant (r) vaccinia-CEA(6D)-TRICOM and rFowlpox-CEA(6D)-TRICOM vaccines with GM-CSF and IFN-alpha-2b in patients with CEA-expressing carcinomas. *Cancer Immunol Immunother*. 2016;65(11):1353-1364.
- 16 Bodet-Milin C, Ferrer L, Rauscher A, et al. Pharmacokinetics and Dosimetry Studies for Optimization of Pretargeted Radioimmunotherapy in CEA-Expressing Advanced Lung Cancer Patients. *Front Med (Lausanne)*. 2015;2:84.
- 17 Schoffelen R, Boerman OC, Goldenberg DM, et al. Development of an imaging-guided CEA-pretargeted radionuclide treatment of advanced colorectal cancer: first clinical results. *Br J Cancer*. 2013;109(4):934-942.
- 18 Gutowski M, Framery B, Boonstra MC, et al. SGM-101: An innovative near-infrared dye-antibody conjugate that targets CEA for fluorescence-guided surgery. *Surg Oncol*. 2017;26(2):153-162.
- 19 Metildi CA, Kaushal S, Pu M, et al. Fluorescence-guided surgery with a fluorophore-conjugated antibody to carcinoembryonic antigen (CEA), that highlights the tumor, improves surgical resection and increases survival in orthotopic mouse models of human pancreatic cancer. *Ann Surg Oncol*. 2014;21(4):1405-11.
- 20 Kaushal S, McElroy M, Luiken GA, et al. Fluorophore-conjugated anti-CEA antibody for the intraoperative imaging of pancreatic and colorectal cancer. *J Gastrointest Surg*. 2008;12(11):1938-1950.
- 21 van Driel PB, van de Giessen M, Boonstra MC, et al. Characterization and evaluation of the artemis camera for fluorescence-guided cancer surgery. *Mol Imaging Biol*. 2015;17(3):413-423.
- 22 Frangioni JV. New technologies for human cancer imaging. *J Clin Oncol*. 2008;26(24):4012-4021.
- 23 Chance B. Near-infrared images using continuous, phase-modulated, and pulsed light with quantitation of blood and blood oxygenation. *Ann NY Acad Sci*. 1998;838:29-45.
- 24 Hekman MC, Boerman OC, de Weijert M, et al. Targeted Dual-Modality Imaging in Renal Cell Carcinoma: An Ex Vivo Kidney Perfusion Study. *Clin Cancer Res*. 2016;22(18):4634-4642.
- 25 Chiorean EG, Coveler AL. Pancreatic cancer: optimizing treatment options, new, and emerging targeted therapies. *Drug Des Devel Ther*. 2015;9:3529-3545.
- 26 Boonstra MC, Prakash J, Van De Velde CJ, et al. Stromal Targets for Fluorescent-Guided Oncologic Surgery. *Front Oncol*. 2015;5:254.
- 27 Tipirneni KE, Warram JM, Moore LS, et al. Oncologic Procedures Amenable to Fluorescence-guided Surgery. *Ann Surg*. 2017;266(1):36-47.

TABLE 1 DEMOGRAPHICS AND DETAILS ON SGM-101 DOSING, SURGICAL PROCEDURE, FLUORESCENCE IMAGING AND CORRELATION WITH HISTOPATHOLOGY

ID	Demographics		SGM-101 Dosing		Surgical procedure	Fluorescence imaging and correlation with histopathology						METASTASES				
	Age (years)	Sexe	CEA serum (ng/mL)	Dose (mg)		Timing (days pre-op)	Procedure	PRIMARY TUMOR			PRIMARY TUMOR			TBR	Histo-pathology	Intensity CEA staining
								Fluorescence primary tumor	TBR	Resection	TBR Pearl	Histo-pathology	Intensity CEA staining			
201	71	m	10.6	5	2	Abandoned, metastases	Yes	1.6	No	-	-	Yes	Liver	1.4	Adenocarcinoma	Moderate
202	61	f	44.2	5	2	Abandoned, unresectable	Yes	1.6	No	-	-	No	Peritoneum	1.8	Adenocarcinoma	Moderate
203	66	m	3.4	5	2	Whipple, RO	Yes	1.4	Yes	4.1	Adeno-carcinoma	Weak	-	-	-	-
204	67	f	3.5	7.5	2	Abandoned, unresectable	Yes	1.4	No	-	-	No	-	-	-	-
205	52	m	5.7	7.5	2	PPPD, RO	Yes	1.6	Yes	1.7	IPMN	Moderate	-	-	-	-
206	68	m	23.5	7.5	2	Abandoned, metastases	-	-	No	-	-	Yes	Liver (segment 2)	1.2	Adenocarcinoma	Strong
207	80	m	4.5	7.5	4	Whipple, RO	Yes	1.4	Yes	3.1	Adeno-carcinoma	Moderate	-	-	-	-
208	70	m	4.9	7.5	4	PPPD, R1	Yes	1.3	Yes	3.3	Adeno-carcinoma	Strong	-	-	-	-
209	71	m	41.1	7.5	4	Abandoned, metastases	Yes	2.3	No	-	-	Yes	Liver**	2.2	Adenocarcinoma	Strong
210	66	f	2.4	10	4	PPPD, RO	Yes	1.5	Yes	2.7	Adeno-carcinoma	Strong	-	-	-	-
211	65	f	34.4	10	4	Total pancreatectomy, RO	Yes (head)	1.4	Yes	3.8	Adeno-carcinoma	Strong	-	-	-	-
212	70	m	2.8	10	4	Abandoned, unresectable	Yes (tail)*	1.4	Yes	3.4	Adeno-carcinoma	Strong	-	-	-	-

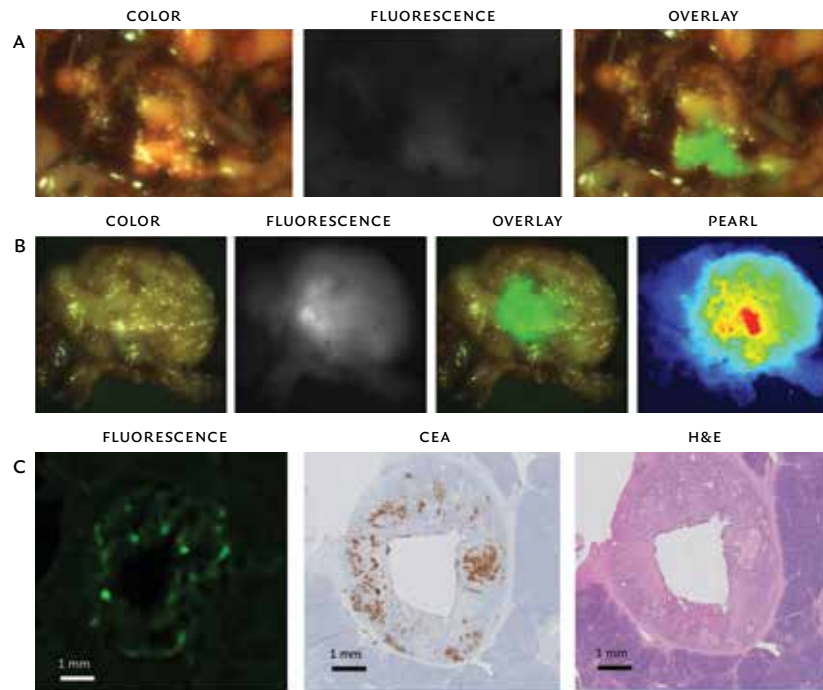
CEA: carcinoembryonic antigen, f: female, IPMN: intraductal papillary mucinous neoplasm, m: male, PPPD: Pylorus Preserving Pancreaticoduodenectomy, TBR: tumor-to-background ratio / * second primary tumor / ** a possible liver metastases (3 mm) was also seen on CT and MRI

FIGURE 1 TUMOR AND BACKGROUND FLUORESCENCE SIGNAL (IN ARBITRARY UNITS; AU) AND MEAN TUMOR-TO-BACKGROUND RATIO (TBR) PER DOSE GROUP.



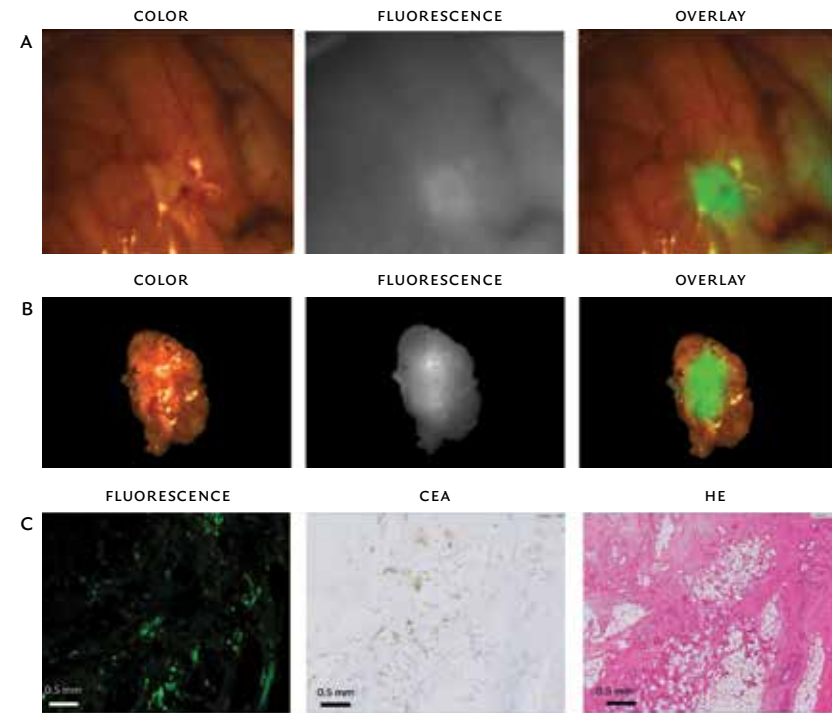
The influence of SGM-101 dose and timing on fluorescence signal and TBR seems limited in this study.

FIGURE 2 FLUORESCENCE DETECTION OF A PRIMARY PANCREATIC TUMOR.

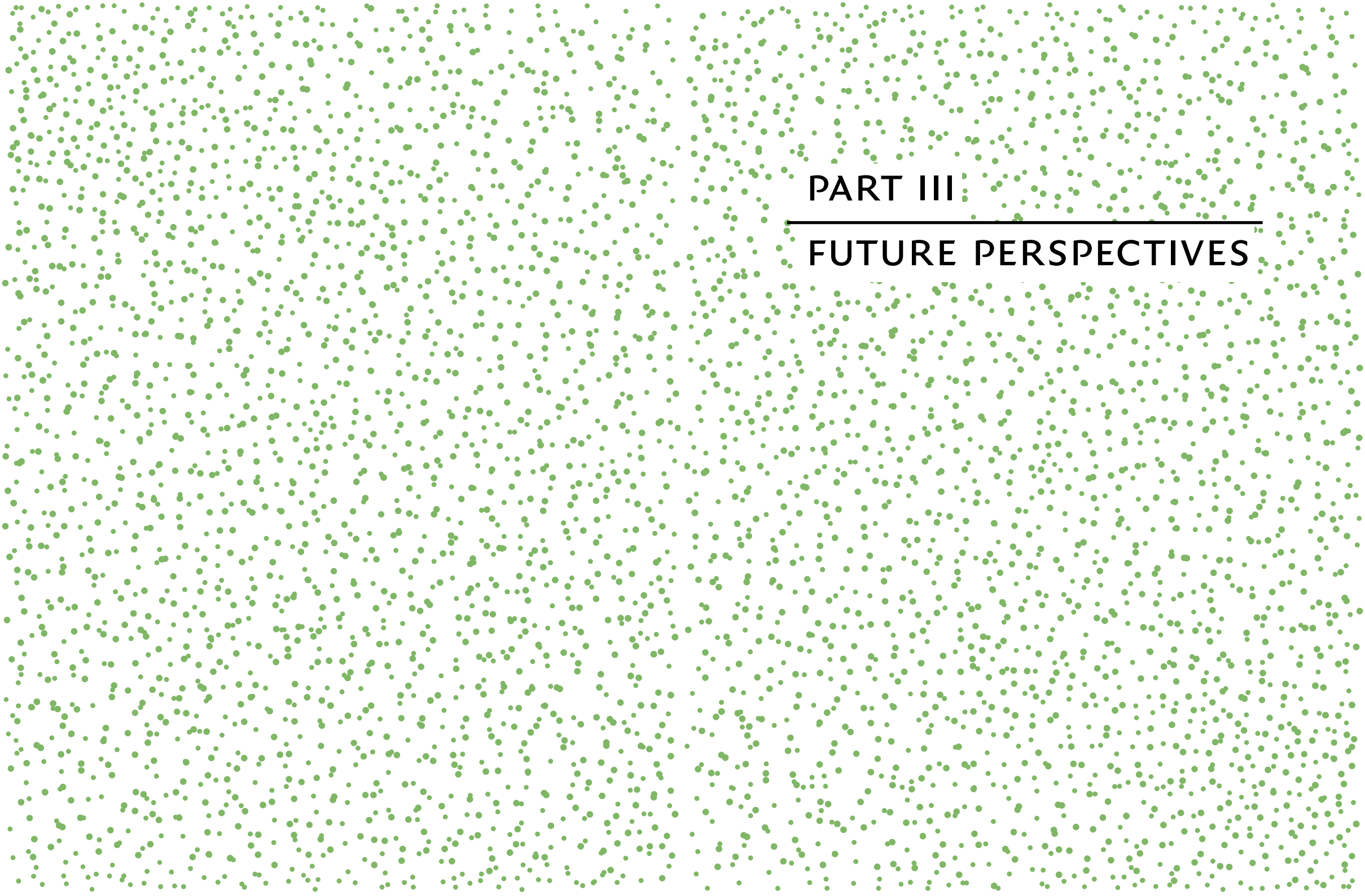


A. Color (left column), fluorescence (middle column), and merged (right column) images of intraoperative imaging of a pancreatic tumor using the Quest imaging system.
 B. Color (left column), fluorescence (middle left column), merged (middle right column) images of ex vivo imaging of slice from the same pancreatic tumor using the Quest imaging system and with the Pearl imager (right column).
 C. Histopathologic evaluation and fluorescence signal in a primary pancreatic tumor. Fluorescence microscopy (left column) shows accumulation of SGM-101 in tumor cells. The fluorescence pattern is consistent with carcinoembryonic antigen (CEA) expression measured using immunohistochemistry (IHC, middle column), which corresponds to the site containing tumor cells visible on hematoxylin and eosin (H&E) staining (right column). Please note: acuity of the images is suboptimal compared to the intraoperative setting as these TIFF images (8 bits) were subtracted from intraoperative videos.

FIGURE 3 FLUORESCENCE DETECTION OF A PERITONEAL AND LIVER METASTASIS OF A PANCREATIC TUMOR.



A. Color (left column), fluorescence (middle left column), and merged (middle right column) images of intraoperative imaging of a peritoneal metastasis of a pancreatic tumor and images of ex vivo imaging of slice from the same metastasis (right column) using the Quest imaging system.
 B. Color (left column), fluorescence (middle left column), and merged (middle right column) images of intraoperative imaging of a liver metastasis of a pancreatic tumor and images of ex vivo imaging of slice from the same metastasis (right column) using the Quest imaging system. Please note: acuity of the images is suboptimal compared to the intraoperative setting as these TIFF images (8 bits) were subtracted from intraoperative videos.



PART III

FUTURE PERSPECTIVES

Chapter 8

Image guided surgery using near-infrared fluorescence: road to clinical translation of novel probes for real time tumor visualization

SPIE 2017 Feb 8

CHARLOTTE HOOGSTINS, HENRICUS HANDGRAAF, LEONORA BOOGERD,
JACOBUS BURGGRAAF, ALEXANDER VAHRMEIJER

ABSTRACT

Fluorescence imaging is a novel intraoperative technique for guiding oncologic surgeons toward radical tumor resections. Application of various fluorescent agents in exploratory clinical trials has already yielded promising results. The field of fluorescence imaging must now move beyond the proof-of-concept phase toward clinical application and implementation. This shift encompasses several hurdles, including standardization, advanced-phase study endpoints, regulatory affairs and routine implementation, which need to be addressed by the community in close collaboration with all stakeholders. These challenges, and the possible actions to overcome them and promote and accelerate clinical implementation of fluorescence imaging, are summarized in this paper.

INTRODUCTION

During oncologic surgery visual inspection under white light and palpation are the principal methods to differentiate cancerous from normal tissue. This distinction is of great clinical importance as positive margins and residual disease are associated with increased local recurrence, the need for adjuvant treatment and poor prognoses [1-4]. Due to limited visual contrast under white light and the inaccuracy of other intraoperative techniques used for assessment of tumors (e.g. frozen section) margin positivity rates are high [1, 5, 6].

With the use of real-time fluorescence guidance, intraoperative contrast between cancerous and benign tissue can be enhanced, likely enabling improvement of surgical outcomes. For visualization of cancer, fluorescence imaging makes use of either endogenous tissue properties (autofluorescence) or administered exogenous fluorescent contrast agents. The latter accumulate in tumor tissue by physiological processes (e.g. enhanced permeability and retention [EPR] effect) or by specific targeting [7].

Near-infrared (NIR, 700–900 nm) fluorescent light is able to penetrate 5-10 mm of tissue and causes almost no autofluorescence, making NIR fluorescent contrast agents particularly suitable for intraoperative imaging [8, 9]. Because the human eye cannot see light in the NIR spectrum, dedicated imaging devices are needed to detect the fluorescence emission of these agents.

In 1998 the first clinical trial describing successful fluorescence imaging of brain tumors using 5-aminolevulinic acid (5-ALA, a metabolic precursor that causes to accumulation of fluorescent porphyrins in malignant glioma tissue) was published [10]. Since then several different fluorescent contrast agents for different targets and many imaging devices for different applications have become available. Clinical trials with these various agents have led to valuable insights to optimize this new technology.

It is essential that the field of intraoperative imaging now moves forward towards clinical implementation. But despite the availability of both fluorescent agents and imaging devices, the fluorescence imaging technology is not consistently employed [11]. The data from first clinical trials supports the use of many of these agents and devices [12-15]. However translational hurdles impede implementation.

These translational hurdles include standards for imaging devices and fluorescent agents, the design and endpoints of larger advanced-phase clinical trials, obtaining regulatory approval and the application in routine surgical practice. For successful clinical translation these issues need to be addressed on a

community level. In this overview these hurdles will be described in more depth and potentially useful strategies will be suggested.

CLINICAL TRANSLATION BEYOND THE PROOF-OF-CONCEPT

INTRODUCTION ● Standardization and quality control play a key role in all radiological modalities. However, standardized and community adopted approaches to qualify NIR fluorescence imaging devices and sensitivity of a fluorescent agents are still lacking. Such standards should be introduced to allow consistent settings of imaging devices and accomplish the correlation of fluorescence with the presence of tumor. Moreover, the use of standardized methodology will be of added value for regulatory approval.

STANDARDS FOR IMAGING DEVICES ● Multiple imaging devices have been developed for clinical imaging but there are no objective specifications regarding sensitivity [16]. For successful fluorescence imaging of clinically relevant concentrations of a certain fluorescent agent, a minimum requirement for the detection of contrast between the signal arising from a suspected lesion and from normal tissue should be identified for imaging devices. Otherwise a lack of fluorescence contrast might be wrongfully attributed to failure of the fluorescent agent when in fact the imaging device is not sensitive enough.

For quantification of the appropriate settings and measurement of the sensitivity of NIR fluorescence imaging devices several approaches can be used. Specificity and sensitivity testing with phantoms that mimic the tissue scattering of background tissue combined with a range of fluorescence signals matching the clinical setting was demonstrated to be of added value [17]. Another option suited for intraoperative fluorescence assessment is thresholding. Using samples from a known cancerous tissue and known normal tissue, the fluorescence intensity of an unknown tissue can be quantified. Despite their value, both approaches are in its self not adequate to be relied upon exclusively for clinical translation, as for instance tumor heterogeneity and tumor size, are not taken into account [18].

Upon completion of the assessment of sensitivity, specificity and working conditions of the different imaging devices, each imaging device should be equipped with an unambiguous list of instruction regarding its use to allow for consistent use. This will enhance the reproducibility in the setting of clinical trials, especially as we are on the verge of large, multicenter trials.

STANDARDS FOR FLUORESCENT AGENTS ● Not only the imaging devices require standardization, the evaluation of performance of fluorescent agents, e.g. sensitivity, is also in need of standardization [19]. To correlate fluorescence with the presence of disease and determine the sensitivity of the fluorescent agent both fluorescence intensity and tumor status need to be quantified. For the quantification of fluorescence signal, the absolute fluorescence signal can be used, but more commonly the fluorescence signal relative to the background signal (tumor-to-background ratio; TBR) is used. The signal is quantified in regions of interest (ROI) of both tumor and background that are manually selected on images. However, manual selection is subject to bias and has low reproducibility. It is worthwhile to pursue other means of quantitation as for instance, automated algorithms to determine the TBR, and investigate their potential value for use in the clinic.

Tumor status can be assessed with histologic analysis using hematoxylin and eosin (H&E) staining. Despite being the gold standard, analysis of H&E staining has various pitfalls, in particular sampling error, which can complicate correlation with fluorescence signal. This is especially relevant for small lesions, e.g. micro metastases. Using a combined approach with ultra-slicing and (pan) keratin staining, this issue can be mitigated. However, as these techniques are too time-consuming for routine use in the daily practice, technical innovation in this area is clearly needed. These challenges concerning both imaging devices and fluorescent agents should be addressed on a community level by formulating novel standards for assessing the sensitivity and by subsequently monitoring the use of these standards.

ENDPOINTS FOR ADVANCED-PHASE CLINICAL TRIALS ● In recent years multiple early-phase clinical trials have assessed the safety, feasibility and appropriate dose and timing of various fluorescent agents. Typically, these early-phase trials are followed by prospectively designed, multicenter phase 3 clinical studies to demonstrate the effectiveness of the agent [20]. Such advanced-phase trials preferably have clear endpoints that can be objectively assessed, like overall survival, progression-free survival or tumor size measurements. However, these traditional endpoints can be time-consuming and expensive to pursue and may be better suited for therapeutic rather than diagnostic agents. The use of well-chosen surrogate endpoints could accelerate the approval of imaging agents by limiting the size, length, complexity and costs of advance phase trials [11]. A possible surrogate endpoint could be therapeutic efficacy, defined as the percentage of change in management following the application of a test,

in this case fluorescence guided surgery. This could apply to positive margins, up or down staging of disease stage or need for adjuvant therapy. It may also be considered to use the patient quality of life as an endpoint. Admittedly, this may be difficult as it would also have to take into account that the outcome of these novel diagnostic techniques may result in abandoning surgery because it is unlikely to be curative and offering the patient palliative care only. Also, functional outcomes could be dominated by adjuvant therapy, which is commonly performed in case of positive resection margins. Other endpoints that could be considered are related to healthcare economics, such as reduction of operation time, re-surgery and costs.

REGULATORY APPROVAL

INTRODUCTION ● Obtaining regulatory approval from the US Food and Drug Administration (FDA) or its European counterpart, the European Medicines Agency (EMA) is essential for the clinical translation of imaging agents. Before approving a new drug, effectiveness of the drug needs to be demonstrated in ‘adequate and well-controlled clinical studies’.

REGULATORY APPROVAL OF IMAGING PRODUCTS ● The FDA does not rigidly enforce this and allows published reports of clinical studies, including exploratory studies at a single site to support approval of imaging agents [20]. However, for published reports, it is recommended that attention is paid to the methodological details as specified in the checklist developed by the Cancer Imaging Program from the National Institute of Health (NIH). This route can be especially helpful in case of investigational agents that lack patent protection and thus have little commercial interest, like indocyanine green (ICG). Approval is subsequently based on risk and benefit considerations that are applicable to all drugs and biologic products. In addition, specific considerations apply to diagnostic imaging drugs. The FDA guidance documents for approval of imaging products (section 351(a) of the Public Health Service Act (42 U.S.C. 262 (a)) states: ‘the ability to locate and outline normal structures or distinguish between normal and abnormal anatomy can speak for itself with respect to the clinical value of the information and will not require additional information substantiating clinical usefulness.’ In addition it is suggested that one-time use imaging agents might even warrant other regulatory models than therapeutic drugs [11]. By all means a close cooperation between academia, industry, and regulatory agencies is indispensable for approval.

IMAGING DEVICE AND AGENT AS A COMBINATION PRODUCT ◉ The marking of a fluorescent agent and imaging device as a combination product for regulatory approval is still subject to discussion [18, 19]. It is not clear if a fluorescent agent should be paired with a specific device, or that fluorescent agents and imaging devices should obtain independent approval. During a recent meeting of the International Society of Image Guided Surgery the general consensus was to seek approval without restriction of the device to any specific optical imaging agent if the device can successfully image more than one fluorophore within the device's excitation/emission spectrum [18]. When a fluorescent agent is to be paired to a specific model of imaging device e.g. Cysview® (Photocure, Oslo, Norway) with Karl Storz blue light cystoscope (PDD system; Karl Storz GmbH and Co., Tuttlingen, Germany), the entry and adoption of fluorescent agents into clinical practice could be restricted. Considerations regarding combination product development can be discussed during a pre-IND or a subsequent meeting with FDA or EMA.

IMPLEMENTATION IN ROUTINE SURGICAL PRACTICE

INTRODUCTION ◉ The potential of intraoperative fluorescence imaging has been demonstrated by various clinical, mostly early-phase, trials. The challenge is to move the field forward towards clinical implementation.

INCREASING AWARENESS ◉ Economic issues are the mainstay of this challenge. Compared to therapeutic drugs the ratio between revenues and development costs are lower for fluorescent agents. Because the market for imaging agents only represent 1% of the total drug market, revenues for a fluorescent agent will only be sufficient when the agent reaches the global market and is established during routine care [21]. This causes a difference in motivation between academia, focusing on agents with potential scientific benefit, and industry, focusing on agents with potential financial benefit. Academic researcher groups typically lack the financial resources and infrastructure for successful translation, and are thus dependent on outside investments. These investments can come either from the industry or from public funding agencies and governments. Irrespectively, strategies to increase awareness among clinical communities, regulatory and funding bodies, the industry and the general public must be employed to ensure funding.

WIDESPREAD AVAILABILITY IMAGING DEVICES ◉ Another hurdle is the availability of imaging devices. Currently, imaging devices are almost exclusively

available in the setting of clinical trials. To stimulate adoption of the technique dedicated, low-cost imaging devices will have to become available for conventional surgical practices. In a routine setting it will not be feasible for surgeons or operating room personnel to frequently adjust the settings (e.g. gain or camera exposure time) of the device. Clear instructions and when possible automated settings will therefore be essential for swift acceptance of the technique.

GENERAL CONCLUSION

Intraoperative fluorescence imaging has great potential to revolutionize oncologic surgery by using fluorescence guidance to distinguish normal from cancerous tissue enabling more radical resections and optimal clinical results. The field is expanding rapidly and numerous fluorescent agents and imaging devices have been developed and studied recently. Despite remarkable developments in the clinical trial setting, the technique has not been translated to a broader surgical practice. This is due to several challenges and hurdles that are yet to be overcome. Standards for qualifying an imaging device and for quantifying sensitivity of a fluorescent agent are needed to ensure accurate and reproducible results. Endpoints for advanced-phase studies that demonstrate effectiveness and yet are not time-consuming and expensive need to be formulated. Both will facilitate the regulatory approval process, especially since the FDA allows published reports of clinical studies, provided they are methodologically sound, to support approval of imaging agents. Awareness of the field needs to be raised to ensure funding. All these challenges warrant a close collaboration between the different parties involved, including academia, clinicians, industry and regulatory and funding bodies. Moreover the fluorescence imaging community has to jointly address the topics regarding standardization, regulatory approval and clinical implementation. With clear standards and a joint approach, data from clinical trials can be aggregated and used to advance the entire field.

REFERENCES

- 1 Iczkowski KA, Lucia MS. Frequency of positive surgical margin at prostatectomy and its effect on patient outcome. *Prostate Cancer*. 2011;2011:673021.
- 2 O'Kelly Priddy CM, Forte VA, Lang JE. The importance of surgical margins in breast cancer. *J Surg Oncol*. 2016;113(3):256-263.
- 3 Raziee HR, Cardoso R, Seevaratnam R, Mahar A, Helyer L, Law C, Coburn N. Systematic review of the predictors of positive margins in gastric cancer surgery and the effect on survival. *Gastric Cancer*. 2012;15 Suppl 1:S116-124.
- 4 Smits RW, Koljenovic S, Hardillo JA, Ten Hove I, Meeuwis CA, Sewnaik A, Dronkers EA, Bakker Schut TC, Langeveld TP, Molenaar J, Hegt VN, Puppels GJ, Baatenburg de Jong RJ. Resection margins in oral cancer surgery: Room for improvement. *Head Neck*. 2016;38 Suppl 1:E2197-2203.
- 5 Woolgar JA, Triantafyllou A. A histopathological appraisal of surgical margins in oral and oropharyngeal cancer resection specimens. *Oral Oncol*. 2005;41(10):1034-1043.
- 6 Atkins J, Al Mushawah F, Appleton CM, Cyr AE, Gillanders WE, Aft RL, Eberlein TJ, Gao F, Margenthaler JA. Positive margin rates following breast-conserving surgery for stage I-III breast cancer: palpable versus nonpalpable tumors. *J Surg Res*. 2012;177(1):109-115.
- 7 Keereweer S, Kerrebijn JD, van Driel PB, Xie B, Kaijzel EL, Snoeks TJ, Que I, Hutteman M, van der Vorst JR, Mieog JS, Vahrmeijer AL, van de Velde CJ, Baatenburg de Jong RJ, Lowik CW. Optical image-guided surgery--where do we stand? *Mol Imaging Biol*. 2011;13(2):199-207.
- 8 Chance B. Near-infrared images using continuous, phase-modulated, and pulsed light with quantitation of blood and blood oxygenation. *Ann N Y Acad Sci*. 1998;838:29-45.
- 9 Frangioni JV. In vivo near-infrared fluorescence imaging. *Curr Opin Chem Biol*. 2003;7(5):626-634.
- 10 Stummer W, Stocker S, Wagner S, Stepp H, Fritsch C, Goetz C, Goetz AE, Kiefmann R, Reulen HJ. Intraoperative detection of malignant gliomas by 5-aminolevulinic acid-induced porphyrin fluorescence. *Neurosurgery*. 1998;42(3):518-525; discussion 525-516.
- 11 Weissleder R, Schwaiger MC, Gambhir SS, Hricak H. Imaging approaches to optimize molecular therapies. *Sci Transl Med*. 2016;8(355):355ps316.
- 12 van Dam GM, Themelis G, Crane LM, Harlaar NJ, Pleijhuis RG, Kelder W, Sarantopoulos A, de Jong JS, Arts HJ, van der Zee AG, Bart J, Low PS, Ntziachristos V. Intraoperative tumor-specific fluorescence imaging in ovarian cancer by folate receptor-alpha targeting: first in-human results. *Nat Med*. 2011;17(10):1315-1319.
- 13 Rosenthal EL, Warram JM, de Boer E, Chung TK, Korb ML, Brandwein-Gensler M, Strong TV, Schmalbach CE, Morlandt AB, Agarwal G, Hartman YE, Carroll WR, Richman JS, Clemons LK, Nabell LM, Zinn KR. Safety and Tumor Specificity of Cetuximab-IRDye800 for Surgical Navigation in Head and Neck Cancer. *Clin Cancer Res*. 2015;21(16):3658-3666.
- 14 Kennedy GT, Okusanya OT, Keating JJ, Heitjan DF, Deshpande C, Litzky LA, Albelda SM, Drebin JA, Nie S, Low PS, Singhal S. The Optical Biopsy: A Novel Technique for Rapid Intraoperative Diagnosis of Primary Pulmonary Adenocarcinomas. *Ann Surg*. 2015;262(4):602-609.
- 15 Hoogstins CE, Tummers QR, Gaarenstroom KN, de Kroon CD, Trimboos JB, Bosse T, Smit VT, Vuyk J, van de Velde CJ, Cohen AF, Low PS, Burggraaf J, Vahrmeijer AL. A Novel Tumor-Specific Agent for Intraoperative Near-Infrared Fluorescence Imaging: A Translational Study in Healthy Volunteers and Patients with Ovarian Cancer. *Clin Cancer Res*. 2016;22(12):2929-2938.
- 16 Zhu B, Sevick-Muraca EM. A review of performance of near-infrared fluorescence imaging devices used in clinical studies. *Br J Radiol*. 2015;88(1045):20140547.
- 17 Zhu B, Rasmussen JC, Sevick-Muraca EM. A matter of collection and detection for intraoperative and noninvasive near-infrared fluorescence molecular imaging: to see or not to see? *Med Phys*. 2014;41(2):022105.
- 18 Rosenthal EL, Warram JM, de Boer E, Basilion JP, Biel MA, Bogyo M, Bouvet M, Brigman BE, Colson YL, DeMeester SR, Gurtner GC, Ishizawa T, Jacobs PM, Keereweer S, Liao JC, Nguyen QT, Olson JM, Paulsen KD, Rieves D, Sumer BD, Tweedle MF, Vahrmeijer AL, Weichert JP, Wilson BC, Zenn MR, Zinn KR, van Dam GM. Successful Translation of Fluorescence Navigation During Oncologic Surgery: A Consensus Report. *J Nucl Med*. 2016;57(1):144-150.
- 19 Snoeks TJ, van Driel PB, Keereweer S, Aime S, Brindle KM, van Dam GM, Lowik CW, Ntziachristos V, Vahrmeijer AL. Towards a successful clinical implementation of fluorescence-guided surgery. *Mol Imaging Biol*. 2014;16(2):147-151.
- 20 Rieves D, Jacobs P. The Use of Published Clinical Study Reports to Support U.S. Food and Drug Administration Approval of Imaging Agents. *J Nucl Med*. 2016;57(12):2022-2026.
- 21 Opacic T, Paefgen V, Lammers T, Kiessling F. Status and trends in the development of clinical diagnostic agents. *Wiley Interdiscip Rev Nanomed Nanobiotechnol*. 2016.

Chapter 9

Setting Standards for Reporting and Quantification in Fluorescence-guided Surgery

Mol Imaging Biol. 2018 May 29

CHARLOTTE HOOGSTINS*, JAN JAAP BURGGRAAF*, MARJORY KOLLER, HENRICUS HANDGRAAF, LEONORA BOOGERD, GOOITZEN VAN DAM, ALEXANDER VAHRMEIJER, JACOBUS BURGGRAAF

* shared first authorship

ABSTRACT

PURPOSE Intraoperative fluorescence imaging (FI) is a promising technique that could potentially guide oncologic surgeons toward more radical resections and thus improve clinical outcome. Despite the increase in the number of clinical trials, fluorescent agents and imaging systems for intraoperative FI, a standardized approach for imaging system performance assessment and post-acquisition image analysis is currently unavailable.

PROCEDURES We conducted a systematic, controlled comparison between two commercially available imaging systems using a novel calibration device for FI systems and various fluorescent agents. In addition, we analyzed fluorescence images from previous studies to evaluate signal-to-background ratio (SBR) and determinants of SBR.

RESULTS Using the calibration device, imaging system performance could be quantified and compared, exposing relevant differences in sensitivity. Image analysis demonstrated a profound influence of background noise and the selection of the background on SBR.

CONCLUSIONS In this article we suggest clear approaches for the quantification of imaging system performance assessment and post-acquisition image analysis, attempting to set new standards in the field of FI.

INTRODUCTION

Image-guided surgery (IGS) is a relatively new and emerging platform, in which imaging techniques are applied intraoperatively. The goal of IGS is to provide the surgeon with real-time information on tissue in the surgical field, aiding in surgical decision making [1]. Fluorescence imaging (FI) is ideal for intraoperative applications due to fast acquisition times (milliseconds), flexibility in application and portability [2]. Various tumor-targeted near-infrared (NIR) fluorescence agents have been successfully studied in clinical trials [3-6]. Moreover, there is great potential for a broad range of clinical applications besides oncology, such as infectious and inflammatory diseases [7]. Consequently, new study groups, industry as well as hospitals are increasingly interested to explore and implement this technology in clinical care.

As NIR light (wavelength 600-900 nm) is invisible to the human eye, dedicated imaging systems are needed to detect the fluorescence signal and to form a two-dimensional (2D) image demarking its tissue distribution. The intraoperative detection of an imaging agent depends on various biological and optical factors (Table 1). The considerable increase in the number of clinical trials in the FI field has led to the development of a variety of FI systems [8]. However, as the imaging system represents the last link in the chain, sensitivity (i.e. detection limit) of the imaging system is crucial [9]. It is therefore important to ascertain if an imaging system is sensitive enough for the application of interest. Phantoms that mimic relevant concentrations of a fluorescent agent in scattering and absorption media can aid in the quantification of the imaging system performance. However, guidance or standard documents describing sensitivity assessment for imaging systems, whether or not including phantoms, is currently lacking [10, 11].

The interplay between biological and optical factors ultimately results in a fluorescence image, in which the fluorescence signal in both the target and background can be semi-quantified. Using ImageJ (National Institute of Health, Bethesda, USA, a public domain image processing and analysis program) or proprietary software provided with the imaging system software, area and pixel value statistics in user-defined selections, known as a region of interest (ROI), can be analyzed. Standardized methods for selection of ROIs are not available, making this procedure prone to selection bias. Using the measured fluorescence signal in the ROIs of target and background, the signal-to-background ratio (SBR, also reported as target or tumor-to-background ratio [TBR]) is calculated (equation 1).

$$SBR = \frac{(\text{MEAN SIGNAL TUMOR})}{(\text{MEAN SIGNAL BACKGROUND})}$$

The SBR is the key determinant of sensitivity and detectability in FI and is frequently reported as a relevant endpoint in (pre-)clinical studies. Tichauer *et al.* advocate that noise originating from the background can influence the contrast between target and background and suggest an alternative measure, the contrast-to-noise ratio (CNR) (equation 2) [12].

$$CNR = \frac{(\text{MEAN SIGNAL TUMOR} - \text{MEAN SIGNAL BACKGROUND})}{(\text{STANDARD DEVIATION BACKGROUND})}$$

Although it is theoretically plausible that CNR may of added value, this read-out has not yet been applied in daily practice. Thus, a comparison between TBR and CNR of in vivo obtained images is needed.

Intraoperative FI holds great promise to revolutionize surgery, but the ability to quantify FI, for reasons of comparison between centers and the imaging systems, will be a critical factor for successful application of the imaging technique. Just as the field is in the process of gathering the evidence through well-designed phase II/III clinical trials necessary for routine clinical application, standards are needed to assure standardization and to assess if imaging systems are adequately sensitive and fluorescence images can be accurately quantified [11, 13, 14]. Therefore, we conducted a systematic, controlled in vitro comparison between two commercially available, state-of-the-art clinical imaging systems using a novel designed calibration device for FI systems and various fluorescent agents to evaluate important performance characteristics of fluorescence imaging. In addition, we evaluated the effect of ROI selection and background noise on SBR calculation by analyzing 271 fluorescence images from previous studies [3, 15-20]. Based on these results, we propose an easily applicable, standardized approach to quantify and report imaging device performance and fluorescence image analysis.

METHODS

IMAGING SYSTEM PERFORMANCE ● The CalibrationDisk™ (SurgVision, t Harde, the Netherlands) is a calibration device for FI systems. The disk can hold 8 clear polypropylene tubes of 0.65 ml (Catalog # 15160, Sorenson, BioScience, Inc, Murray, USA) (Figure 1). The device consists of two parts; an upper disk

which holds the tubes in place and a base on which the upper disk can rotate. The upper disk has round windows that allow measurement of signal intensity in each tube. By rotating the disk, different concentrations of a tracer can be imaged at the same position and under the same excitation conditions providing assessment of homogeneity in illumination of the field of view. We performed the experiment with two different commercially available imaging systems with distinctly different modes of operation; imaging system A and imaging system B. Both systems are state-of-the-art clinical systems optimized for intraoperative NIR imaging providing real-time fluorescence images and white light overlays. System A, a cooled system, has two cameras, one for white-light image acquisition and one for fluorescence image acquisition of a single NIR channel (825 to 850 nm). System B uses a single camera for imaging two fluorescence channels (far red 700 to 830 nm and NIR 830 to 1100 nm) and a white-light channel. Four different NIR fluorescent agents including two dyes (indocyanin green (ICG) [Pulsion Medical Systems Munich, Germany] and IRDye 800CW [LI-COR Biosciences, Lincoln, NE, USA]) and two molecularly targeting fluorescent tracers (bevacuzimab-IRDYE800CW [21] and a folate-NIR fluorophore (OTL38) [3]) were used to make dilution series in Intralipid 2%. All dilution series consisted of 21 concentrations, starting at 10,000 nanomolar and, following one on one dilution with Intralipid 2%, ending at 10 picomolar. Vials containing the 21 different concentrations were divided into three sets of seven (low, medium and high concentration). A background or '0-vial' containing Intralipid 2% without a fluorescent agent was added to each set (Figure 1).

Each set was stacked into the CalibrationDisk™ and imaged at 3 different exposure times (low, medium, high) and 3 different gain settings (low, medium, high) with both imaging systems. A low, medium, high setting of gain and exposure time were used rather than absolute values, as both imaging systems had a different maximum gain and exposure time. Imaging was done in a dark room under identical conditions, including an identical working distance of 20 cm. System A provides high quality and resolution 16-bits TIFF images. For system B, images were subtracted from videos (.qifs format) in the corresponding software suite, resulting in 8-bits TIFF images. Images were exported to ImageJ for gray value intensity analyses. Sensitivity was defined as the lowest concentration detectable at maximal settings (high gain, high exposure time). To mimic SBR in the clinical setting, we determined at what concentration a SBR >2 between the pertaining vial and background vial was achieved. For a fair comparison of different bits size images, fluorescence intensity values were indexed for maximal imaging system value and plotted on log₁₀ fluorophore

concentration versus log₁₀ fluorescence signal graphs. Linearity was defined as the slopes of linear fits to the log-log data. An optimal imaging system provides a doubling in signal strength for every 2-fold increase in concentration, resulting in a fitted linear slope of 1 in this logX-logY plot).

As a reference, the performance of the two intraoperative FI systems was compared to the Pearl Impulse preclinical imager (LI-COR Biosciences, Lincoln, NE, USA). This system contains an ambient-light-free chamber and can be used as a standard of the maximal linearity and sensitivity achievable. Analysis of images obtained with the Pearl imaging system was done using the software suite provided with the device.

FLUORESCENCE IMAGE ANALYSIS ● We evaluated 271 images available from previous studies to evaluate the effect of ROI selection and background noise on SBR. We randomly selected a representative sample of intraoperative and ex-vivo images from both animal and human studies in different tumor types using different fluorescent agents and imaging systems (Table 2).

On these images we drew a ROI around the (histologically confirmed) tumor. To evaluate the effect of ROI selection we drew two different ROIs of similar area size in the background: the darkest region adjacent to the tumor ROI and the lightest region adjacent to the tumor. Lastly, we drew a ROI using our preferred method selecting the region surrounding the tumor ROI remaining within the anatomical structure in which the tumor is present. This can be done in ImageJ by subtracting the tumor ROI from the overlapping background, using the ROI manager menu and selecting the 'More' button followed by the 'XOR' button. Figure 2 displays a representative example of ROI selection. Mean gray values and the standard deviation of the pixels within one ROI were assessed using ImageJ. To evaluate the effect of background noise we applied both SBR and CNR equation on the values obtained with ImageJ.

RESULTS

IMAGING SYSTEM PERFORMANCE ● By assessing the lowest concentration visible with an imaging system, sensitivity of the system can be determined. Using the CalibrationDisk™ the lowest detectable concentration can easily be assessed for each agent and imaging system (Figure 3). We found, irrespective of the fluorescent agent used, that system A is superior to system B in terms of sensitivity. The lowest detectable concentration with system A is 1 nM, for system B this is 500 nM. For comparison, the Pearl Impulse detects concentrations

as low as 0.05 nM. Gain and exposure time settings influenced sensitivity of the system, with high settings leading to maximal sensitivity for both systems, nevertheless these settings did not effect the mutual differences between system A and B.

Moreover, SBR-values > 2 (compared to the background vial) could be achieved from the low concentration set (0.61 nM) using system A, while system B could only achieve a SBR > 2 at concentrations exceeding 312.5 nM. Thus, in vitro performance of system A was superior to system B in terms of SBR.

Analysis of the linearity of imaging system A and B reveals striking differences, with system A being superior, approaching the linearity of the Pearl Impulse. For the low and medium concentrations, the detection limit of the system was reached, therefore signals measured by system B remain in the same range resulting in a horizontal line on the log₁₀ graph. However, for the high concentrations system B does display a linear gradient similar to system A and the Pearl Impulse (Figure 4).

FLUORESCENCE IMAGE ANALYSIS ● The method applied for ROI selection had a profound influence on both SBR and CNR. Figure 2 shows the influence of background selection on CNR and TBR. Obviously, selection of a darker background will increase the SBR. As figure 2 effectively displays, a sufficient SBR (> 2) can be achieved by adapting background ROI selection. In addition, the area size of the background ROI influences the CNR. As the selection of a small area as background results in a small standard deviation, CNR is higher when smaller ROIs are selected.

DISCUSSION

Quantitative ability of a FI system will play a crucial role in the clinical adoption of intraoperative FI. Despite repeated calls from the FI community, guidelines or standards for quantification of the performance of imaging systems or the analysis of fluorescence images are still lacking [11, 13, 14]. As clinical trials are expanding, the need of a performance test was regarded highly urgent and as such we propose a simple and low-cost imaging system performance test, that can be applied to every fluorescent agent and imaging system. We demonstrate how this test can be performed and how data can be interpreted. In addition, we evaluated a representative sample of 271 fluorescence images. Based on the effect of ROI selection and background noise on SBR calculation, we also propose a routine procedure for quantification of fluorescence images.

IMAGING SYSTEM PERFORMANCE ● Sensitivity of two different imaging systems for intraoperative use was assessed. The goal of our experiment was not to quantify performance of an individual imaging systems, but to demonstrate how to compare different imaging systems and predict clinical performance in an experimental setting. Hence we decided to select systems with a distinct mechanism of action and anonymize both systems. For the imaging system assessment, we used the CalibrationDisk™ and tubes filled with descending concentrations of different fluorescent agents. Various types of other phantoms are described in literature. The use of solid polyurethane phantoms, with TiO₂ particles mimicking scattering and quantum dots mimicking different concentrations of a fluorophore, is suggested by Zhu *et al.* [9]. Benefit of these solid phantoms is their longer shelf life that allows repeated measurements over time. Disadvantages are that these phantoms are difficult to construct. More importantly, however, is that while quantum dots mimic the fluorescence of the agent it does not use the actual fluorescent tracer that will be used in humans and thus provides only a distal proxy of the crucial information. Others have suggested the use of more tissue like-phantoms made from gelatin [22, 23]. The fluorescent inclusions, used to mimic tumors, are prepared using a custom-made silicone mold, which is filled with agarose mixture containing a relevant concentration of the fluorescent agent. Alternatively, hydroxyapatite (HA) crystals loaded with Pam78, a fluorescent derivative of the bisphosphonate pamidronate, calibrated against the relevant concentration of the fluorescent agent can be used. Background tissue is made from gelatin to which various ingredients can be added to mimic absorption (hemoglobin or pink India ink), scattering (using Intralipid or milk powder) and autofluorescence (ICG). The fluorescent inclusions can be incorporated at various depths in the gelatin base. Although close to the clinical setting, the manufacturing of these tissue-like phantoms is laborious and the shelf-life is limited. For training purposes these phantoms are probably superior, but for sensitivity and comparability testing of imaging systems most features seem superfluous. The use of the CalibrationDisk™ allowed determination of the lowest concentration detectable and the ability to quantify concentrations. This data can be used to compare imaging systems or to predict clinical performance and can consequently simplify the task of selecting the right system for a certain application. However, users of imaging systems should be aware that the generated in vitro data is a simplification of the in vivo reality. In vivo optical tissue properties influence the ability to discriminate the signal from its background, sufficient knowledge and careful consideration of these limitations remains of the utmost importance. Moreover various other

factors besides sensitivity may play a role in the selection process. Dsouza et al. suggest six key features for imaging systems [10]:

- Real-time overlay of white-light reflectance and fluorescence images;
- Fluorescence-mode operation with ambient room lighting present;
- High sensitivity to tracer of interest;
- Ability to quantify fluorophores in situ;
- Ability to image multiple fluorophores simultaneously;
- Maximized ergonomic use.

Although we focused on the sensitivity point, the other points are equally relevant when deciding on the optimal imaging system for a certain application. In addition, the costs should also be taken into account.

FLUORESCENCE IMAGE ANALYSIS ◉ The basic principle for FI is the excitation of fluorophores using a light source and the subsequent detection of photons emitted by the excited fluorophore using the imaging system. The detection of emitted photons is influenced by tissue optical properties like absorption and scattering (including reflection). Absorption of photons is a consequence of tissue specific absorption properties, of which in humans blood is the main absorber [24]. Scattering is the change of the direction of a photon in tissue. Scattering events can cause decreased signal strength and source localization, as occurs with fatty tissue. The effect of these phenomena is increased when a photon has to travel through more tissue, thus with greater tissue depths. Reflection seen at the surface of tissues causes diffusion of the signal and consequently reduced detection. Besides the targeted fluorophore, excitation can cause endogenous fluorophores within the tissue to fluoresce as well (e.g. autofluorescence). Noise is the sum of autofluorescence, scattering and reflection events and can make it difficult to discern the actual fluorescence signal. A SBR >2 is generally considered adequate to differentiate target from background [25]. Nevertheless, there are clinical trials in which SBR values below 2 are described as sufficient for intraoperative FI [26]. Despite routine use in optical imaging, including nuclear medicine, the cut-of value of 2 seems to be based on marginal evidence and the clinical relevance of this cut-of seems at least questionable. CNR is the ratio of the absolute difference between background and tumor signal and the standard deviation of the background. Rewriting the CNR formula shows that the CNR is strongly dependent on the SBR (equation 3).

$$\text{CNR} = \frac{(\text{SBR}-1) * ((\text{MEAN SIGNAL BACKGROUND}))}{(\text{STANDARD DEVIATION BACKGROUND})}$$

The use of CNR is theoretically favorable over SBR to quantitate in vivo obtained (patient) imaging data as it is more comprehensive measure and thus provides extra information. Following the three-sigma-rule, an empirical statistic rule often used in descriptive statistics, a CNR of 3 or higher indicates that the average tumor signal is present only in approximately 0.135% of the background selection [27]. It could therefore be argued that the CNR has a more evidence-based cut-off value.

However, this does not instantaneously mean that the CNR can be declared superior to SBR, as both quantitative measures are critically dependent on the ROI selection. Background ROI selection has an important influence on the mean background signal (SBR and CNR) and its standard deviation (CNR), rendering CNR is equally prone to selection bias as SBR. To increase reproducibility in FI research ROI selection process should be standardized and described more in detail in scientific articles. We suggest a ROI selection procedure that is representative and least prone to selection bias. However, as selection is done manually, bias cannot be excluded completely. The gold standard remains performance of biodistribution studies describing the percentage of the dose per gram of tumor and background tissue.

CONCLUSION ◉ In conclusion, assessing the sensitivity in terms of the detection limit of an imaging system is easy and yields relevant data. Data can be used to compare imaging systems or to predict clinical performance, which allows selecting the right system for a certain application. Importantly, other factors, including costs and ergonomics should also be taken into account. Although CNR is partly a result of SBR, it does provide additional information regarding the noise and allows a more scientific base for a cut-of-value. Irrespective of the use the SBR or CNR formula, for contrast quantification, selection of a representative background and tumor ROI is of the utmost importance. Manual ROI selection without a clearly defined procedure, allows bias, potentially misrepresents CNR and SBR results and has low reproducibility. In general, researcher and clinicians should be aware of these possibilities and limitations of FI systems and image quantification.

REFERENCES

- 1 Vahrmeijer AL, Hutteman M, van der Vorst JR, van de Velde CJ, Frangioni JV (2013) Image-guided cancer surgery using near-infrared fluorescence. *Nat Rev Clin Oncol.* 10:507-18.
- 2 Themelis G, Yoo JS, Soh KS, Schulz R, Ntziachristos V (2009) Real-time intraoperative fluorescence imaging system using light-absorption correction. *J Biomed Opt.* 14:064012.
- 3 Hoogstins CE, Tummers QR, Gaarenstroom KN, et al. (2016) A Novel Tumor-Specific Agent for Intraoperative Near-Infrared Fluorescence Imaging: A Translational Study in Healthy Volunteers and Patients with Ovarian Cancer. *Clin Cancer Res.* 22:2929-38.
- 4 Rosenthal EL, Warram JM, de Boer E, et al. (2015) Safety and Tumor Specificity of Cetuximab-IRDye800 for Surgical Navigation in Head and Neck Cancer. *Clin Cancer Res.* 21:3658-66.
- 5 van Dam GM, Themelis G, Crane LM, et al. (2011) Intraoperative tumor-specific fluorescence imaging in ovarian cancer by folate receptor-alpha targeting: first in-human results. *Nat Med.* 17:1315-9.
- 6 Harlaar NJ, Koller M, de Jongh SJ, et al. (2016) Molecular fluorescence-guided surgery of peritoneal carcinomatosis of colorectal origin: a single-centre feasibility study. *Lancet Gastroenterol Hepatol.* 1:283-90.
- 7 Tipirneni KE, Rosenthal EL, Moore LS, et al. (2017) Fluorescence Imaging for Cancer Screening and Surveillance. *Mol Imaging Biol.* 19:645-655
- 8 Zhang RR, Schroeder AB, Grudzinski JJ, et al. (2017) Beyond the margins: real-time detection of cancer using targeted fluorophores. *Nat Rev Clin Oncol.* 14:347-64.
- 9 Zhu B, Rasmussen JC, Sevic-Muraca EM (2014) A matter of collection and detection for intraoperative and noninvasive near-infrared fluorescence molecular imaging: to see or not to see? *Med Phys.* 41:022105.
- 10 DSouza AV, Lin H, Henderson ER, Samkoe KS, Pogue BW (2016) Review of fluorescence guided surgery systems: identification of key performance capabilities beyond indocyanine green imaging. *J Biomed Opt.* 21:80901.
- 11 Pogue BW, Gioux S, Hoogstins CES, et al. (2017) Image guided surgery using near-infrared fluorescence: road to clinical translation of novel probes for real time tumor visualization. *SPIE Proceedings 10049(Molecular-Guided Surgery: Molecules, Devices, and Applications III):100490X.*
- 12 Tichauer KM, Samkoe KS, Sexton KJ, Gunn JR, Hasan T, Pogue BW (2012) Improved tumor contrast achieved by single time point dual-reporter fluorescence imaging. *J Biomed Opt.* 17:066001.
- 13 Snoeks TJ, van Driel PB, Keereweer S, et al. (2014) Towards a successful clinical implementation of fluorescence-guided surgery. *Mol Imaging Biol.* 16:147-51.
- 14 Rosenthal EL, Warram JM, de Boer E, et al. (2016) Successful Translation of Fluorescence Navigation During Oncologic Surgery: A Consensus Report. *J Nucl Med.* 57:144-50.
- 15 Tummers QR, Hoogstins CE, Gaarenstroom KN, et al. (2016) Intraoperative imaging of folate receptor alpha positive ovarian and breast cancer using the tumor specific agent EC17. *Oncotarget.* 7:32144-55.
- 16 Verbeek FP, Tummers QR, Rietbergen DD, et al. (2015) Sentinel Lymph Node Biopsy in Vulvar Cancer Using Combined Radioactive and Fluorescence Guidance. *Int J Gynecol Cancer.* 25:1086-93.
- 17 Handgraaf HJM, Boonstra MC, Prevo H, et al. (2017) Real-time near-infrared fluorescence imaging using cRGD-ZW800-1 for intraoperative visualization of multiple cancer types. *Oncotarget.* 8:21054-66.
- 18 Hutteman M, van der Vorst JR, Mieog JS, et al. (2011) Near-infrared fluorescence imaging in patients undergoing pancreaticoduodenectomy. *Eur Surg Res.* 47:90-7.
- 19 Handgraaf HJ, Boogerd LS, Verbeek FP, et al. (2016) Intraoperative fluorescence imaging to localize tumors and sentinel lymph nodes in rectal cancer. *Minim Invasive Ther Allied Technol.* 25:48-53.
- 20 Tummers QR, Verbeek FP, Prevo HA, et al. (2015) First experience on laparoscopic near-infrared fluorescence imaging of hepatic uveal melanoma metastases using indocyanine green. *Surg Innov.* 22:20-5.
- 21 Koch M, de Jong JS, Glatz J, et al. (2017) Threshold Analysis and Biodistribution of Fluorescently Labeled Bevacizumab in Human Breast Cancer. *Cancer Res.* 77:623-31.
- 22 De Grand AM, Lomnes SJ, Lee DS, et al. (2006) Tissue-like phantoms for near-infrared fluorescence imaging system assessment and the training of surgeons. *J Biomed Opt.* 11:014007.
- 23 Pleijhuis R, Timmermans A, De Jong J, De Boer E, Ntziachristos V, Van Dam G (2014) Tissue-simulating phantoms for assessing potential near-infrared fluorescence imaging applications in breast cancer surgery. *J Vis Exp.* 91:51776.
- 24 Chance B. (1998) Near-infrared images using continuous, phase-modulated, and pulsed light with quantitation of blood and blood oxygenation. *Ann NY Acad Sci.* 838:29-45.
- 25 Boonstra MC, Tolner B, Schaafsma BE, et al. (2015) Preclinical evaluation of a novel CEA-targeting near-infrared fluorescent tracer delineating colorectal and pancreatic tumors. *Int J Cancer.* 137:1910-20.
- 26 Liberale G, Vankerckhove S, Caldon MG, et al. (2016) Fluorescence Imaging After Indocyanine Green Injection for Detection of Peritoneal Metastases in Patients Undergoing Cytoreductive Surgery for Peritoneal Carcinomatosis From Colorectal Cancer: A Pilot Study. *Ann Surg.* 264:1110-5.
- 27 Colquhoun D (2014) An investigation of the false discovery rate and the misinterpretation of p-values. *R Soc Open Sci.* 1:140216.

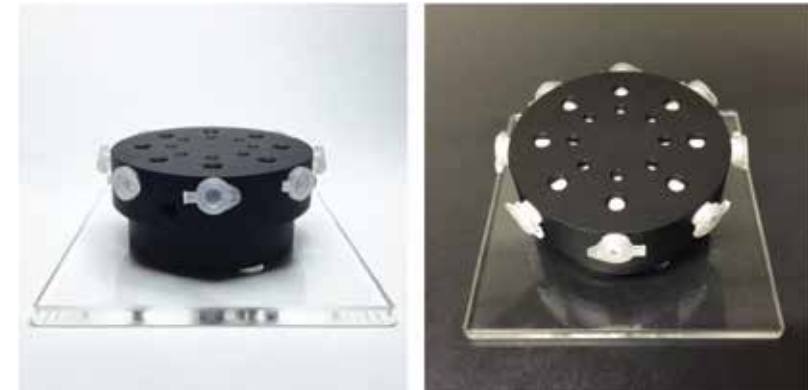
TABLE 1 FACTORS OF INFLUENCE ON THE SIGNAL TO BACKGROUND RATIO

Concentration probe to reach tumor	Imaging	Tumor qualification for scientific reporting
Specific delivery of a tracer to tumor (i.e. vascularization of the tumor, Enhanced Permeability and Retention [EPR])	Imaging settings (exposure time, camera distance, gain, darkness of room)	Software (image format, program settings)
Tumor-specific receptor-ligand kinetics (receptor availability, binding and dissociation constants)	Optical qualities (scattering, absorption, autofluorescence, depth of penetration)	Background and tumor selection
Clearance	Camera system	Radiating underlying tissue
Dosing	Noise	TBR or CNR

TABLE 2 SPECIFICATIONS OF THE IMAGES USED FOR FLUORESCENCE IMAGE ANALYSIS

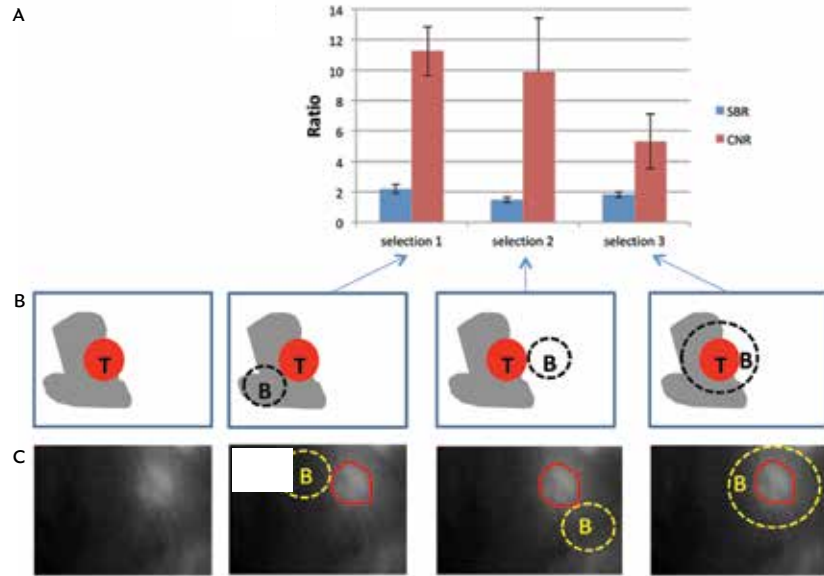
	Imaging system	Probe	Tumor type
Animal	Pearl	Trastuzumab-DTPA[111in]	Breast
		CRGD-ZW800-1	Colorectal
Human	Artemis Flare	ICG	Liver
			Pancreas
			Vulvar SLN
			Rectal
		OTL38	Ovarian
		EC17	Ovarian

FIGURE 1 THE CALIBRATIONDISK™



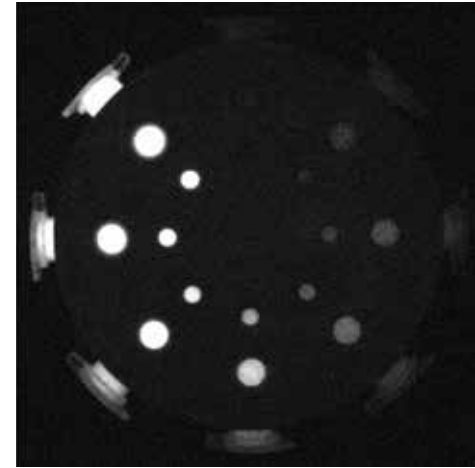
The CalibrationDisk™ (SurgVision, t Harde, the Netherlands) loaded with 8 clear polypropylene tubes of 0.65 ml (Catalog # 15160, Sorenson, BioScience, Inc, Murray, U.S.A.)

FIGURE 2 THE INFLUENCE OF BACKGROUND SELECTION



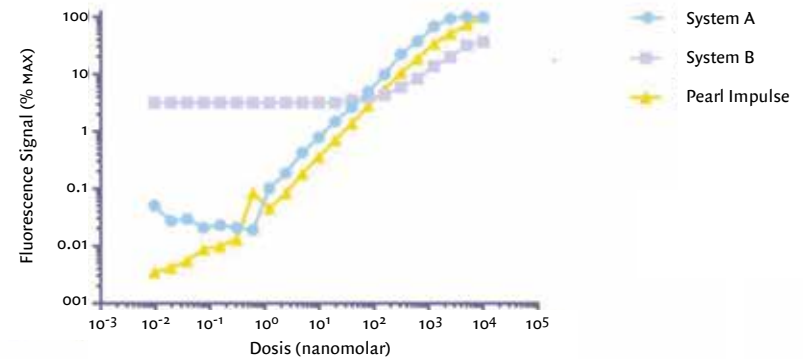
A. The influence of background selection on CNR and TBR.
 B. A schematic example of different background selections.
 C. Intraoperative image of a fluorescent metastatic lymph node with different background selections.

FIGURE 3 FLUORESCENCE IMAGING OF THE CALIBRATIONDISK™

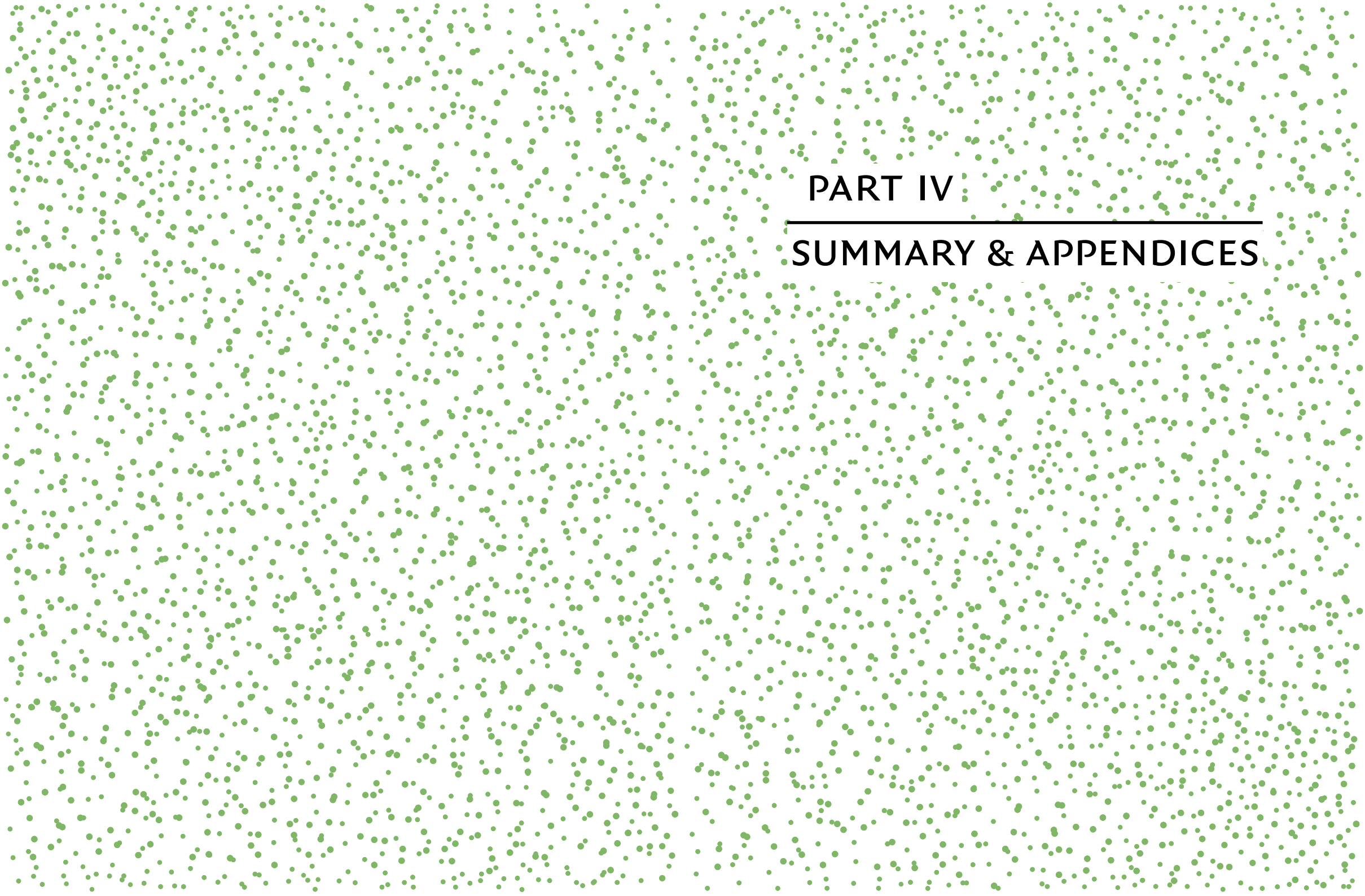


Fluorescence imaging of the CalibrationDisk™ containing 7 vials with ascending concentrations of a fluorescent agent diluted in Intralipid 2% and at 12 o'clock position a background or '0-vial' containing Intralipid 2% without a fluorescent agent.

FIGURE 4 LINEARITY OF FLUORESCENCE SIGNAL STRENGTH



Analysis of the linearity of imaging system A and B compared to the Pearl Imager. An optimal imaging system provides a doubling in signal strength for every 2-fold increase in concentration, resulting in a slope of 1 (linear fit with 45° angle in logX-logY plot).

The background of the entire page is a dense, repeating pattern of small, light green dots. The dots are arranged in a grid-like fashion, creating a textured, dotted effect.

PART IV

SUMMARY & APPENDICES

Chapter 10

Summary

Intraoperative visualization of tumors could be enhanced by the use of near-infrared (NIR) fluorescent contrast agents. The fluorescence imaging field first focused on clinically available contrast agents that do not specifically bind to tumor cells. Nowadays the focus is shifting more towards novel contrast agents that target receptors overexpressed on tumor cells. Part one of this thesis illustrates the road towards the use of tumor-targeted fluorescent agents, by highlighting the disadvantages of the use of non-targeted fluorescent contrast agents and demonstrating how to select biomarkers for tumor targeted fluorescence imaging. In part two of this thesis the clinical translation of tumor-targeted agents is exemplified by describing the introduction of three different agents for several indications (ovarian cancer, breast cancer and pancreatic cancer) in four clinical trials. Part three focusses on the future perspectives of image-guided fluorescence surgery. The road toward clinical application and implementation, associated challenges, and the possible actions to overcome them are summarized in this part.

PART ONE: ROAD TOWARDS TUMOR-TARGETED AGENTS ● In chapter two we hypothesize, based on mouse models, that indocyanine green (ICG) cumulates in tumor tissue as a result of enhanced permeability and retention (EPR), allowing NIR fluorescence imaging using in ovarian cancer. In the ten patients included in this study, eight metastatic lesions were detected, which were all NIR fluorescent. However, 13 non-malignant lesions were also NIR fluorescent, resulting in a false-positive rate of 62%. As a consequence of this high false-positive rate, NIR fluorescence imaging using ICG based on the EPR effect was deemed unsatisfactory for the detection of ovarian cancer metastases, stressing the need for tumor-specific intraoperative agents. In chapter three we assess the suitability of different biomarkers as potential targets for tumor-targeted imaging of peritoneal metastases (PM) of colorectal carcinoma (CRC). Following immunohistochemical stainings on tissue samples, overexpression of the epithelial cell adhesion molecule (EPCAM) and carcinoembryonic antigen (CEA) was seen in 100% of PM samples while overexpression of other biomarkers (e.g. Tyrosine-kinase Met and folate receptor α) was limited (20% of PM samples). This demonstrates that both EPCAM and CEA are suitable targets for fluorescence imaging of PM in patients with CRC.

PART TWO: CLINICAL TRANSLATION OF TUMOR-TARGETED AGENTS ● In chapter four we describe the use of EC17, a folate receptor alpha (FR α)-targeting agent that fluoresces at 500 nm, in twelve ovarian and three breast cancer patients

undergoing surgical resection. Although EC17 allowed detection of tumor-specific fluorescence signal in both breast and ovarian cancer, autofluorescence caused false-positive lesions in ovarian cancer and difficulty in discriminating breast cancer-specific fluorescence from background signal. We therefore concluded FR α is a favorable target for fluorescence-guided surgery, but imaging in the NIR fluorescence light spectrum is required to minimize autofluorescence and further improve intraoperative tumor detection.

Subsequently we performed a first-in-human trial with the successor of EC17, OTL38 a near-infrared (796 nm) fluorescent folate analogue. In chapter five we describe a combined study in 30 healthy volunteers and in 12 patients who had epithelial ovarian cancer and were scheduled for cytoreductive surgery. Intravenous infusion of OTL38 in healthy volunteers yielded an optimal dosage range and time window for intraoperative imaging. In patients with ovarian cancer, OTL38 accumulated in folate receptor alpha-positive tumors and metastases, enabling the surgeon to resect an additional 29% of malignant lesions without hindrance from autofluorescence. Based on these results, we further assessed the use of OTL38 in 6 patients with early stage ovarian cancer undergoing a surgical staging procedure in chapter six. The use of OTL38 allowed intraoperative distinction between a malignant and benign primary tumor. However the anticipated added value of NIR fluorescence imaging in staging procedures, the detection of occult metastases, could not be demonstrated in this study as metastatic lesions were not present in any of the patients. Moreover, fluorescence imaging led to resection of non-malignant lymph nodes following binding of OTL38 to tumor associated macrophages in lymph nodes. Chapter seven describes SGM-101, a NIR fluorescent-labeled anti-carcinoembryonic antigen antibody. We performed a feasibility study using SGM-101 in twelve patients undergoing a surgical exploration for pancreatic cancer. Similar to the folate analogues, we found specific accumulation of the fluorescent contrast agent in both primary tumors and peritoneal and liver metastases. However, the mean tumor-to-background ratios (TBRs) were more modest in comparison to TBRs in the ovarian cancer studies. In addition, false negativity was seen twice as a consequence over overlaying blood or tissue that blocked the fluorescent signal. This highlights a common drawback of fluorescence imaging: limited depth penetration.

PART THREE: FUTURE PERSPECTIVES ● In chapter eight we pose that the field of fluorescence imaging must move beyond the proof-of-concept phase. In order to achieve clinical application and implementation several hurdles need to be

addressed by the fluorescence imaging community. These include standards for qualifying an imaging device and for quantifying sensitivity of a fluorescent agent, which are needed to ensure accurate and reproducible results. In addition endpoints for advanced-phase studies that demonstrate effectiveness and yet are not time-consuming and expensive need to be formulated. Moreover clear standards and well-chosen endpoints will facilitate the regulatory approval process. In chapter nine we attempt to set new standards by conducting a systematic, controlled comparison between two commercially available imaging systems using a novel calibration device. Moreover we evaluated the calculation of the signal-to-background ratio (SBR), a key determinant of sensitivity and detectability in fluorescence imaging. Using the calibration device, imaging system performance could be quantified and compared, exposing relevant differences in sensitivity. We show a profound influence of background noise and the selection of the background on SBR. SBR calculation without a clearly defined procedure, allows bias, potentially misrepresents study results and has low reproducibility.

Chapter 11

Nederlandse samenvatting

BEELDGELEIDE CHIRURGIE MET FLUORESCENTIE

Chirurgie is nog steeds de hoeksteen van de behandeling van solide tumoren. Tijdens de operatieve verwijdering van deze tumoren is de chirurg grotendeels afhankelijk van het zien en voelen van subtiele veranderingen om onderscheid te kunnen maken tussen gezond en kwaadaardig weefsel. Als gevolg hiervan kan er onnodig gezond weefsel worden uitgenomen of kan er kwaadaardige weefsel achterblijven (incomplete resectie). Beeldgeleide chirurgie kan de chirurg tijdens het opereren van extra visuele informatie voorzien waardoor er duidelijker onderscheid gemaakt kan worden tussen kwaadaardig en normaal weefsel. Voor dit onderscheid wordt gebruik gemaakt van fluorescent contrastmiddelen. Een externe lichtbron exciteert bepaalde moleculen (fluoroforen) in het contrastmiddel. Omdat fluorescentielicht onzichtbaar is voor het menselijk oog, wordt een speciaal camerasysteem gebruikt om de signalen van de fluoroforen op te vangen. Aanvankelijk werd gebruik gemaakt van fluorescente contrastmiddelen die door toevallige processen in bepaalde tumoren ophopen. Dit proefschrift beschrijft de toepassing van nieuwe fluorescente contrastmiddelen die specifiek aan tumorcellen binden.

In het eerste gedeelte van dit proefschrift worden de processen beschreven die geleid hebben tot de toepassing van deze tumor-specifieke contrastmiddelen. In deel twee van dit proefschrift worden vier klinische onderzoeken beschreven waarin gebruik gemaakt wordt van tumor-specifieke contrastmiddelen. Deel drie richt zich op de toekomstperspectieven van beeldgeleide chirurgie met fluorescentie.

DEEL EEN: DE WEG NAAR TUMOR-SPECIFIEKE CONTRASTMIDDELEN ● Hoofdstuk een is een algemene inleiding over het gebruik van fluorescentie bij beeldgeleide chirurgie. In hoofdstuk twee beschrijven we onderzoek naar het contrastmiddel indocyanine groen (ICG) – een niet tumor-specifieke fluorofoor. Op basis van muismodellen verwachtten wij, dat ICG ophoopt in tumorweefsel als gevolg van verhoogde permeabiliteit en retentie (EPR). Door dit effect zou fluorescentie beeldvorming met ICG de detectie van uitzaaiingen van eierstokkanker kunnen verbeteren. Bij de tien patiënten die in dit onderzoek waren geïncludeerd, werden acht uitzaaiingen van eierstokkanker gedetecteerd, die allemaal fluorescent waren. Maar er werden ook 13 niet-kwaadaardige laesies gevonden die wel fluorescent waren, wat resulteerde in een fout-positief percentage van 62%. Hieruit concludeerden we dat fluorescentie beeldvorming met ICG niet geschikt is voor de detectie van uitzaaiingen van het ovariumkanker en dat hiervoor tumor-specifieke contrastmiddelen nodig zijn.

In hoofdstuk drie beschrijven we de resultaten van onderzoek naar potentiële aangrijpingspunten voor tumor-specifieke contrastmiddelen voor het opsporen van peritoneale (buikvlies) metastasen (PM) van colorectaal carcinoom (CRC). Met immunohistochemische kleuringen op weefselmonsters werd vastgesteld dat het epitheliale celadhesiemolecuul (EPCAM) en carcino-embryonaal antigeen (CEA) tot over-expressie komen in 100% van de PM-monsters, terwijl over-expressie van andere biomarkers beperkt was. Zo hebben we aangetoond dat zowel EPCAM als CEA geschikte aangrijpingspunten zijn voor fluorescentiebeeldvorming van PM bij patiënten met CRC.

DEEL TWEE: KLINISCHE TRANSLATIE VAN TUMOR-SPECIFIEKE CONTRASTMIDDELEN ◉ In hoofdstuk vier beschrijven we het gebruik van EC17, een tumor-specifiek contrastmiddel dat aangrijpt op de folate receptor alpha (FR α). De golflengte waarbij dit middel fluoresceert (500 nm) is relatief laag. EC17 wordt toegediend aan twaalf patiënten met eierstokkanker en drie patiënten met borstkanker die chirurgische resectie van de tumor ondergingen. Het gebruik van EC17 leidde tot detectie van tumor-specifiek fluorescentiesignaal bij zowel borst- als ovariumkanker. Hierdoor konden er bij patiënten met eierstokkanker zelf 16% meer kwaadaardige laesies verwijderd worden. Door de lage golflengte ontstond er autofluorescentie van gezond weefsel waardoor relatief veel fout-positieve laesies werden gedetecteerd en er sprake was van een niet-optimaal contrast tussen tumor en normaal weefsel. We concludeerden daarom dat FR α een gunstig doelwit is voor beeldgeleide chirurgie maar dat een hogere golflengte in het nabij-infrarode gebied een voorwaarde is voor een tumor specifiek contrastmiddel.

Vervolgens voerden we een onderzoek uit met OTL38 dat net als EC17 een analoog van folaat is, maar waarbij de fluorescentie plaatsvindt bij golflengtes in het nabij-infrarode gedeelte van het lichtspectrum. In hoofdstuk vijf beschrijven we een gecombineerde studie bij 30 gezonde vrijwilligers en 12 patiënten met eierstokkanker die een operatie ondergaan. Door het onderzoek met OTL38 bij gezonde vrijwilligers konden we voorafgaand aan het onderzoek bij patiënten zowel optimale doseringen als het optimale tijdvenster tussen toediening van de stof en intra-operatieve beeldvorming vaststellen. Bij patiënten met ovariumkanker cumuleerde OTL38 in de tumor en uitzaaiingen, waardoor de chirurg 29% meer kwaadaardige laesies kon weghalen, zonder hierbij gehinderd te worden door autofluorescentie.

Op basis van deze resultaten hebben we, zoals in hoofdstuk zes beschreven, het gebruik van OTL38 verder onderzocht bij 6 patiënten met ovariumkanker

in een vroeg stadium die een chirurgische stadiëringsprocedure ondergingen. Door OTL38 kon tijdens de operatie onderscheid gemaakt worden tussen een kwaadaardige en goedaardige primaire tumor. Omdat er bij geen van de patiënten uitzaaiingen aanwezig waren konden we hier geen toegevoegde waarde van OTL38 aantonen.

In hoofdstuk zeven beschrijven onderzoek met de stof SGM-101, een tumor-specifiek contrastmiddel dat bindt aan CEA. We onderzochten SGM-101 bij twaalf patiënten met alveesklierkanker die een operatie ondergingen. We konden vaststellen dat SGM-101 cumuleerde in zowel de tumoren als de uitzaaiingen. Maar, de contrast verhouding tussen de tumor laesies en de achtergrond (tumor-to-background ratio [TBR]) was minder in vergelijking met de bovengenoemde onderzoeken (OTL38 en EC17). Bovendien werd tweemaal door overliggend bloed of weefsel het fluorescentiesignaal tijdens de operatie gemist. Het feit dat de fluorescentie met name geschikt is voor oppervlakkige gebruik (beperkte dieptepenetratie) is een algemeen bekend nadeel van de techniek. Onze conclusie was dat SGM-101 in de huidige vorm niet van toegevoegde waarde is voor beeldgeleide chirurgie bij patiënten met alveesklierkanker.

DEEL DRIE: TOEKOMSTPERSPECTIEVEN ◉ In hoofdstuk acht stellen we dat het onderzoeksveld van fluorescentiebeeldvorming verder moet gaan dan de proof-of-concept-fase. Om klinische toepassing en implementatie van de techniek te bereiken, moeten verschillende uitdagingen door alle betrokkenen in het onderzoeksveld samen worden aangepakt. De belangrijkste uitdagingen zijn het opstellen van standaarden, die nodig zijn om nauwkeurige en reproduceerbare resultaten te garanderen. Daarnaast moeten eindpunten voor vervolgonderzoek, die én de effectiviteit van de techniek aantonen én niet te tijdrovend of te duur zijn, geformuleerd worden. Consensus binnen het onderzoeksveld over deze standaarden en eindpunten is wat ons betreft essentieel voor de uiteindelijke registratie van fluorescente contrastmiddelen door de geneesmiddelen autoriteiten. In hoofdstuk negen doen wij zelf een voorstel voor nieuwe standaarden. We laten aan de hand van een systematische, gecontroleerde vergelijking van twee commercieel verkrijgbare camera-systemen zien hoe je met behulp van een nieuw kalibratie-apparaat de sensitiviteit van het camera-systeem voor een contrastmiddel kan kwantificeren. Daarnaast evalueerden we de berekening van de TBR, de belangrijkste uitkomstmaat in het fluorescentie onderzoek. Hierbij laten we zien dat zowel achtergrondruis als de selectie van de achtergrond grote invloed hebben op de TBR.

LIST OF PUBLICATIONS

Hoogstins CES, Boogerd LS, Sibinga Mulder BG, Mieog JS, Swijnenburg RJ, van de Velde CJ, Farina Sarasqueta A, Bonsing BA, Framery B, Pèlegriin A, Gutowski M, Cailler F, Burggraaf J, Vahrmeijer AL. Image-guided surgery in patients with pancreatic cancer: first results of a clinical trial using SGM-101, a novel carcinoembryonic antigen-targeting, near-infrared fluorescent agent. *Ann Surg Oncol*. 2018 July 28

Hoogstins CES, Burggraaf JJ, Koller M, Handgraaf H, Boogerd L, van Dam G, Vahrmeijer A, Burggraaf J. Setting Standards for Reporting and Quantification in Fluorescence-Guided Surgery. *Mol Imaging Biol*. 2018 May 29.

Hoogstins CES, Boogerd LS, Gaarenstroom KN, de Kroon CD, Beltman J, Trimbos JB, Bosse T, Vuyk J, Low PS, Burggraaf J, Vahrmeijer AL. Feasibility of Folate Receptor-targeted Intraoperative Fluorescence Imaging during Staging Procedures for Early Ovarian Cancer. Publication pending *Eur J Gynaecol Oncol*

Boogerd LS, **Hoogstins CES***, Schaap DP, Kusters M, Handgraaf HJ, van der Valk MJ, Hilling DE, Holman FA, Peeters KC, Mieog JS, van de Velde CJ, Farina Sarasqueta A, van Lijnschoten I, Framery B, Pelegriin A, Gutowski M, Nienhuijs SW, de Hingh IH, Nieuwenhuijzen GA, Rutten HJ, Cailler F, Burggraaf J, Vahrmeijer AL. Safety and effectiveness of SGM-101, a fluorescent antibody targeting carcinoembryonic antigen, for intraoperative detection of colorectal cancer: a dose-escalation, pilot study. *Lancet Gastroenterol Hepatol*. 2018 Jan 17

Boogerd LS, **Hoogstins CES***, Gaarenstroom KN, de Kroon CD, Beltman JJ, Bosse T, Stelloo E, Vuyk J, Low PS, Burggraaf J, Vahrmeijer AL. Folate receptor- α targeted near-infrared fluorescence imaging in high-risk endometrial cancer patients: a tissue microarray and clinical feasibility study. *Oncotarget*. 2017 Dec 11

Hoogstins CES, Weixler B, Boogerd LS, Hoppener DJ, Prevoo HA, Sier CF, Burger JW, Verhoef C, Bhairosingh S, Farina Sarasqueta A, Burggraaf J, Vahrmeijer AL. In search for optimal targets for intraoperative fluorescence imaging of peritoneal carcinomatosis from colorectal cancer. *Biomark Cancer*. 2017 Aug 28

Handgraaf HJM, Boogerd LSF, Höppener DJ, Peloso A, Sibinga Mulder BG, **Hoogstins CES**, Hartgrink HH, van de Velde CJH, Mieog JSD, Swijnenburg RJ,

Putter H, Maestri M, Braat AE, Frangioni JV, Vahrmeijer AL. Long-term follow-up after near-infrared fluorescence-guided resection of colorectal liver metastases: A retrospective multicenter analysis. *Eur J Surg Oncol*. 2017 Aug

Boogerd L, Vuijk FA, **Hoogstins CES**, Handgraaf H, van der Valk M, Kuppen P, Sier C, van de Velde C, Burggraaf J, Fariña-Sarasqueta A, Vahrmeijer AL. Correlation Between Preoperative Serum Carcinoembryonic Antigen Levels and Expression on Pancreatic and Rectal Cancer Tissue. *Biomark Cancer*. 2017 May 17

Hoogstins CES, Handgraaf HJ, Boogerd LS, Burggraaf J, Vahrmeijer AL. Image guided surgery using near-infrared fluorescence: road to clinical translation of novel probes for real time tumor visualization. *SPIE* 2017 Feb 8

Hoogstins CES, Tummers QR, Gaarenstroom KN, de Kroon CD, Trimbos JB, Bosse T, Smit VT, Vuyk J, van de Velde CJ, Cohen AF, Low PS, Burggraaf J, Vahrmeijer AL. A novel tumor-specific agent for intraoperative near-infrared fluorescence imaging: a translational study in healthy volunteers and patients with ovarian cancer. *Clin Cancer Res*. 2016 Jun 15

Tummers QR, **Hoogstins CES***, Gaarenstroom KN, de Kroon CD, van Poelgeest MI, Vuyk J, Bosse T, Smit VT, van de Velde CJ, Cohen AF, Low PS, Burggraaf J, Vahrmeijer AL. Intraoperative imaging of folate receptor alpha positive ovarian and breast cancer using the tumor specific agent EC17. *Oncotarget*. 2016 May 31

Boogerd LS, Boonstra MC, Beck AJ, Charehbili A, **Hoogstins CES**, Prevoo HA, Singhal S, Low PS, van de Velde CJ, Vahrmeijer AL. Concordance of folate receptor- α expression between biopsy, primary tumor and metastasis in breast cancer and lung cancer patients. *Oncotarget*. 2016 Apr

Tummers QR, **Hoogstins CES***, Peters AA, de Kroon CD, Trimbos JB, van de Velde CJ, Frangioni JV, Vahrmeijer AL, Gaarenstroom KN. The value of intraoperative near-infrared fluorescence imaging based on enhanced permeability and retention of indocyanine green: feasibility and false-positives in ovarian cancer. *PLoS One*. 2015 Jun 25

Hoogstins CES, Becker SJ, Ring D. Contralateral electrodiagnosis in patients with abnormal median distal sensory latency. *Hand (NY)*. 2013 Dec

* Shared first authorship

CURRICULUM VITAE

Charlotte Hoogstins werd op 21 augustus 1987 geboren te Amsterdam. In 2005 behaalde zij haar eindexamen aan het Stedelijk Gymnasium te Haarlem, waarna zij Geneeskunde ging studeren aan de Rijksuniversiteit Groningen. Tijdens haar studie was zij betrokken bij de organisatie het van International Student Congress of Medical Sciences (ISCOMS) en werkte zij als vrijwilliger bij de kindertelefoon. Daarnaast was zij actief lid van de Groningse Studenten Vereniging Vindicat. Tijdens haar coschappen in Zwolle zat zij in het bestuur van de Stichting Benefietdiner Isala Ziekenhuis, waarmee dat jaar 35.000 euro werd ingezameld voor een project van Artsen zonder Grenzen. Haar wetenschappelijke stage deed zij bij de Orthopaedic Hand and Upper Extremity Surgery van het Massachusetts General Hospital in Boston, hier raakte zij geïnspireerd door het wetenschappelijk onderzoek. Na het behalen van haar artsexamen in maart 2013 begon zij als eerste arts-onderzoeker van de Image-Guided Surgery groep zowel in het Leids Universitair Medisch Centrum (LUMC) onder leiding van dr. A.L. Vahrmeijer en prof. dr. C.J.H. van de Velde als in het Centre for Human Drug Research (CHDR) onder leiding van prof. dr. J. Burggraaf en prof. dr. A.F. Cohen. Tijdens deze periode gaf zij verschillende poster- en podiumpresentaties op (inter)nationale congressen, die gewaardeerd werden als het beste abstract (Symposium Experimenteel Onderzoek Heelkundige Specialismen 2015, Groningen) en waarmee een reisstipendium werd gewonnen (World Molecular Imaging Congress 2015, Honolulu Hawaii). In 2017 startte zij als ANIOS Chirurgie in het Flevoziekenhuis te Almere (opleiders dr. P.C.M. Verbeek en dr. K.H. in 't Hof). Momenteel is zij werkzaam als ANIOS Chirurgie in het Academisch Medisch Centrum te Amsterdam (opleider dr. E.J.M. Nieveen van Dijkum).

Charlotte is gelukkig getrouwd met Christiaan Swellengrebel en woont in Amsterdam.

DANKWOORD

Mijn dank gaat in de eerste plaats uit naar alle patiënten die onbaatzuchtig deel hebben genomen aan het onderzoek. Hun moed en hun positieve instelling zijn een ware inspiratie. Ook gaat mijn dank uit naar de gezonde vrijwilligers die het aan durfden om mee te doen aan onderzoek met nieuwe middelen. Zonder beiden zou dit proefschrift er niet zijn geweest.

Daarnaast wil ik de volgende mensen bedanken die de afgelopen jaren nauw betrokken geweest zijn bij het onderzoek:

Dr. Vahrmeijer, allerbeste Lex, jouw leiding aan onze groep was uniek, je hebt altijd zoveel ideeën voor onderzoek en geeft ons het vertrouwen om er zelf wat moois van te maken. Ik heb de afgelopen jaren veel van je geleerd, natuurlijk op wetenschappelijk gebied, maar vooral ook door de unieke manier waarop jij met mensen omgaat.

Prof. Burggraaf, allerbeste Koos, met jouw praktische en directe manier van leiding geven, vorm je met Lex een uitstekend team. Met jouw visie en toekomstplannen gaat het Green Team naar de next level. Ik waardeer het enorm dat je altijd betrokken was bij het onderzoek, maar ook bij ons persoonlijk.

Prof. van de Velde, beste professor, ik beschouw het als een eer dat ik onder uw leiding onderzoek heb mogen doen, uw carrière is een grote inspiratiebron voor mij. Ik wil u bedanken voor de tijd die u regelmatig vrij maakte om met mij van gedachten te wisselen over het onderzoek en mijn verdere loopbaan. Xandra, dank voor alle praktische ondersteuning hierbij.

Prof. Cohen, beste Adam, jouw manier van 'out of the box' denken heeft mij bijzonder geprikkeld tijdens mijn onderzoek. Ik wil je bedanken voor alle mogelijkheden die mij geboden zijn dankzij het feit dat ik onder jouw leiding in het CHDR onderzoek te doen.

Dear Marty and Phil, I really enjoyed working with you on the EC17 and OTL38 projects. Your/On Target's perspective has taught me a lot, on both a scientific as well as a drug development level, thank you. Also thanks to Françoise and Surgimab for the opportunity to work together.

Greenteam, dankzij jullie was promoveren een feestje. Q, met je treffende one-liners zoals 'een beller is sneller', wijdde jij mij in in de wereld van het promoveren. Norie, immer 'shinend', samen hebben wij ons staande gehouden tussen alle mannen. Marruk, altijd in voor de Hepatho of een lekker muziekje. Heinrich, keiveel gelachen (om je mooie Brabantse accent), jammer alleen dat je nog steeds geen nikes hebt. Babbel, de benjamin van de groep, highlight van

mijn laatste jaar. Natuurlijk heb ik veel te danken aan de ‘oude’ garde: *Sven, Rutger-Jan, Denise, Bob, Floris* en natuurlijk *Joost*, die mij voor de Green Team scoutte in Boston. Uit onze samenwerking zijn niet alleen heel veel mooie artikelen maar nog veel meer mooie avonden voortgekomen. Ik hoop dat we die traditie nog lang kunnen voortzetten met alle nieuwe aanwinsten.

Dankzij de hulp van vele anderen is dit proefschrift tot stand gekomen, dank daarvoor aan:

Alle *co-auteurs*; de *chirurgen, assistenten chirurgie en OK-assistenten*; de *mede-promovendi* en het *Heelkunde research lab*, in het bijzonder *Marieke, Shadhvi* en *Kees*; de *gynaecologen* en hun assistenten, in het bijzonder *Katja Gaarenstroom, Margriet* en *Dorien*; de *pathologen* en hun assistenten, in het bijzonder *Tjalling Bosse, Arantza Farina Sarasqueta* en *Vincent Smit*; de *anesthesisten*, hun assistenten en de *anesthesie medewerkers*, in het bijzonder *Jaap Vuyk*; alle *collega's* van het *CHDR*; de *trial apotheek*; en de *collega's* van het *Catharina Ziekenhuis (Eindhoven)*, in het bijzonder *Harm Rutten, Miranda Kusters* en *Dennis Schaap*.

De *assistenten en chirurgen* uit het *Flevoziekenhuis*, dank voor een fantastisch begin van mijn klinische carrière en ook de nieuwe *collega's* uit het *AMC*, dank voor de voortzetting daarvan.

Zonder alle leuke afleiding was het natuurlijk helemaal niets geworden, daarvoor dank aan al mijn lieve vriendinnetjes:

Durfjes, Ali, Bettie, Fred, Bel, Marijn en *Sop*; *Teddies, Lien, Mart, Dino, Sab, Kees, Billy* en *Piet*; *Boston babes, Margriet* en *Heleen*; en de *wijnclub*.

Lieve *schoonfamilie, Caroline, Maurits* en de *Hoffen*, dank dat jullie mee leefden en interesse toonden in mijn werk in de afgelopen jaren.

Lieve *pappi, mammi, Fred, Wilson, SJ* en tante *Pien*. Dank voor jullie onvoorwaardelijke steun en vertrouwen. Jullie zijn de basis waarop ik verder heb kunnen bouwen; zonder jullie was ik nooit zo ver gekomen.

Allerliefste *Chris*, *ij's my* toevlug. Dankzij jouw steun is het gelukt! Ik geniet zo van het leven met jou (en daar is nu nog meer tijd voor!)

